TALLINNA TEHNIKAÜLIKOOL
MEHAANIKATEADUSKOND

Mehaanikainstituut
Tehnilise mehaanika õppetool

EMD70LT

Hardi Niiler

EKVIVALENTNE JÄÄ PAKSUS LAEVA TEGELIKU JÄÄ TAKISTUSE HINDAMISEKS

Autor taotleb
tehnikateaduse magistri
akadeemilist kraadi

Tallinn
2015

AUTORIDEKLARATSIOON

Deklareerin, et käesolev lõputöö on minu iseseisva töö tulemus.
Esitatud materjalide põhjal ei ole varem akadeemilist kraadi taotletud.
Töös kasutatud kõik teiste autorite materjalid on varustatud vastavate viidetega.

Töö valmis Kristjan Tabri juhendamisel

“.....”.....2015 a.

Töö autor

..... allkiri

Töö vastab magistritööle esitatavatele nõuetele.

“.....”.....2015 a.

Juhendaja

..... allkiri

Lubatud kaitsmisele.

..... eriala/õppekava kaitsmiskomisjoni esimees

“.....”.....2015 a.

..... allkiri

TALLINNA TEHNIKAÜLIKOOL
MEHAANIKATEADUSKOND

Faculty of Mechanical Engineering
Chair of Technical Mechanics

EMD70LT

Hardi Niiler

EQUIVALENT ICE THICKNESS FOR EVALUATING SHIP RESISTANCE IN ICE

Thesis submitted in partial fulfilment
of the requirements for the degree of
Master of Science in Technology

Tallinn
2015

TTÜ Mehaanikainstituut

Tehnilise mehaanika õppetool

MAGISTRITÖÖ ÜLESANNE

2015. aasta kevadsemester

Üliõpilane: Hardi Niiler, 120371MATMM
Õppekava MATM02/11 – Tootearendus ja tootmistehnika
Eriala: Laevaehitus
Juhendaja: Kristjan Tabri, D.Sc. (Tallinna Tehnikaülikool)
Konsultandid: Professor Pentti Kujala (Aalto Ülikool)
Mikko Suominen, M.Sc (Aalto Ülikool)

MAGISTRITÖÖ TEEMA:
Ekvivalentne jää paksus laeva tegeliku jää takistuse hindamiseks
Equivalent ice thickness for evaluating ship resistance in ice

Lõputöös lahendatavad ülesanded ja nende täitmise ajakava:

Nr	**Ülesande kirjeldus**	**Täitmise tähtaeg**
1	**Magistritöö kava esitamine**	**15.07.2014**
2.	**Andmete analüüs, mõõtmiste teostamine**	**28.08.2014**
3.	**Ekvivalentse jää paksuse arendus**	**28.11.2014**
4.	**Esialgse versiooni esitamine**	**11.01.2015**
5.	**Lõputöö lõplik versioon**	**1.04.2015**

Lahendatavad insenertehnilised ja majanduslikud probleemid:
Magistritöö eesmärk on teostada jää paksuste mõõtmised ja neid analüüsida. Analüüsis tuleb kasutada kolme erineva meetodi tulemusi. Mõõtmistulemuste põhjal tuleb leida Antarktika jääle ekvivalentne paksus mis vastaks laeva tegelikule taksitusele jääs.

Töö keel: inglise keel

Kaitsmistaotlus esitada hiljemalt 18.05.2015 **Töö esitamise tähtaeg:** 25.05.2015

Üliõpilane Hardi Niiler /allkiri/ …….. kuupäev 18.05.2015

Juhendaja Kristjan Tabri /allkiri/ ……. kuupäev 18.05.2015

Acknowledgements

This thesis was carried out with the collaboration of Aalto University School of Engineering and Finnish Meteorological Institute, as a part of ANTLOAD (Variation of Antarctic Ice Thickness and its Effect on the Load Level of Ice Navigation) project and funded by the Academy of Finland.

I would like to thank Tallinn University of Technology for giving such an opportunity and enabling to study at the Aalto University Master's Programme in Maritime Engineering.

I would like to express my sincere gratitude to my supervisor, Professor Pentti Kujala, for his valuable guidance and advices. I am also grateful to my instructors, M.Sc. Mikko Suominen and Kristjan Tabri for their support and comments throughout the thesis writing.

Finally, I would also like to thank my family and friends for their support during the thesis writing process.

Espoo, 2015

Hardi Niiler

Table of contents

Acknowledgements vii

List of symbols x

Abbreviations xi

1. Introduction 1

2. Characteristics of ice conditions 4

2.1 Ice cover 5

2.2 Sea ice properties 11

3. Ship resistance in ice 13

4. Equivalent ice thickness 16

5. Description of measurements 18

5.1 Description of the voyage 18

5.2 Instrumentation and description of the vessel 19

5.3 Ice thickness measurements 20

5.3.1 Visual observations 20

5.3.2 Electromagnetic system 21

5.3.3 Stereo camera system 23

6. Case study 26

6.1 Measurements selection 26

6.2 Visual observations 27

6.3 Stereo camera measurements 29

6.4 The EM measurements 30

6.5 Conclusion of the three method's results 31

7. Application for equivalent ice thickness 34

7.1 Measurement results based on ship navigation parameters 34

7.2 More detailed analysis with the four selected cases 37

8. Discussion 40

9. Conclusion 43

Kokkuvõte 44

Bibliography 45

List of Appendices

Appendix 1 48
Appendix 2 49
Appendix 3 54
Appendix 4 64
Appendix 5 65
Appendix 6 71

List of symbols

B	breathe of the ship
C	ice concentration
d	distance of ice track
d_{ow}	distance of open water
F_v	vertical force
g	gravitational constant
H_{eq}	equivalent ice thickness
H_i	level ice thickness
H_p	primary electromagnetic field
H_R	ridge height
L_{wl}	length of waterline
R_B	ice breaking resistance component
R_c	ice crushing resistance component
R_i	level ice resistance
R_{ice}	total level ice resistance
R_{ow}	open water resistance
R_S	ice submerging resistance component
R_T	total resistance
R_V	resistance increase due to velocity
R_x	receiver coil
T	draught of the ship
T_x	transmitter coil
v	speed of the ship

Z_E	distance from the sensor to the bottom of sea ice
Z_I	total thickness of sea ice
Z_L	distance from the sensor to the surface of ice or snow
α	water entrance angle
$\Delta\rho$	density difference between water and ice
η	ridge volume factor
κ	snow layer thickness coefficient
κ	snow layer thickness coefficient for equivalent ice
μ	friction coefficient between ice and structure
μ_0	magnetic permeability
ρ_{ice}	ice density
ρ_w	water density
σ_b	ice bending strength
ϕ	stem angle
ψ	angle between normal of the surface and vertical vector

Abbreviations

ASPeCt	Antarctic Sea Ice Processes & Climate
EM	electromagnetic induction sounding
FMI	Finnish Meteorological Institute
GPS	global positioning system
RAW	digital negative
SC	stereo camera system

1. Introduction

Ship resistance in ice is important because human activity is increasing in Earth's Polar Regions. The Polar Regions are The Arctic Ocean in the North and the continent of Antarctica in the South. These areas receive less intensive solar energy because of the oblique sun angle. The climate in these areas is characterized by extremely cold temperatures during the winter, resulting in thicker ice and greater snow thicknesses compared to, for example, Baltic winter conditions. The polar areas saw less human activity in the past century, but now that activity is growing. The main reason for this growth is scientific progress and ongoing research, which allows for better evaluation of real ice conditions, and according to this construct vessels, using long-term methods are capable of operating there mainly in the summer if lighter ice conditions are present. However, perhaps in the future during the winter season, the efficiency of icebreakers may be better than it is now. This would allow for year-round safe transport, which will be necessary for starting oil drilling in polar areas.

Based on publication data, the equivalent ice thickness concept has not really been studied systematically, but some generalizations can be made. "Equivalent ice thickness describes ship performance in general ice conditions where the ice ridges are smaller than those that would stop the vessel" (Riska, 2011). The description of this general ice condition requires the following data: coverage of ice and level ice thickness. These parameters are given versus the coverage of each thickness: average maximum thickness of ice ridges and the density of the ridges. This information is mainly available on weather web pages under the marine weather section where charts of ice conditions are located. These ice charts, which are based on satellite images, allow for the evaluation of the ice thickness as equivalent and present the ice chart in a color-coded format, but the entire process takes time and ice conditions change regularly. As a result, these data cannot be depended upon.

Average-size ice ridges can cause a high resistance, and usually the resistance is higher than the ship's actual thrust. Therefore, the ship must penetrate the ridges by using inertia. The capability of ridge penetration is a prerequisite for icebreaking ships, for which the requirement is for a certain size of ice ridge that should be penetrated by one ram with a certain initial speed. The level ice performance is possible to verify in full scale, and therefore, ridge penetration and level ice performance are taken together using so-called

equivalent level ice thickness. An explanation for the equivalent level ice thickness is the average thickness of all ice in the area calculated from level ice thickness and ridges. The ridges part is divided uniformly to the level ice, where it is assumed that ridges are of triangular cross section with a certain base angle (Riska, 2011).

The snow cover on top of the ice affects ship performance because snow influences frictional forces. As the icebreaking ships are made with a flat bow, the effect of the snow is amplified. The present common practice is to use equivalent ice thickness, where the coefficient for snow is commonly set at 1/3 (Riska, 2011).

It is known that, in nature, level ice does not exist, although the ice thickness maps indicate that it does. This argument is supported by the paper in which the transit speed and equivalent ice thickness are compared to the performance of the *MT Uikku* in level ice. When the results are translated into equivalent transit speed in ice, the equivalent ice thickness is approximately 1.5 times the level ice thickness (Hänninen, 2004).

Another option is to formulate an equation of ridge spacing distribution, where the equation explains ridge fields in terms of ridge height and ridge spacing for a certain area. The spacing distribution value is used as a coefficient for ridged ice. In which the volume of ice rubble in a ridge equals the volume of the consumed parent ice. The ridge rubble is then thought of as added thickness to the level ice sheet (Lensu, 2003). However, such method requires several year's analysis to formulate realistic term of ridges.

The other important part is ice resistance evaluation with a calculated method where measured ice thickness results are used. For that purpose Lindqvist's (1989) straightforward method for the calculation of ice resistance can be used to assess the actual thrust of the ship, which is measured from the shaft-line. An equivalent thickness must be found using this method.

All previously mentioned equivalent ice thickness concepts and works with performance data are based on Baltic region ice conditions. Currently, similar studies of Antarctic data cannot be found. These ice thickness determination methods are still in development because of the need to know the ice-induced loads on the ship's hull and how thick the ice which induces such loads actually is.

The scope of the work is to discover a reasonable way to describe the Antarctic sea ice average ice thickness as equivalent ice thickness. The relevant definition from Kaj Riska:

“If a ship is navigating in level ice of 40 cm in thickness, this will result in the same load level as irregular ridged ice of an equivalent thickness of 40 cm” (Riska, 2009). Although the work considers this definition for ice resistance. Figuratively it means that level ice, which is hard to find, is reallocated irregularly with ridged ice and level ice over the same surface, which is due sea ice. The flow of the work is to calculate the equivalent ice thickness of measured ice and calculate resistance in order to compare with vessel actual thrust during that time and assess the results. All the work is based on real measurements taken by the Polar research vessel *S.A. Agulhas II* in Antarctic sea ice in 2013 – 2014.

2. Characteristics of ice conditions

The current chapter describes the Antarctic region (see Figure 2.1) generally and which data are used in this thesis. The focus is on ice conditions that are relevant for this work and physical and mechanical properties of ice.

Figure 2.1 Map of Antarctica

Antarctica is a land mass surrounded by an ocean. The salinity there is about 3.4%, which notably affects sea ice formation compared to the Baltic Sea. Ocean temperature must reach -2°C to freeze. The formation differences appear with brine rejection, which is a process that occurs during sea ice formation where salt is pushed from forming ice into the seawater by brine drainage channels. This brine drainage significantly affects the properties of sea ice. The open ocean allows the forming sea ice to move more freely than closed sea ice, resulting in higher drift speeds and possibilities to form ridges. Antarctic sea ice extends mostly latitudes 60°-70°S. However, there is no land boundary to the north and the sea ice is free to float northward into warmer waters, where it eventually melts. Therefore, almost all of

the sea ice that forms during the Antarctic winter melts during the summer season (National Snow & Data Center). As a result, Antarctic ice is typically 1 to 2 m thick and the occurrence of multiyear ice is low in high seas. About 80% of the Antarctic multiyear ice store is in the Weddell Sea (ASPeCt). Furthermore, on Antarctic sea ice occur the biggest snow falls. Because of the thin ice, the weight of the snow often depresses the sea ice surface below the sea level, which creates the possibility to form snow ice (Maksym, 2012). Statistical ice conditions from literature (Worby, et al., 2008) in spring for Weddell Sea area can be seen in Table 2.1, where the values are with standard deviations in brackets.

Table 2.1 Ice conditions in spring for Antarctic Weddell Sea (east) (Worby, et al., 2008)

Ice concentration [tenth], Mean (std)	8.2 (2.4)
Level ice thickness [m], Mean (std)	0.63 (0.35)
Average ice thickness [m], Mean (std)	0.89 (0.64)
Ridge height [m], Mean (std)	0.74 (0.52)
Snow thickness [m], Mean (std)	0.16 (0.12)

2.1 Ice cover

Ice cover has been described in various ice types because the ice appears in nature in many different forms. The following describes of these sea ice types that are typical for first-year ice and relevant for the equivalent ice thickness point of view.

Level ice is an undamaged continuous ice sheet with a flat surface. In real conditions it is hard to find at sea. But it is the simplest term to define ice conditions with one thickness value, and it is used, for example, in power prediction calculations. Also, icebreaking vessel performance is typically specified with minimum speed in a given level ice thickness. First-year level ice can freeze up to 2 m thick, but normally it is less. Generally ice growth process in rough ocean is called pancake cycle (see Figure 2.2).

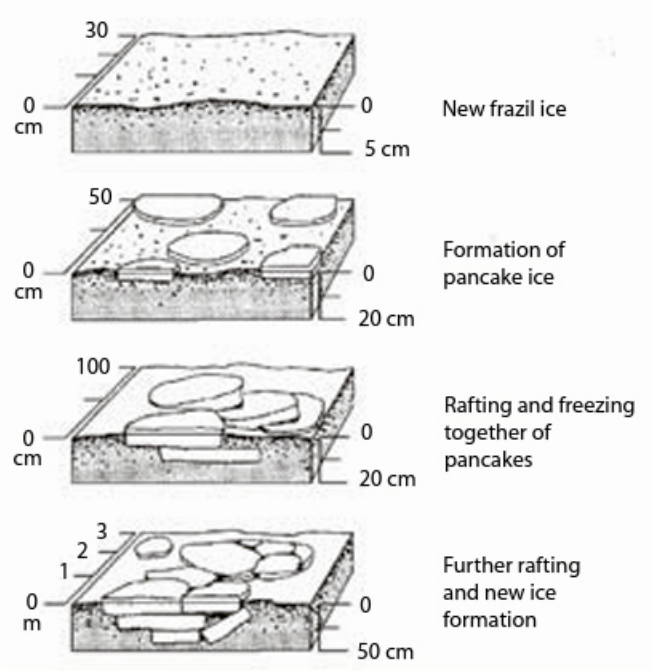

Figure 2.2 The pancake cycle (Lange, et al., 1989)

Firstly forms frazil ice, which is a collection of loose, randomly oriented ice crystals in water. After that the frazil crystals accumulate into circular disks, called pancake ice. As the pancake ice is in motion then rafting or ridging occurs and pancakes grow. Then the pancake ice cement together and consolidate into ice sheet, which continues to grow through the winter. This ice may be called level ice. In Table 2.2 can be seen Antarctic level ice thickness statistical values for winter, summer and annual with standard deviations in brackets (Worby, et al., 2008).

Table 2.2 Statistics of Antarctic level ice thickness (Worby, et al., 2008)

	Level ice thickness, [m], Mean (std)			
Location	Period	Winter	Summer	Annual
Weddell Sea		0.40 (0.23)	0.58 (0.55)	0.50 (0.44)
Bellinghausen-Amundsen Sea		0.39 (0.22)	1.91 (1.03)	0.63 (0.67)
Ross Sea		0.49 (0.29)	1.12 (1.04)	0.84 (0.87)

Ice floe is a large patch of flat floating ice (see Figure 2.3). The size is greater than 20 meters across. They are formed from solid ice sheet. The ice floes are dominant in melting season and appear most in the marginal sea ice zone, which is located between open ocean and the interior ice pack. In the marginal sea ice zone are relatively small ice floes, mostly less than 100 m in diameter. Likewise the melt rate of ice floes increase significantly for floe sizes smaller than 30 m because of lateral melting effect increase. Therefore, the floe size

distribution is an important parameter to describe ice conditions and melting (Toyota, et al., 2011).

Figure 2.3 Ice floe (Auch, 2008)

Example of floe size distribution for the Antarctic Weddell Sea can be seen on Figure 2.4, where the measurements were implemented at the end of the winter season (2006), when the sea ice extent is about annual maximum.

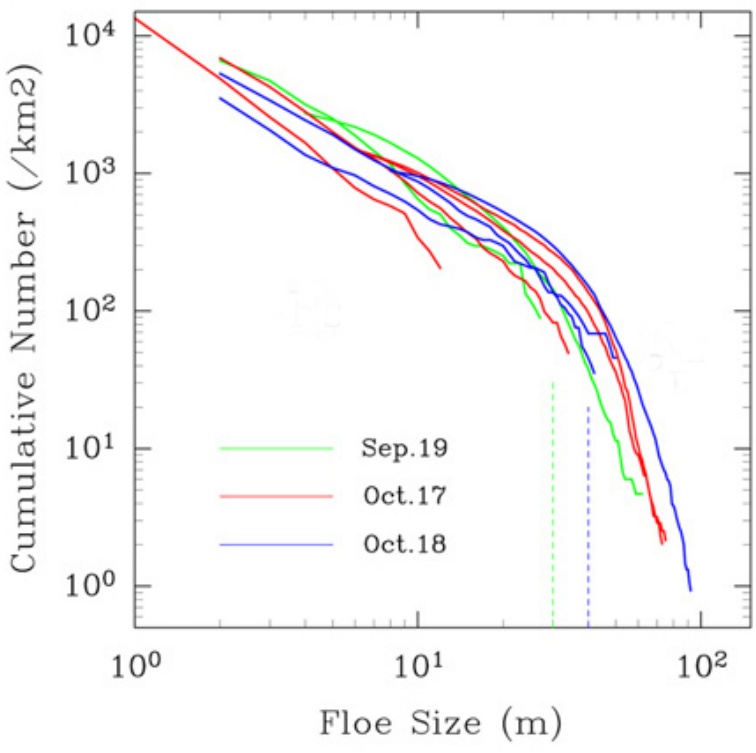

Figure 2.4 Floe size distribution (Toyota, et al., 2011)

Rafted ice forms when one ice sheet or floe overrides another. This process is possible through the actions of external forces like wind and currents. Sometimes a distinction between rafting and ridging is not so clear, but based on Parmerter (1975), thin ice (< 17 cm) rafts and thick ice form ridges.

Figure 2.5 Rafted Ice (SMHI, 2014)

A ridge is a long, narrow pile of ice blocks that are forced upwards. See Figure 2.6.

Figure 2.6 Sea ice ridge (Usher, 2005)

An idealized ridge has a triangular sail above the water level and a similar keel below the water level, but typically the keel size is several times greater than the sail height. See Figure 2.7, where the ridge cross-section parts are illustrated. Ridges form when two ice sheets are moved by wind and currents against each other and break. After that a ridge starts to freeze together and the spaces between the ice blocks below the waterline consolidate. Over time the ridge becomes stronger. Basic dimensions of Antarctic (Weddell, Amundsen, and Ross Sea) first-year ridges are presented in Table 2.3.

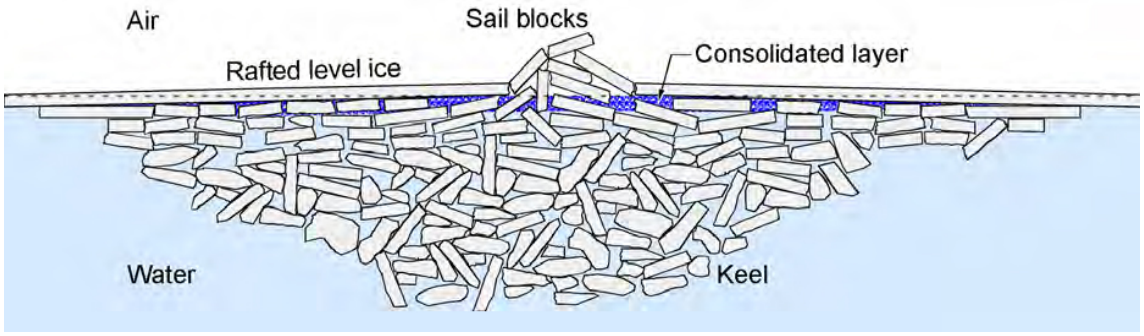

Figure 2.7 Typical sea ice ridge cross-section (Ehle, 2011)

Table 2.3 Basic dimensions of Antarctic first-year ridges (Tina Tin, 2003)

Variable	Antarctic
Keel width [m]	27 ± 17
Max keel depth [m]	3.65 ± 1.82
Keel angle α [^{o}]	15 ± 8
Keel area [m^2]	73 ± 72
Level ice thickness [m]	0.75 ± 0.28
% underestimation by level approximation [%]	55 ± 17

Table 2.3 illustrates the Antarctic first-year ridge's physical dimensions, with mean and ± one standard deviation. The ridge's keel width is about 27 meters. The maximum keel depth of Antarctic ridges is 3.65 meters. Keel angle is about 15^o degrees. Level ice thickness is 0.75 meters. The Antarctic level ice thickness is approximated by the surrounding level ice, and in this way the underestimation is approximately 55%, which explains why it is so thin. The measurements are more or less from the late nineties and were done from drill profiles. Table 2.3 results are only presented to give a general idea of ice conditions, because the measurements are carried out in different ways and at different times.

Another key parameter for ridges is porosity, which is caused by structural voids between ice blocks, and material porosity, which is made of air and water pockets in the ice. Based on literature, the total porosity for Antarctic ridged ice is 0.35 (Tina Tin, 2003).

Ice concentration: a unit less parameter what describes the relative amount of area covered by ice, compared the total areal extent of ice and water. As an example, concentration describes how much of a 10 km by 10 km square is covered by ice. Typically it is reported as a percentages, in tenths or fraction from 0 to 1. A value 100 % means that the square is completely covered by ice. Normally the 90% and up is considered solid ice. It is done

primarily in situ measurements from ships and aircraft and can be done by eye or using photos. Another method is to use a satellite images (see Figure 2.8) but sometimes it is hard to identify what is ice and what is open water. Also clouds can prevent the usage of satellite. Furthermore they require a validation by in situ measurements, because the ice is in constant motion and conditions can change rapidly.

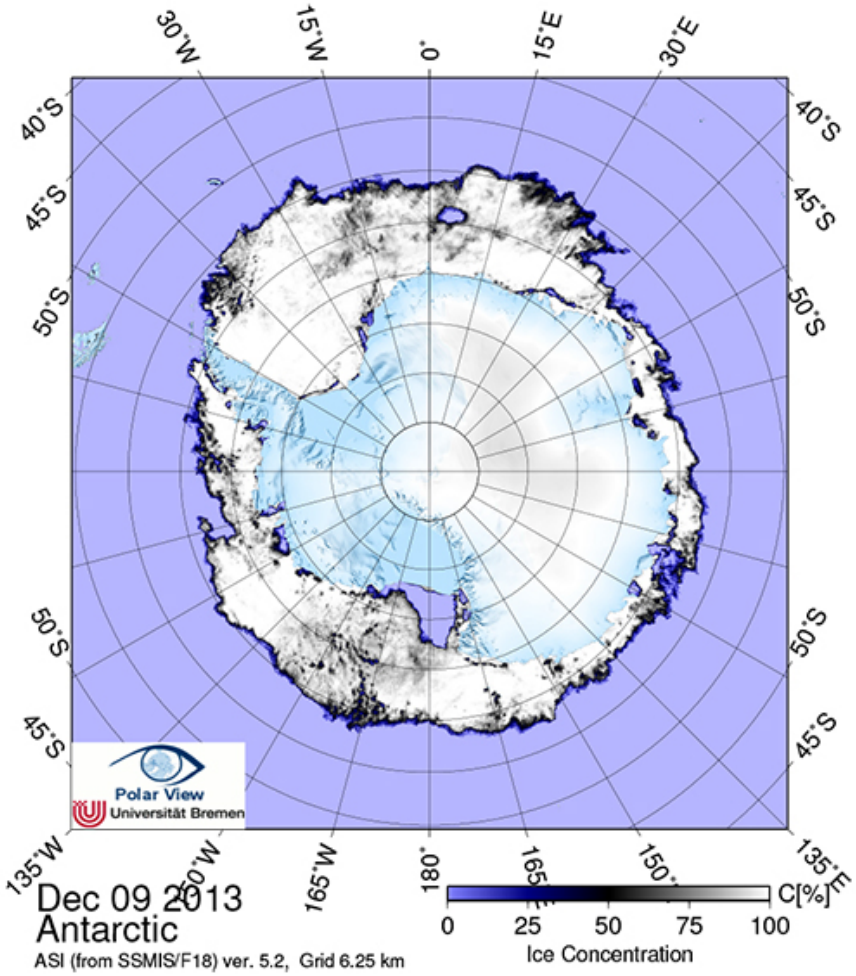

Figure 2.8 Antarctic satellite image (University of Bremen)

2.2 Sea ice properties

Engineering properties of sea ice refers to the strength and stiffness of sea ice. These values can vary over a wide range. They are highly dependent on temperature, orientation, structure, brine volume, porosity, strain rate, and scale. Furthermore, sea ice properties appear to depend on the measurement procedure, and the results are quite sensitive to the qualities of the ice samples. Therefore, single values cannot be given and statistical data should be used,

which is safer if considering the consequences that a too-low value may cause, for example, an oil spill or a structural collapse.

In this work the bending strength is the most relevant parameter, because the ship breaking ice by bending. However the process when measuring the bending strength of ice by simply supported beam, there are assumption's that the ice in the beam is homogenous and perfectly elastic. Likewise bending strength is not an initial material property but more like index value. The bending strength is dependent on the brine volume and ice/brine ratio changes with temperature, which means that porosity grows with temperature and bending strength decrease.

Engineering properties for this work are also taken from real measurements that are implemented during the Antarctic voyage. As the work is based on a real state, sea ice properties are taken from real measurement results and summed up in Table 2.3 by one average value for each parameter and also include statistical parameters from the literature (Schwarz, 1981) for comparison. The full review of sea ice mechanical properties are presented in Appendix 4 (Kujala, et al., 2014).

Table 2.3 Engineering properties of sea ice

	Antarctic (Schwarz, 1981)	Antarctic during the voyage (Kujala, et al., 2014)	
Parameter	Value	Value	Unit
Bending strength	398	173	[kPa]
Compressive strength	4.34	0.737	[Mpa]
Density	875	790	[kg/m^3]
Salinity of speciments	0.58	0.11	[%]
Temp of speciments	-3.6	-0.7	[C°]

Based on Table 2.3 data, we can say that during the Antarctic voyage, the ice engineering properties are much lower and, in general, the ice is much weaker. Probable cause for this is the summer season in Antarctica and a quite high ice temperature that causes the strength to be reduced. The ice samples were also porous and granular.

3. Ship resistance in ice

Ship ice resistance calculation method development began when Robert Runeberg published the first ice resistance formula in 1889 (Runberg, 1889). One hundred and twenty-five years have elapsed since then. Throughout this period, over thirty different ice resistance formulas have been published. Most of them have focused on level ice resistance. The most recognizable names include Enkvist (1972), Kasteljan et al. (1979), Ionov (1985), Lindqvist (1989), and Riska (1997). Several of the formulas are somehow connected or slightly differ in variables used (Riska, et al., 1997).

A quite common assumption is that the open water and level ice resistance components R_{ow} and R_i can be separated and superimposed to obtain the total resistance R_T.

$$R_T = R_{ow} + R_i \tag{3.1}$$

However, about 75% of the resistance of a typical vessel in open water is frictional resistance. On the other hand, most of the underwater part of the hull of a vessel is covered with ice floes when operating in level ice. This means that a type of boundary layer does not exist, which is typical for open water conditions because the hull is covered by ice. This means that ice resistance and the resistance of a vessel in open water cannot be added. Thus R_i only represents the arithmetic difference between resistance of the ship in ice-covered waters and resistance of the ship in open water (Kämäräinen, 1993).

Based on the literature, the quite established division of ice resistance into components is breaking resistance R_B, ice submerging resistance R_S, and resistance increase due to velocity (Kämäräinen, 1993).

$$R_i = R_B + R_S + R_V \tag{3.2}$$

For the scope of this thesis, ice resistance is needed to compare the ship's actual thrust. Thrust is a linear reactive force that is exerted by propeller and should be in balance with ship resistance. As this thesis does not cover the deep resistance methods of study, this work is based on Lindqvist's (1989) established and proven method because it is well defined and validated in full scale. In addition, this method accounts for the changing mechanical properties of ice unlikely with the newer Riska method, which is defined for Baltic Sea ice by constants and is not so applicable for Antarctic sea ice's mechanical properties.

The Lindqvist (1989) method is a straightforward method for the calculation of the ice resistance of ship. The whole icebreaking process is simplified. It does not handle scientific exactitude. Its primary use is to be a tool for the evaluation of ship ice resistance. The main purpose is to estimate the resistance level and to indicate how resistance is affected by the main dimensions, the hull form, and friction. The main resistance components in this method are breaking, submersion, and speed dependence. The assumption for the icebreaker hull form can be seen in Figure 3.1, where the underwater form is composed of flat surfaces to make calculations compact. The hull form is defined by stem angle ϕ, water entrance angle α, angle between normal surface and vertical vector ψ, length of waterline L_{wl}, draught T, and breath B. In calculations ice is defined by thickness h, bending strength $\sigma_{b,}$ and density ρ. In addition, the friction coefficient between the ship and ice is μ, gravitational constant g, and density difference between the water and ice $\Delta\rho$.

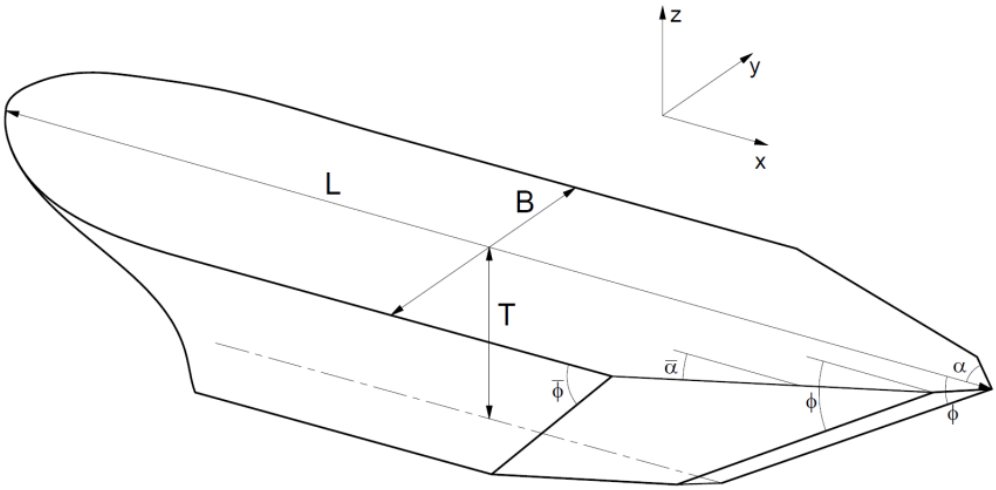

Figure 3.1 Approximation of hull form (Lindqvist, 1989)

Furthermore, to keep the calculations short, both deflection of the ice and trimming of the vessel are excluded. It can cause an underestimation of the breaking resistance. It is well-known that in very thick ice, the ship trims considerably; therefore these simplifications can cause underestimations.

The Lindqvist method formulas are presented as follows:

Angle ψ between normal surface and vertical vector is calculated as:

$$\psi = \text{atan}\left(\frac{\tan(\phi)}{\sin(\alpha)}\right) \tag{3.3}$$

Crushing component is calculated as follows:

$$F_u = 0.5 \cdot \sigma_b \cdot H_{ice}^2 \tag{3.4}$$

$$R_c = F_u \cdot \left(tan(\phi) + \mu \frac{cos(\phi)}{cos(\psi)}\right) \cdot \left(1 - \mu \frac{sin(\phi)}{cos(\psi)}\right)^{-1} \tag{3.5}$$

Breaking by bending component:

$$R_b = 0.003 \cdot \sigma_b \cdot B \cdot \left(\frac{H_{ice}^{1.5}}{\sqrt{m}}\right) \cdot \left(tan(\psi) + \mu \frac{cos(\phi)}{sin(\alpha) \cdot cos(\psi)}\right) \cdot \left(1 + \frac{1}{cos(\psi)}\right) \tag{3.6}$$

Submersion component:

$$R_s = \Delta\rho \cdot g \cdot H_{ice} \cdot B \left[T \frac{B+T}{B+2T} + \mu \left(0.7 L_{wl} - \frac{T}{tan(\phi)} - \frac{B}{4 \cdot tan(\alpha)}\right) + \right.$$

$$\left. + T \cdot cos(\phi) \cdot cos(\psi) \cdot \left(\frac{1}{sin^2(\phi)} + \frac{1}{tan^2(\alpha)}\right)^{0.5}\right] \tag{3.7}$$

Total level ice resistance with a speed-dependent component can be calculated as follows:

$$R_{ice} = (R_c + R_b) \cdot \left(1 + 1.4 \frac{v}{\sqrt{g \cdot h}}\right) + R_s \left(1 + 9.4 \frac{v}{\sqrt{g \cdot L_{wl}}}\right) \tag{3.8}$$

In this equation *v* is the ship speed and the total level ice resistance is the sum with previously presented components. The speed dependency of this formula is too simple, but in this work it cannot influence the result because the speed rate is quite low.

4. Equivalent ice thickness

The idea behind the equivalent ice thickness is to define an equivalent average level ice thickness which gives the same resistance level as encountered by a ship when it navigates in ice conditions with varying amounts of level ice and ridges (Kujala, 1996). As the sea ice field is never homogeneous, then it is better to refer to the ice thickness with one parameter like equivalent ice thickness that contains all the ice forms in some certain area and is given by one simple thickness value like level ice thickness. As well the ice resistance calculation formulas contain mainly a single value to evaluate the ship's performance in full scale.

Methods for evaluating the ice thickness in such a way have been used earlier for Baltic Sea ice but not yet for Antarctic sea ice. The first option is the geometric method, where the main parameters to describe the ice field are level ice thickness H_i, average ridge thickness H_R, and the ice concentration C. This concept is illustrated in Figure 4.1. Ice concentration C is calculated as all the distance d minus the distance of the open water d_{ow}, which is divided by distance d.

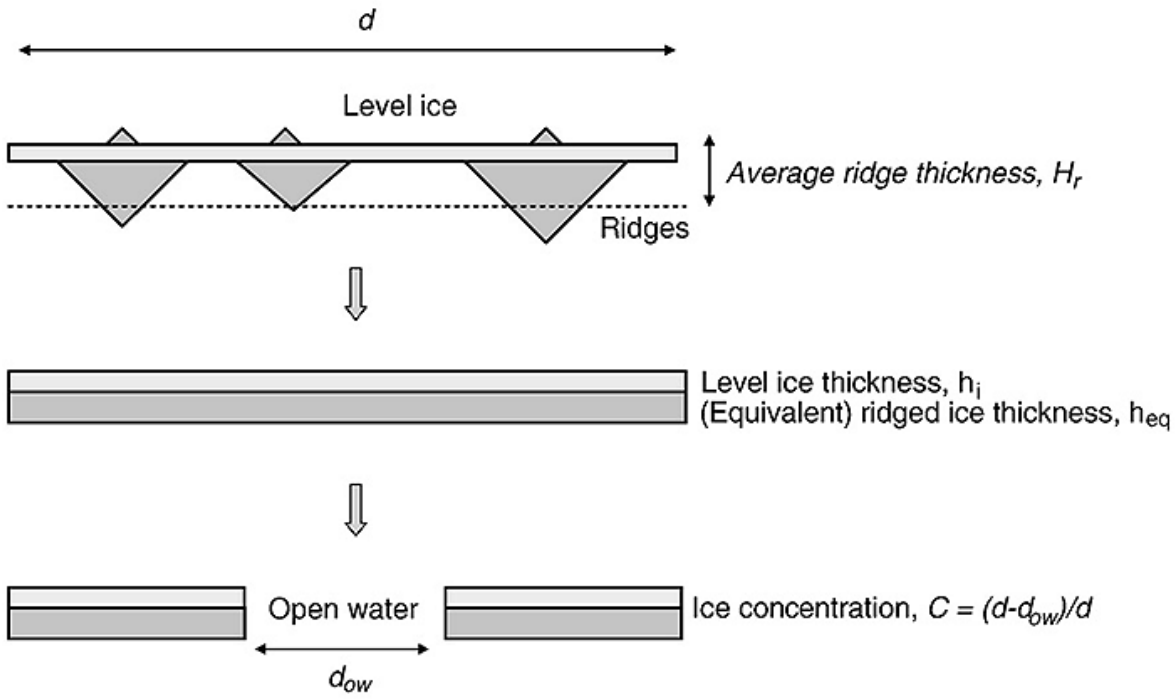

Figure 4.1 Concept of level ice, ridged ice thickness and ice concentration (Ville Kotovirta, 2009)

The ridges are assumed to be of triangular cross section with base angel α. Ridge thickness is H_R and this thickness usually ignores the sail. Ridge density per km is μ. The ridged ice

thickness is calculated as by Riska, where $\frac{1}{tan\alpha} \cdot H_R^2$ component is the ridge cross-section area. The full form is presented in the equation (4.1).

$$H_{eq} = (C - 2 \cdot \frac{1}{tan\alpha} \cdot \mu \cdot H_R) \cdot h_i + \mu \cdot \frac{1}{tan\alpha} \cdot H_R^2 \quad (4.1)$$

Another way is to use Lensu (2003) method, where ridges as ice rubble mass are added to a level ice sheet. Measurements for this method development are taken in the Baltic Sea. Equivalent ice thickness H_{eq} is calculated from level ice thickness H_{level}, ridge sail height h, ridge density μ, and ridge volume factor η = 0.129.

$$H_{eq} = H_{level} + \eta \cdot \mu h^2 \quad (4.2)$$

In this work the calculation model is quite simple. Basically the equivalent thickness is calculated as a geometric in formula (4.1), but here the ridge's porosity is taken into account and snow. The coefficient for ridge porosity p is 0.35 (Tina Tin, 2003). The snow part is applied as a level ice thickness where the snow layer thickness coefficient κ is 1/3 of the level ice thickness equivalent (Riska, 2011). The final form of the equation which is used in the work is presented in formula (4.3)

$$H_{eq} = (h_i + \frac{1}{3} h_s + h_{eq}) \cdot C \quad (4.3)$$

where level ice thickness is h_i, snow thickness is h_s, ridged ice equivalent is h_{eq}, and ice concentration is C. The component of ridged ice equivalent (h_{eq}) looks as follows:

$$h_{eq} = \frac{1}{tan\alpha} \cdot \mu \cdot H_R^2 \cdot C_p \quad (4.4)$$

where C_p is ridge porosity component and is calculated as follows:

$$C_p = 1 - p \quad (4.5)$$

5. Description of measurements

This chapter presents a description of the voyage, vessel, measurement systems, and a pre-analysis of visual observation and selection of measurements. The full-scale measurements were conducted on board *S.A. Agulhas II* in the Antarctic waters during 2013-2014. The measurements were conducted continuously and around the clock. Ice thickness was measured with three different methods. The main facts of this chapter's information are taken from the report (Kujala, et al., 2014).

5.1 Description of the voyage

The ship departed South Africa city Cape Town on November 28, 2013. From there the ship headed to the zero Meridian, along which they headed to Antarctica. On December 7, the ship encountered ice the first time and on December 23, the ship arrived to the Akta Bukta which is close to the Neumayer (the German Antarctic research station). On December 24, the ship navigated to the Pinguin Bukta where the helicopter flights to SANAE were conducted. On December 30, the ship continued towards South Georgia and the South Sandwich Islands for the buoy run, during which the weather buoys are maintained. Arrival took place there January 4, when also the ice ended. After that the ship visited South Georgia and started the whole observation period. The ship was back in ice on January 23 to get through the pack ice to Pinguin Bukta. On January 26, the ship started the voyage to Akta Bukta and arrived there 28 January. The voyage back to departure city Cape Town started on January 31 and the last ice was observed 1 February. The ice conditions change during the voyage can be seen on Figure 5.1.

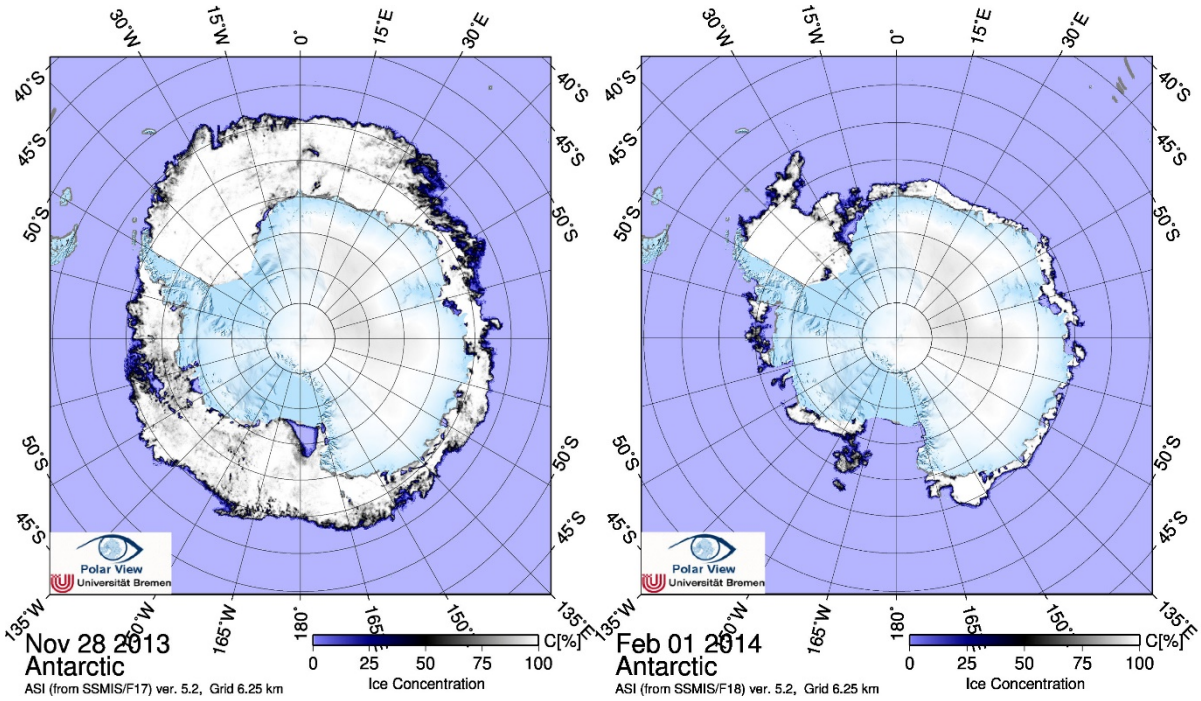

Figure 5.1 Concentration map from the beginning and end of the voyage

5.2 Instrumentation and description of the vessel

The *S.A. Agulhas II* is the polar supply and research vessel built in the year 2012. The vessel was built to polar ice class PC 5 and the strength of the hull in accordance with Det Norske Veritas (DNV) ICE-10 class rules. Furthermore, it is the first polar research vessel with a passenger vessel certificate. The main dimensions of the ship are presented in Table 5.1.

Table 5.1 The main dimensions of the ship

Length, bpp. [m]	121.8
Breadth, mould. [m]	21.7
Draught, design [m]	7.65
Deadweight at design displacement [t]	5000
Service speed [kn]	14.0

Brief description of thrust measurement system. Propeller-generated thrust was measured on the port side shaft line by strain gauges in a Wheatstone bridge configuration (Bekker, et al., 2014). The gauges were mounted parallel with the centerline of the shaft, and the location was just behind a thrust bearing where thrust force is transferred to the hull. The calculated thrust measurement frequency was 500 Hz using the Manner Telemetry System (Bekker, et al., 2014). The measurement frequency is very high for use directly in this work. Therefore,

the data is reshaped so that it represents the one-second average thrust, which is better to use and accurate for calculated ship ice resistance comparisons in future work. As the thrust is measured only from one shaft line then the total thrust is obtained by multiplying the measured thrust with two.

5.3 Ice thickness measurements

Ship ice resistance calculation methods have gone through a long development that has helped to evolve a methodology for measuring the thickness of the ice in order to get more accurate results with less effort. This subsection presents the ship-borne measurement methods in probable development order.

5.3.1 Visual observations

Visual observations are made using a measurement stick that is fixed to the vessel side on the level of deck 3.5 (see Figure 5.2). Measurement stick units are tenths (10 cm) and these are marked per tenths by alternating black and white markings.

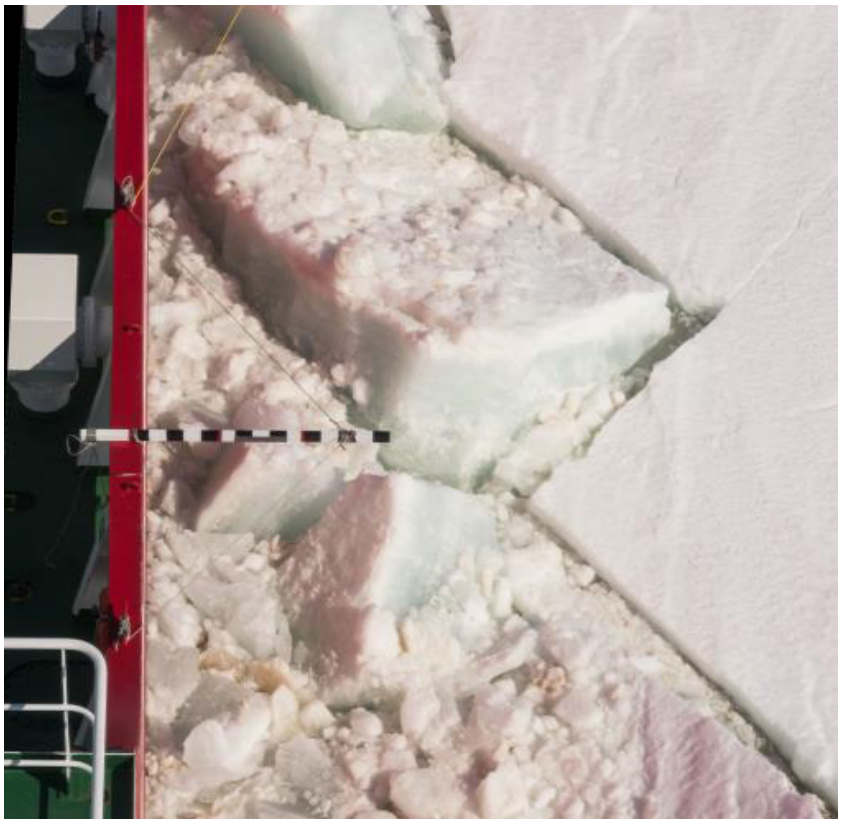

Figure 5.2 Measurement stick (Kujala, 2013)

The observer performs visual observations at the bridge, where the eye level is at deck 9.5. The viewer evaluates the turned ice thickness with measurement stick units and marks them down in ten-minute periods to form the occurrence percentages in tenths. Other comments like snow min/max thickness, vibration, ramming, ice concentration, ice flow size and general comments are also noted for each ten-minute period. An example of ice concentration and ice thickness observations can be seen on Figure 5.3.

Ice concentration in tenths												Ice thickness [cm] in tenths												
open wate	0-10	10-20	20-30	30-40	40-50	50-60	60-70	70-80	80-90	90-100	sum	0-20	20-40	40-60	60-80	80-100	100-120	120-140	140-160	160-180	180-200	200-250	250-300	300+	sum
						2			8		10			1.0	5.0	2.0	2.0							10
									10		10				2.0	2.0	2.0		4.0						10
								3	7		10			2.0	6.0	2.0									10
3	1		2	2	2						10		2.0	5.0	3.0										10
						2		4	4		10		1.0	6.0	3.0										10
				2				3	5		10		.8	1.6	3.5	2.5	1.6								10
2	2							4	2		10		1.2	2.2	2.8	2.3	1.6								10
				2				3	5		10		1.2	1.1	2.1	2.5	2.2	.0		.5	.4	.2			10
							3	2	5		10			.2	2.1	1.6	1.4	1.4	.3			3.0			10
								2	8		10					1.4	2.4	3.5	.8	.5	1.4	.2			10

Figure 5.3 Example of visual observations table

Accuracy of the measurements cannot be very high because the instrument location is far from the observer and observations done by various people during the voyage; additionally, in low light conditions it is difficult to identify the ice edge and read the measurement stick reading. Furthermore, this method is selective and random because when the thickest ice does not turn, thinner ice is measured. In general, the measurements give a good overview of ice conditions and are a good starting point for measurement analysis because the results are instantly legible.

5.3.2 Electromagnetic system

The electromagnetic induction sounding (EM) system is a portable set of sensors that is hung overboard from the fore ship. Figure 5.4 shows the actual installation on *S.A. Agulhas II*.

Figure 5.4 Installation of the EM system (Kujala, 2013)

The principle by which the EM sensor measures the total ice thickness is shown in Figure 5.5. The system consists of a Geonics EM-31 electromagnetic inductive sensor to measure the distance Z_E from the sensor to the bottom of sea ice, which is actually the surface of the sea water. The EM measurement frequency was mainly 20 Hz and the readings were averaged to form one thickness for one meter of the track.

The EM sensor has a transmitter coil (T_x) and a receiver coil (R_x) at each end. A primary magnetic field generated by T_x penetrates snow and ice, and induces an eddy current near the sea water surface. This is due to the high contrast in conductivity between resistive sea ice and conductive sea water. A secondary magnetic field caused by the eddy current is detected by R_x. The ratio of intensities between the primary and secondary EM field is approximately related to the apparent conductivity. A laser distance sensor (Noptel) detects the distance from the sensor to the surface of ice or snow, Z_L. Total thickness: $Z_I = Z_E - Z_L$ (Shotaro Uto, 2006).

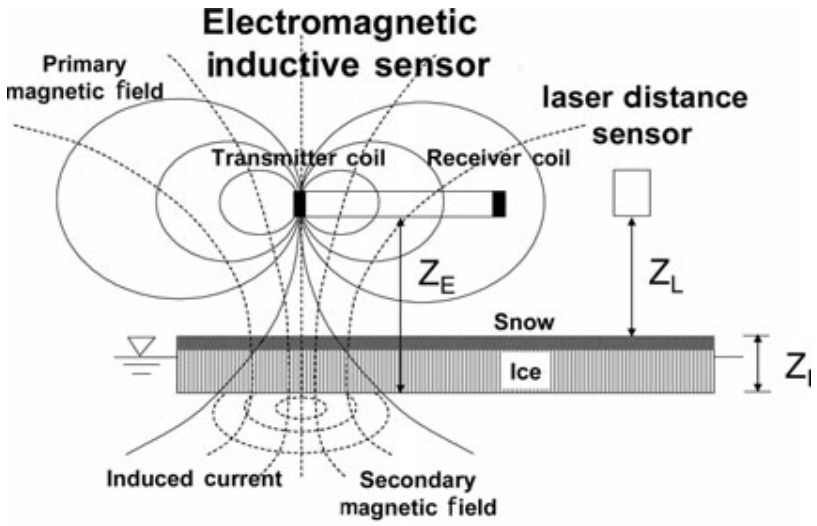

Figure 5.5 Principle of EM observation of total thickness of sea ice (Shotaro Uto, 2006)

5.3.3 Stereo camera system

The stereo camera system is composed of two identical cameras that are fixed to the pipeline, a measurement computer with camera controlling software, and set of hard drives for stereo images. A picture of the *S.A. Agulhas II* stereo cameras can be seen in Figure 5.6.

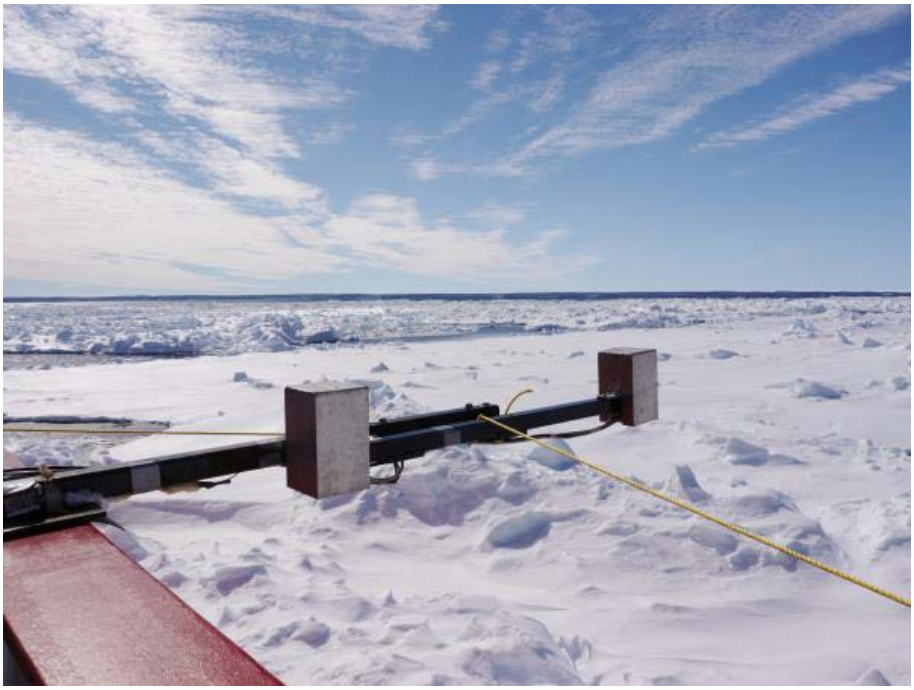

Figure 5.6 Picture of installed stereo cameras (Kujala, 2013)

The system is self-acting until the hard drives are full of stereo images or a hardware/software error occurs. The camera frame rate was 2 – 3 frames per second (FPS) during the last voyage, which is sufficient to get images of turned ice for performing later measurements on a computer screen using the special MATLAB semi-automatic measurements code. Actually, this means that for each hour up to 10,000 stereo images are taken, but as the system does not choose when to record, the quantity of useless images is high. Moreover the original images are in RAW files and data load for hard dives is large.

Figure 5.7 Stereo camera image (Kujala, 2013)

The stereo camera system's ability currently lies in only taking stereo images of ice, but during development it will be possible to run automatic ice measurements in some way. One sample image is presented in Figure 5.7, which is a good turned ice block where both ice edges are clear enough to take a thickness measurement with the perpendicular method. The user defines the edges of the turned ice block with the aid of the computer code and the ice thickness is the shortest distance between the edges. In addition, snow thicknesses were measured in images where the edges between ice and snow were visible and snow thickness was more than some centimeters.

Another option was to use a triangle method for when the ice block is at an angle and direct edge-to-edge result is not true. The triangle idea is firstly to select an ice block surface by three points and to allow software to define a plane (see Figure 5.8), where the yellow lines represent the planes and the red line the ice thickness measurement between the planes. The

second step is to select other plane edge and then let software calculate ice thickness between the planes.

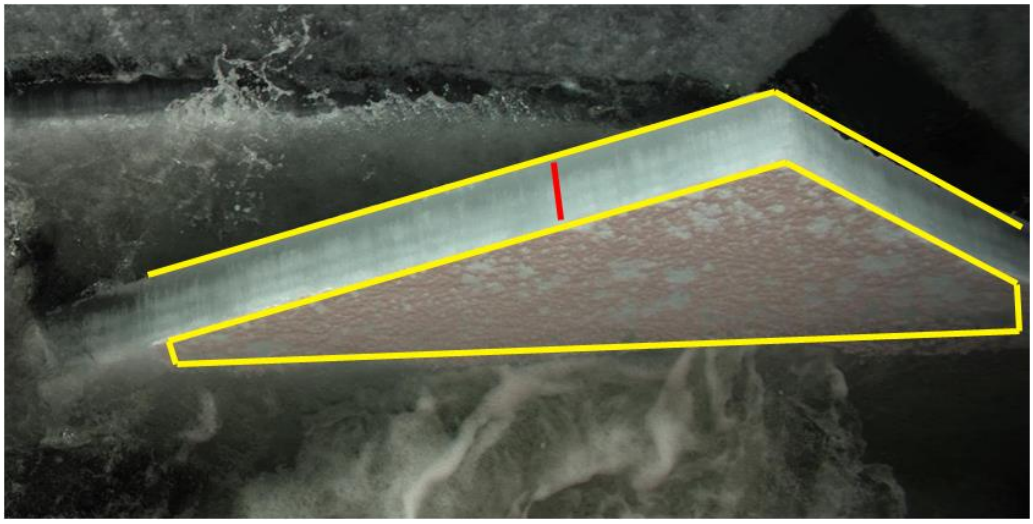

Figure 5.8 Ice block at an angle (Kujala, 2013)

6. Case study

This chapter's aim is to go through the Case 1 as an example and explain how the measurements results are processed in three methods for all the selected cases. As all processing work with the cases was similar at this step, then the rest of them will not be repeated here. Furthermore, each sub-chapter results are in a slightly different form, but the final statistical parameters are in the same form. The last part is a comparison of all the ice thickness distributions for Case 1 and summary table of all the cases.

6.1 Measurements selection

During the research vessel voyage the visual observations were made and noted via the MS Excel table. The analysis during the work has shown that the effective way is starting with these measurement results pre-analysis, because the table gives a good overview of ice conditions and data is readable directly, variously the stereo camera or the EM measurements.

The pre-analyses were made to identify good measurement hours. Criteria for this purpose are no ramming's during the hour, high ice concentration, and ice thickness occurs more in higher thickness ranges.

The results of pre-analysis are ten selected hours that are suitable for future investigation. The ten hours of data were selected so that they cover all the previously defined measurements methods as well. The complete table of the ten-hour visual observations is presented in Appendix 1. For comparison of the measurement results the ten different hours of data were used. The selected time periods are presented in Table 6.1, where two cases are from the end of 2013 and six from beginning of 2014.

Table 6.1 Selected cases for analysis

Case 1	2013-12-09 11:00 – 12:00
Case 2	2013-12-09 12:00 – 13:00
Case 3	2014-01-23 21:00 – 22:00
Case 4	2014-01-23 22:00 – 23:00
Case 5	2014-01-24 02:00 – 03:00
Case 6	2014-01-24 04:00 – 05:00
Case 7	2014-01-27 04:00 – 05:00
Case 8	2014-01-31 21:00 – 22:00
Case 9	2014-02-01 04:00 – 05:00
Case 10	2014-02-01 08:00 – 09:00

A general description of ice conditions during the selected cases based on visual observations. The vessel was operating during the cases quite smoothly, and there was no need for ramming. The ice concentration was about 80-90%, which means that most of the time the vessel was operating in very close ice without open water. The ice thickness generally was around 1 meter and the entire range was about 0.5 to 2 meters, which is quite a high range, but they can be regarded as extremes. The first two cases do not contain information about snow thickness but eight later periods have notes of snow; the snow thickness range was 0.1 to 0.6 meters. Ice floe size was decreasing in time due to the Antarctic summer season lasting from December to February.

6.2 Visual observations

Visual observation ice thickness divisions are presented in tenths of ice thickness, in interval of 10 minutes each, which makes six short periods for one selected case. Table 6.2 shows Case 1 measurement divisions where each row is the short period division for thicknesses and the sum must be 10.

Table 6.2 Visual observation ice thickness for Case 1

Ice thickness [cm] in tenths													
0-	**20-**	**40-**	**60-**	**80-**	**100-**	**120-**	**140-**	**160-**	**180-**	**200**	**250**	**300+**	**sum**
20	**40**	**60**	**80**	**100**	**120**	**140**	**160**	**180**	**200**	**250**	**300**		
		2.0	4.0	3.0	1.0								10
		2.0	3.0	2.0	1.0	1.0	1.0						10
			4.0	5.0	1.0								10
		2.0	2.0	5.0	1.0								10
		1.0	2.0	2.0	3.0		1.0		1.0				10
			2.0	5.0	2.0	1.0							10

The thicknesses there are as occurrence percentages for given classes and the mean thickness is calculated from the observations as a weighted average. For further analysis the tenths were converted to probabilities and summed together for one-hour probability distribution. The next step was to find the mean and standard deviation for Table 6.2 values by manual calculations. The results can be seen in Table 6.3, where *bin* is the ice thickness class or range, *div* is division of the sum of measurements, where one thickness class values are joined and divided by quantity, and mean is the sum of *bin* time's *div*. The empty rows there show that in this thickness class the occurrence was zero and there were no measurements.

An example for clarity, thickness column 40-60 cm in Table 6.2 is used for the *div* value, the *bin* 0.4 m in Table 6.3 is calculated as follows:

$$div = \frac{0.20+0.20+0+0.20+0.10+0}{6} = 0.117 \tag{6.1}$$

The mean thickness was calculated as follows:

$$Mean = SUM(bin * div) = SUM(0.047 + 0.170 + 0.293 +$$

$$+0.150 + 0.040 + 0.047 + 0.030 = 0.777 \tag{6.2}$$

$$Variance = \frac{SUM[(Mean-div)^2]}{7} = \frac{1.837}{7} \tag{6.3}$$

Standard deviation $\sigma = \sqrt{Variance} = \sqrt{0.262} = 0.512$ (6.4)

Table 6.3 Mean and Standard deviation for Case 1

bin [m]	div	bin* div	mean-div	(mean-div)^2
0.2				
0.4	0.117	0.047	0.377	0.142
0.6	0.283	0.170	0.177	0.031
0.8	0.367	0.293	-0.023	0.001
1	0.150	0.150	-0.223	0.050
1.2	0.033	0.040	-0.423	0.179
1.4	0.033	0.047	-0.623	0.388
1.6				
1.8	0.017	0.030	-1.023	1.047
2				
2.5				
	Mean	0.777	**Sum**	1.837
	Variance	0.262		
	σ	0.512		

As can be seen from the table, the mean ice thickness is 0.777 m and the standard deviation σ is 0.512 m for Case 1 measurements.

6.3 Stereo camera measurements

Stereo images were processed by the hour for all the cases. All measurements for each case were collected together from all the processed images by script and recorded in a text file with ice thickness, snow thickness (if measured), or none and timestamps for each measurement. The thicknesses are in millimeters and timestamps are in seconds. One row in the results file equals one sample. Furthermore, only this method gives reasonable information about snow thickness, although visual observations contain min/max values of snow thickness. A summary of Case 1 results can be seen in Figure 6.1, where 101 measurements of ice and 51 measurements of snow were plotted.

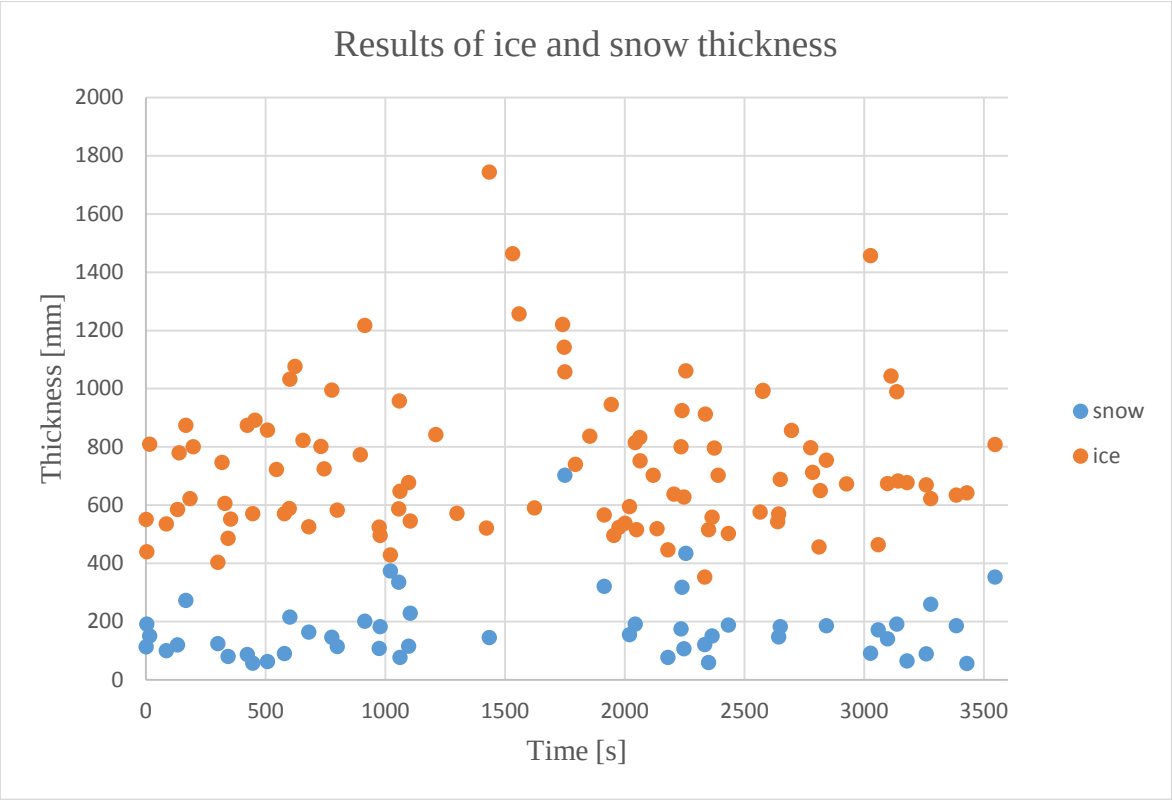

Figure 6.1 Stereo camera results of Case 1

The statistical parameters for ice thickness were calculated by the MATLAB distribution tool, where the data is processed into the same classes as visual observations, where the classes are in increments of 0.20 m. Mean ice thickness is 0.738 m and standard deviation 0.244 m for Case 1. Probabilities for each ice thickness class were saved for future steps. Furthermore, the SC method was the main opportunity to measure snow thickness. For Case 1 the mean snow thickness is 0.176 m and standard deviation is 0.116 m.

6.4 The EM measurements

The processed data from EM measurements is obtained from the Finnish Meteorological Institute (FMI). The data is in simple text files where one row thickness value conforms to a one-meter track including the timestamp, GPS coordinates, and speed.

First, for a prime overview of the thickness values, these were plotted with timestamps and presented in Figure 6.2 with smooth lines due to dense data.

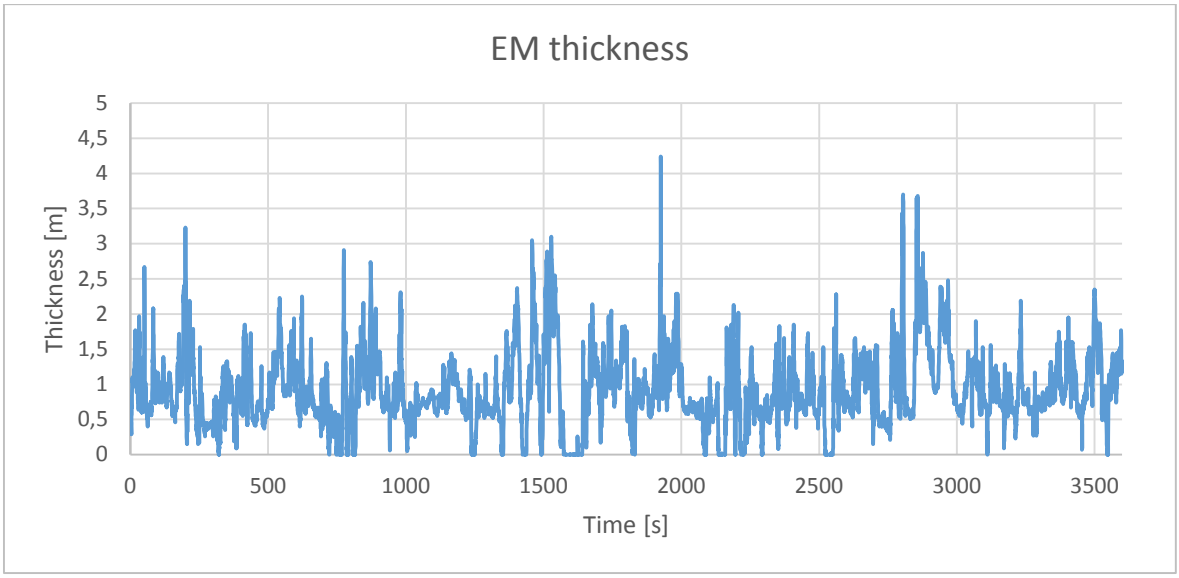

Figure 6.2 EM thicknesses of Case 1

Based on the Figure 6.2 view, it is hard to see what the actual EM thickness will be. It requires further investigation.

The data were processed using a distribution tool because of the over 10,000 values for each case, and integrated tool capabilities and performance is good for statistical calculations. Firstly ice thickness classes as for visual observations and exclusion rules were set to exclude the unreliable measurements from normal distribution. The lower limit excluded data that is less than or equal to 0.09 m. The upper limit excludes data that is greater than or equal to 3 m. The upper limit is derived from borehole real measurements, which results in that over 3 m it will be unreliable. The lower limit value is only selected so that it excludes nearly zero values (water surface). The sampling rate with this method is the highest compared with Visual and SC, and therefore, on Figure 6.2 the thicknesses are plotted by a smooth line.

The statistical parameters for Case 1 from the distribution tool are as follows: the mean thickness is 0.927 m and standard deviation is 0.444 m. The probabilities for each ice thickness class were saved for future steps.

6.5 Conclusion of the three method's results

In Table 6.4 are presented the mean thickness values and standard deviations for normal distributions. Based on these results we can say that the results match quite well and differences are in a reasonable range to use them in further investigation. The EM total thickness also contains the snow, and therefore, it shows a bit higher trend compared with

the other two. But in future steps it can be subtracted using the SC measurements of snow thicknesses.

Table 6.4 Case 1 to 10 statistical parameters

	EM method		**Stereo camera**		**Stereo camera**		**Visual observation**	
	total thickness [m]		snow thickness [m]		ice thickness [m]		ice thickness [m]	
	mean	σ	mean	σ	mean	σ	mean	σ
Case 1	0.927	0.444	0.176	0.116	0.738	0.244	0.777	0.512
Case 2	0.788	0.371	0.161	0.086	0.736	0.218	1.150	0.577
Case 3	0.982	0.512	0.199	0.111	0.909	0.287	0.803	0.400
Case 4	0.868	0.506	0.161	0.063	0.862	0.237	0.540	0.227
Case 5	0.962	0.543	0.194	0.079	0.869	0.296	0.963	0.556
Case 6	1.042	0.634	0.225	0.187	0.988	0.319	1.284	0.523
Case 7	1.265	0.660	0.281	0.125	1.014	0.371	1.319	0.530
Case 8	1.032	0.625	0.396	0.433	0.880	0.349	0.843	0.373
Case 9	0.995	0.592	0.159	0.058	0.942	0.343	1.081	0.530
Case 10	0.881	0.468	0.157	0.110	0.823	0.286	0.702	0.412

The previous three methods provide clarity that the reasonable way to compare these results is probability step curves. The reason for such 0.2 m step curves were the visual observation ice thickness classes, and therefore, the EM and the SC results are also distributed in the same bin rules to make them comparable (see Figure 6.3). From this is seen that the SC and the visual observations match quite well but the curves are about 0.4 m offset relative to each other in thickness axis. Of this can be concluded that the visual observations overestimate the ice thickness measurements, and comparing the EM curve with the previous two the EM distribution is smoother and each ice thickness class includes measurements. Likewise the EM first thickness class contains too many results, which does not make sense for ice thickness because this part can be open water and is taken into account by concentration. The other nine case's probability curves are presented in Appendix 2.

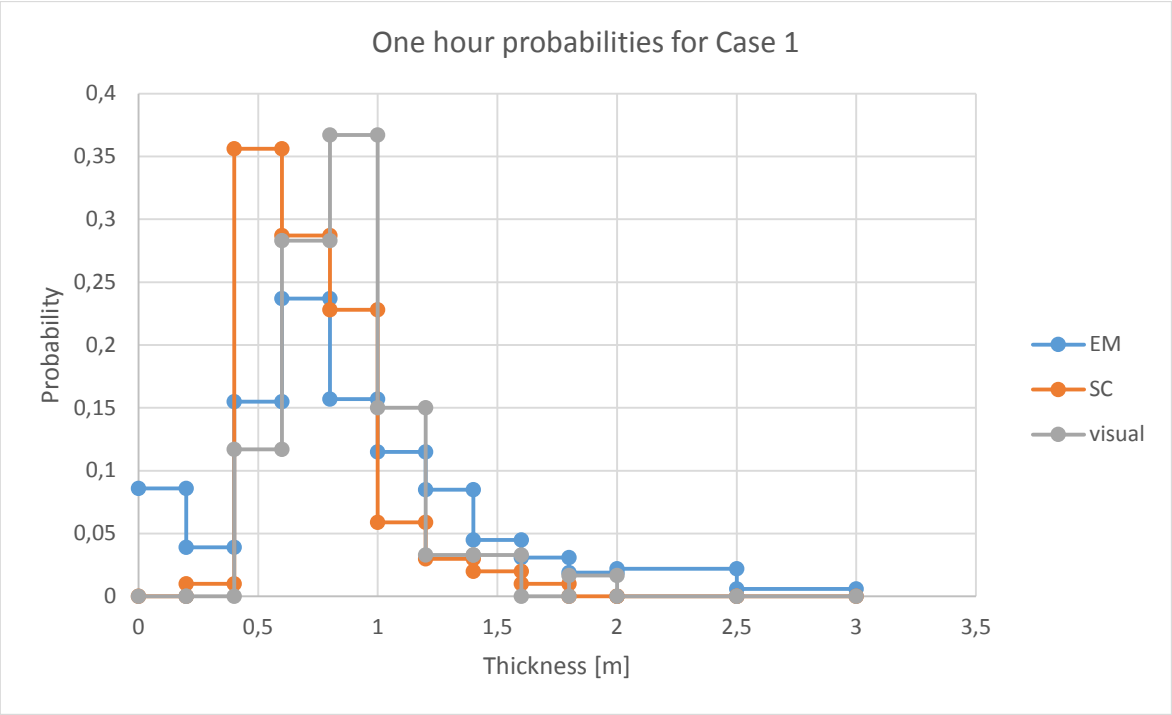

Figure 6.3 Thickness probabilities for Case 1

7. Application for equivalent ice thickness

The idea of this chapter is to define the equivalent ice thickness calculations without the ridges part as the first step in saving work load for ice surface profile analysis; the snow thickness part is also excluded to make the first estimation simpler, and ridges and snow are applied for suitable cases.

7.1 Measurement results based on ship navigation parameters

As the ice conditions affect the ship's actual speed and thrust quite heavily, and this data is available, it is used to get an outline of the ship's operation during Case 1. The thrust and speed ratio is plotted over time and presented in Figure 7.1, which illustrates that the variation ratio of thrust and speed is about two times during the one-hour period. As the variation is high it can be concluded that the ice conditions varied significantly, and shorter periods should be used to get a more accurate estimation of measured thrust and calculated ship resistance in ice.

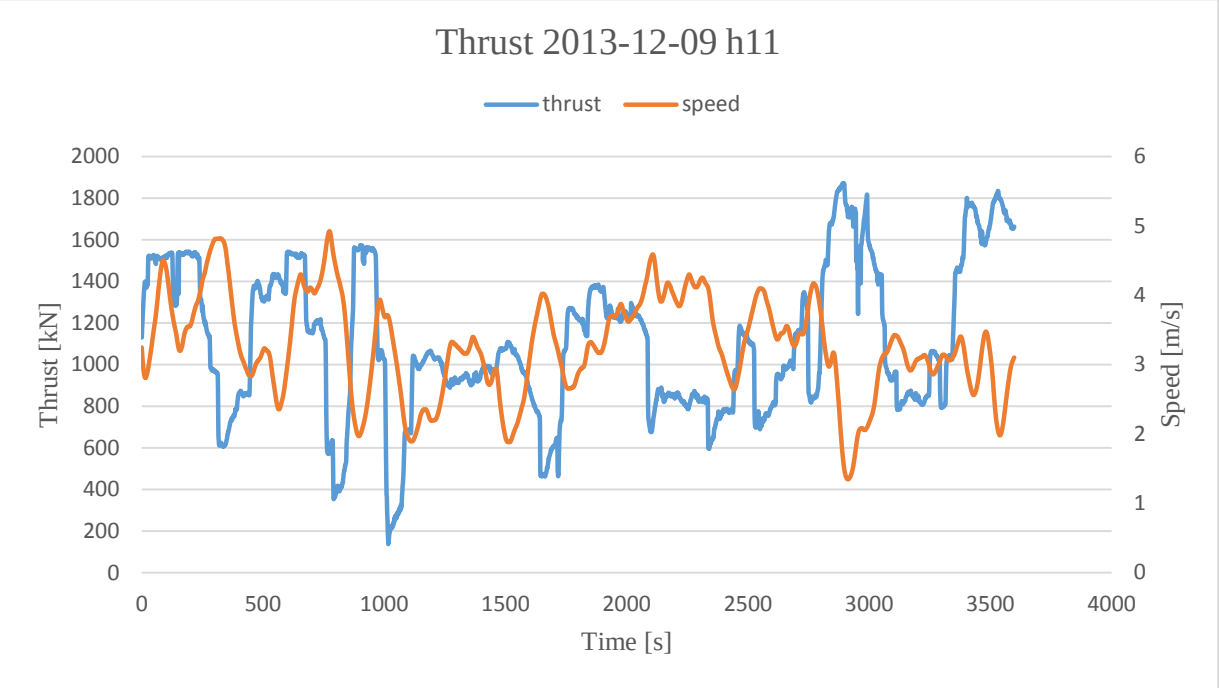

Figure 7.1 Thrust and speed ratio

Based on Figure 7.1, the finer selections have been made and plotted in Figure 7.2, which shows quite smooth navigation during 1750 – 2100 seconds, from which it can be concluded that the ice conditions are fairly smooth. According to this period, new ice measurements

were taken from one-hour data and new mean and standard deviations were calculated. Residual figures for thrust and speed ratio for one hour and short periods are provided in Appendix 3.

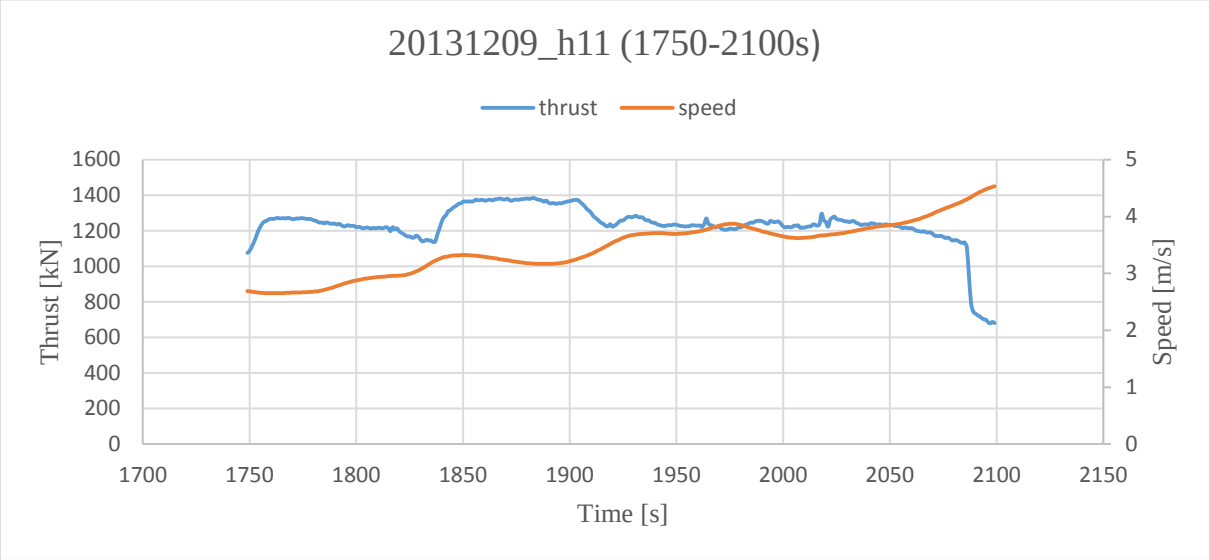

Figure 7.2 Thrust and speed ratio for a short period

Mean and standard deviation for short period ice thicknesses are presented in Table 7.1 and compared with one-hour period values in Table 6.4, the thickness differences are small. However, navigation speed is smoother with a lower standard deviation that enables closer ice resistance calculations in the next chapter.

Table 7.1 Case 1 to 10 short-period values with statistical parameters

	EM method		**Stereo camera**		**Visual observ.**		**Stereo camera**		**Navigation**	
	total thickness[m]		ice thickness[m]		ice thickness[m]		snow thickness[m]		speed [m/s]	
	mean	σ	mean	σ	mean	σ	mean	σ	mean	σ
C 1	0.931	0.434	0.753	0.231	0.700	0.169	0.186	0.116	3.40	0.46
C 2	0.790	0.316	0.738	0.257	1.258	0.289	0.167	0.086	4.36	0.44
C 3	1.181	0.522	1.119	0.233	0.680	0.224	0.207	0.111	2.50	0.24
C 4	0.883	0.344	0.842	0.183	0.660	0.174	0.150	0.063	3.11	0.29
C 5	0.841	0.510	0.865	0.297	1.054	0.404	0.206	0.079	3.36	0.19
C 6	0.975	0.647	0.841	0.255	1.145	0.519	0.237	0.187	4.69	0.75
C 7	1.404	0.627	0.918	0.352	1.473	0.407	0.227	0.125	2.31	0.58
C 8	1.156	0.654	0.838	0.266	1.000	0.432	0.371	0.433	3.35	0.25
C 9	0.979	0.489	0.955	0.226	1.066	0.534	0.179	0.058	4.02	0.29
C10	1.154	0.501	1.062	0.289	0.659	0.289	0.244	0.110	3.57	0.29

In addition to the ice thicknesses, the complete view of snow thicknesses is presented in Table 7.2 where the results of two periods are a one-hour period and a short period, but for the short period the standard deviation has not been calculated due to the limited data and the one-hour standard deviation should be used if needed. These results are also taken into account in resistance calculations in future steps and subtracted from the EM total thicknesses to get a more reasonable ice thickness from the EM measurements.

Table 7.2 Snow thicknesses from SC measurements

	Snow thickness [m]		
	one hour		short period
	mean	σ	mean
Case 1	0.176	0.116	0.186
Case 2	0.161	0.086	0.167
Case 3	0.199	0.111	0.207
Case 4	0.161	0.063	0.150
Case 5	0.194	0.079	0.206
Case 6	0.225	0.187	0.237
Case 7	0.281	0.125	0.227
Case 8	0.396	0.433	0.371
Case 9	0.159	0.058	0.179
Case 10	0.157	0.110	0.244

Ice concentrations for short periods are taken from visual observations and recalculated to percentages. The numerical values can be seen in Table 7.3. These values are used as coefficients for equivalent ice thicknesses in calculations.

Table 7.3 Ice concentration

Ice concentration [%]	
	short period
Case 1	87
Case 2	81
Case 3	88
Case 4	76
Case 5	77
Case 6	78
Case 7	86
Case 8	82
Case 9	80
Case 10	80

The ice resistance is calculated as described in Chapter 3 where the Lindqvist method is presented and input parameters are taken from Tables 2.3 (Kujala values), 7.1, 7.2 and 7.3. The calculated resistances can be seen in Table 7.4, where resistance values are presented for the mean, mean + σ, and mean – σ ice thicknesses. The calculation procedure is shown in Appendix 4.

Table 7.4 Calculated resistance of ice compared with actual thrust

	Resistance of ice [kN]									Thrust [kN]
	EM			SC			Visual			
nr	mean	mean+σ	mean-σ	mean	mean+σ	mean-σ	mean	mean+σ	mean-σ	mean
1	947	1538	383	958	1270	654	888	1114	666	1234
2	833	1278	401	993	1358	637	1741	2170	1321	1577
3	1104	1746	495	1279	1566	999	756	1020	499	507
4	774	1159	402	895	1100	693	694	886	506	514
5	702	1302	133	969	1322	625	1193	1683	719	417
6	995	1931	117	1141	1507	783	1578	2348	839	966
7	1275	2021	573	980	1383	590	1622	2114	1148	918
8	934	1773	1483	1000	1337	671	1204	1764	666	419
9	1020	1686	384	1228	1537	926	1379	2124	667	528
10	1097	1745	478	1291	1666	924	783	1145	431	568

Based on Table 7.4 results the actual thrust and the calculated resistance indicate a great difference between them, and therefore, suitable cases are selected for further analysis. The selection of results has been made taking into account the actual thrust magnitude; higher values look more suitable for equivalent ice thickness investigation because they are more close to the calculated resistances. The selection of four cases is Case 1, Case 2, Case 6, and Case 7, which are highlighted in gray in Table 7.4. The remaining six cases are excluded from further analysis while the actual thrust is about half the size of the calculated resistances.

7.2 More detailed analysis with the four selected cases

The aim was to estimate a more accurate equivalent ice thickness, applying the ridges and snow part to the four cases. The first step was to do the primary review of one-hour probabilities, which are presented in Appendix 2. Case 2 one-hour probabilities show a similarity between EM and SC measurements. Visual observations distribution offset is

about 0.6 m to the thicker side. Thickness probabilities for cases 6 and 7 show similarity. However, both EM distributions are quite flat and the biggest thickness trend for them is somewhere between 0.6-1.0 m. The Visual and SC distributions for cases 6 and 7 are similar but the visual observation distributions show a thicker trend. In general, it is typical for all the cases and it can be concluded that visual observations overestimate the ice thickness.

The second step is to analyze the EM measurements surface profile to identify reasonable ridges (Haas, 1998). In the selected four cases ridge identification was manual work on surface profile figures. Traveled distance for each case was different. All reasonable ridges are tagged by a red circle on the figures, see Appendix 5. Ridge heights are measured directly from the end of the average ice thickness edge, which means that ridge height is the residual part above the ice thickness average line. Average ice thickness is taken from EM measurements, which is EM measurement minus SC snow thickness. The figures are presented in Appendix 5. The obtained results are in Table 7.5.

Table 7.5 Results of ridges

Case	distance	EM average ice thickness	Average ridge h	Ridge count
nr	[m]	[m]	[m]	[piece]
1	1177	0.745	0.805	10
2	2331	0.623	0.684	8
6	2247	0.738	1.572	13
7	1419	1.177	1.414	13

Based on Table 7.3 Ice concentration and Table 7.5 Results of ridges, the equivalent ice values can be seen in Table 7.6, where the equivalent ice thickness is calculates as in the equation (4.3) with added snow and ridges porosity, and calculated resistance with the Lindqvist method in comparison with the ship actual thrust. The calculation procedures can be seen in Appendix 6.

Table 7.6 Calculated resistance with EM equivalent ice thickness vs. actual thrust

Case	Equivalent ice thickness	Calculated resistance	Actual thrust
nr	[m]	[kN]	[kN]
1	0.714	1049	1234
2	0.552	914	1577
6	0.653	1135	966
7	1.099	1392	918

Based on Table 7.6 results, the Case 1 outcome is the best, where the calculated resistance is about 15% smaller. For Case 2, calculated resistance is about 42% smaller. For Case 6 and 7, calculated resistances are correspondingly about 17%, which is good, and 52% bigger which is surely not a sufficient outcome.

Another way is to change the EM average to the SC average ice thickness and repeat the same procedure as for the Table 7.6. The results can be seen in Table 7.7, where the final results are a bit closer to the actual thrust.

Table 7.7 Calculated resistances with SC equivalent ice thickness vs. actual thrust

Case	Equivalent ice thickness	Calculated resistance	Actual thrust
nr	[m]	[kN]	[kN]
1	0.727	1069	1234
2	0.645	1075	1577
6	0.733	1282	966
7	0.877	1095	918

Case 1 variance is 13% of actual thrust. Case 2 variance is 31%. Case 6 variance increases to 33% and Case 7 variance decreases to 19%, which is in quite a good range. In summary, Table 7.7 with SC average ice thicknesses is more close to the actual thrusts, considering that the calculations were made with Lindqvist method and a modified equivalent ice thickness formula with snow layer and ridge porosity factor.

8. Discussion

As far as the author knows, the equivalent ice thickness for evaluating ship resistance in Antarctic sea ice with real measurement data has not been developed before. Therefore the sea ice was analyzed and evaluated as the level ice equivalent.

In the present work a large number of measurement results are investigated. Ice thicknesses were measured by three methods. These three method's results were quite similar, but the standard deviation of the measurements was the smallest for stereo camera measurements. This can be explained by the fact that the other two methods were rather indirect and the results cannot be verified later. As the influence of snow is relatively large in Antarctica, the snow part has been taken into account in the calculations of the equivalent ice thickness. However, the way it was applied is not validated enough, and considering snow as a thin additional ice layer introduces some uncertainty.

The data that was investigated consists of ten one-hour measurements periods. It became clear that all the periods were not suitable for further work and six periods were excluded from the list. The residual four cases were used in the final findings to evaluate the ship's resistance through calculations and compare it with actual thrust.

Ice mechanical properties are taken from in situ measurements, and in the current work the mean value of flexural strength was used. However, the ice is natural material and its properties can change very quickly, and during the selected cases it is assumed to be the same as the mean value from random measurement locations. Comparing the measured flexural strength mean with the Antarctic statistical value, it was more than two times lower and it should be considered critically. In comparison with the statistical values given by Schwarz the calculated resistance decrease about 200 kN, which is primarily caused by the ice density increase. The exact values are given in the following Table 8.1.

Table 8.1 Mechanical properties affect to the resistance

Case	SC equivalent	Calculated resistance	Actual thrust	Calculated resistance by Schwarz
nr	[m]	[kN]	[kN]	[kN]
1	0.727	1069	1234	875
2	0.645	1075	1577	878
6	0.733	1282	966	1060
7	0.877	1095	918	903

During the work, it was found that the Antarctic sea ice equivalent ice thickness resistance with the Lindqvist method was quite close to the measured actual thrust of the ship, even though the Lindqvist method has been developed for the Baltic region. The equivalent ice thickness formula used in the present work was only modified by ridge porosity. The ridge porosity coefficient affected the equivalent ice thickness a few millimeters while the average high of ridges was low, but in a situation where they are high the influence increase. The snow part was applied by coefficient, which was commonly set. However, the ice surface profile data was investigated, where the ridges were counted and measured from ice profile directly, but to identify reasonable ridges and their heights was difficult because the EM data was noisy and it did not give an accurate picture of the ridges. When the equivalent ice thickness is calculated with ridges, modified by porosity, and the snow part is applied then the calculated resistance increases in the range of 81 to 141 kN for the four selected cases. It is about 10 percent of the only level ice resistance.

An unexpected finding was the flow size diameter effect for the vessel's actual performance, which will significantly influence the actual thrust. It is not clear exactly from which diameter the ice flow can be taken as level ice. That means that, if the ship is operating in small-flow-size ice, then it produces less resistance, because the icebreaking process is not complete while the ship pushes ice banks aside, which are much lighter compared with totally closed level ice, and wanted speed obtained with less thrust. The variation of flow sizes for ten cases can be seen in Table 8.2. The previously selected four cases: 1, 2, 6, and 7 reflect that flow size affects the thrust, although Case 7 shows that it does not match with Case 9, where flow size distribution is in a higher class but thrust is lower. This is not conclusively studied in this work because it needs more analysis than these short ten cases, and they might not be sufficient for a more accurate conclusion. Likewise, the flow size is marked down only visually and not validated with another method like the ice thicknesses measurements were. However, the flow size effect in the final finding should be minimal because during these short periods the ship was operating at high power and notes of flow size showed a greater trend.

Table 8.2 Flow sizes from visual observations

Case	Thrust [kN]	Flow [m] < 20	20 100	100 500	500 2000	2000 5000	5000+ Level ice	Sum
1	**1234**	**3**	**2**	**1**	**3**	**1**		**10**
2	**1577**	**1**	**3**	**2**	**4**			**10**
3	507	4	4	2				10
4	514	2	5	3				10
5	417	2	6	2				10
6	**966**		**4**	**6**				**10**
7	**918**	**4**	**6**					**10**
8	419	5	5					10
9	528	1	9					10
10	568	10						10

Finally, in the selected four cases the calculated resistance with the stereo camera measurements fell the most in total compared with the ship's actual thrust, where the variances were 13-33%. The accuracy of this is influenced by ice mechanical properties, which was measured by a relatively small comparison with ice or snow measurements. Likewise the ship's actual thrust measurement system cannot be taken as absolutely accurate, where the thrust is obtained from one shaft line and multiplied by two.

9. Conclusion

The focus of this thesis was on the Antarctic ice conditions analysis and evaluation of ship resistance in these ice conditions. Measurements results are analyzed and presented. They were divided into ice data and ship performance data. The ship actual thrust, ice conditions, measurement methods and calculated ice resistance is studied.

The analyzed results show that ship actual thrust is similar with calculated ice resistances, however there were also variations which is reasonable because ice is natural material and ice conditions are not as smooth as we might expect.

The final results of the calculated equivalent ice thickness resistance compared with actual thrust differed up to 33 %, depending on the case. This result can be considered as good because simplifications have been made and mean values were used.

The comparison of ice thickness measurements with three methods gave quite similar results, although visual observations probability curves were shifted into thicker side. The probability distributions for visual and SC results show dominance for some thickness classes. In conclusion it can be said that all three methods are able to get a satisfactory results, which can be used for making the assessment.

For future studies the flow size effect should be investigated more properly in ship and ice interaction to find out from which size the ice act as level ice and how to take into account the flow size in equivalent ice thickness formula. In addition, as the statistical mechanical properties vary quite a lot of a limited amount of the in-situ measurements, then it will be beneficial to increase them. Furthermore the snow factor should be more studied, because in Antarctic is a lot of snow or ice snow and the current factor may not be appropriate.

Kokkuvõte

Käesolevas magistritöös on uuritud Antaktika merejääd ja leitud sellele ekvivalentne jää paksust, et hinnata laeva tegelikku takistust jääs. Täismõõtmelised mõõtmised viidi läbi Antarktika vetes laevalt *S.A Agulhas II* aastatel 2013-2014. Arvutustes on kasutades Lindqvist'i valemit. Ekvivalentse jää paksuse kontseptsioon on võetud kui geomeetriline meetod, kus kogu jää võetakse arvesse mingi pindala kohta ja tulemus on antud ühe paksuse väärtusena. Ekvivalentse jää paksuse leidmiseks on kasutatud reaalsete mõõtmiste andmeid sileda jää paksuse, rüsijää paksuse, lume paksuse ja jää kontsentratsiooni kohta. Samuti on arvesse võetud rüsijää poorus.

Töö põhineb kümnel eelnevalt valitud juhtumil, kus iga juhtumi kesvuseks on üks tund. Jää paksused on leitud kolme erineva meetodiga, stereo piltidelt, visuaalse vaatluse ja elektromagnetlainte abil kõigile kümnele juhtumile. Nende kolme meetodi tulemusi on võrreldud tõenäosusjaotustel ja need näitavad üsna sarnaseid tulemusi, mis annab kinnitust, et mõõtmistulemused on realistlikud. Rüsijää paksus on mõõdetud elektromagnetlainete abil genereeritud jää profiili graafikutelt. Lume paksus mõõdeti stereo piltidelt. Jää kontsentratsioon on võetud arvesse visuaalse vaatluse põhjal. Arvutuslikult saadud jää takistust on võrreldud laeva sõuvõllilt mõõdetud keskmise tõukejõuga. Seejärel valiti nende hulgast neli sobilikku juhtumit, et neid detailsemalt uurida. Kus juhtumid lühendati kümnele minutile, et saada ühtlasemaid navigatsiooni parameetreid laevale jää takistuse arvutamiseks.

Tulemused näitavad, et laeva tegelik tõukejõud on sarnane arvutatud jää takistusega, kuigi töö lõppfaasis käsitletud neljal erineval juhtumil võisid tulemused erineda kuni 33%. Seda tulemust võib pidada heaks kuna jääolud polnud nii ühtlased kui oleks võinud ja jää mehaanilised parameetrid polnud mõõdetud nii tihedalt kui jää paksused.

Bibliography

ASPeCt Multi-year ice [Online] // Antarctic Sea Ice Processes & Climate. - September 5, 2014. - http://aspect.antarctica.gov.au/home/glossary-and-image-library/multi-year-ice.

Auch Jason Image (cropped) - Antarctic mountains, pack ice and ice floes.jpg [Art].

Bekker Anriëtte [et al.] Full-scale measurements on a polar supply and research vessel during maneuver tests in an ice field in the Baltic Sea [Conference] // The 33rd International Conference on Ocean, Offshore and Arctic Engineering OMAE33. - San Francisco : [s.n.], 2014. - Vols. OMAE2014-24128.

Daley Katherine Use of Equivalent Ice Thickness in Winter Navigation Restrictions [Report]. - Espoo : Helsinki University of Technology Ship Laboratory, 2004.

Ehle Daniela Analysis of Breaking through Sea Ice Ridges for Development of Prediction Method [Report]. - Essen : The University of Duisburg-Essen, 2011.

Haas Christian Evaluation of ship-based electromagnetic-inductive thickness measurements of summer sea-ice in the Bellingshausen and Amundsen Seas, Antarctica [Report]. - Bremerhaven : Alfred Wenger Institute, 1998.

Hänninen Samuli The Determination of The Equivalent Ice Thickness using Performance data of MT Uikku and Ice Thickness maps [Conference] // 17th International Symposium on Ice. - Saint Petersburg : Helsinki University of Technology, Ship Laboratory, 2004. - pp. 309-318.

Kujala Pentti [et al.] Full-Scale Measurements on board S.A. Agulhas II in the Antarctic Waters 2013-2014 [Report]. - Espoo : Aalto University, 2014.

Kujala Pentti Measurements on board S.A. Agulhas II in the Baltic Sea and Antarctic waters [Kul-24.3500 Winter Navigation (Kul-24_3500_measurements_in_antarctica.pdf)]. - Helsinki : Aalto University School of Engineering, 2013.

Kujala Pentti Semi-empirical Evaluation of Long Term Ice Loads on a Ship Hull [Journal]. - Espoo : Helsinki University of Technology, Ship Laboratory, 1996.

Kämäräinen Jorma Evaluation of Ship Ice Resistance Calculation Methods. Licentiate's thesis. [Report]. - Espoo : Helsinki University of Technology, Faculty of Mechanical Engineering, 1993.

Lange M. A. [et al.] Development of Sea Ice in the Weddell Sea [Journal]. - [s.l.] : Annals of Glaciology, 1989. - Vol. 12.

Lensu Mikko The Evolution of Ridged Ice Fields [Report]. - Espoo : Helsinki University of Technology Ship Laboratory, 2003.

Leppäranta Matti and Myrberg Kai Physical Oceanography of the Baltic Sea [Book]. - Helsinki : Springer, 2009.

Lindqvist Gustav A Straightforward Method for Calculation of Ice Resistance of Ships [Conference] // POAC. - Luleå : Wärtsilä Marine Industries Arctic Sea Transportation, 1989. - pp. 722-735.

Maksym T., S.E. Stammerjohn, S. Ackley, and R. Massom Antarctic sea ice - A polar opposite? [Journal] // Oceanography. - 2012. - pp. 140-151.

Mikko Suominen Jakke Kulovesi, Mikko Lensu, Jonni Lehtiranta, Pentti Kujala A Comparison of Shipborne Methods for Ice Thickness Determination [Conference] // 22nd IAHR International Symposium on Ice. - Singapore : Aalto University, 2014. - p. 8.

National Snow & Data Center National Snow & Data Center [Online]. - September 3, 2014. - http://nsidc.org/cryosphere/seaice/characteristics/difference.html.

Parmerter R. Reid A model of Simple Rafting in Sea Ice [Report]. - Washington : Department of Aeronautics and Astronautics, University of Washington, 1975.

Riska Kaj [et al.] Performance of Merchant Vessels in Ice in The Baltic - Report No 52 [Report]. - Espoo : The Winter Navigation Research Board, 1997.

Riska Kaj Definition of The new Ice class IA Super+ - Research Report No 60 [Report]. - Helsinki : The Winter Navigation Research Board, 2009.

Riska Kaj Ship – Ice Interaction in Ship Design: Theory and Practice [Conference] // Cold Regions Science and Marine Technology. - [s.l.] : ILS Oy and University of Science and Technology, 2011. - pp. 1-30.

Schwarz Joachim Sea Ice Investigation in the Weddell Sea [Journal]. - [s.l.] : Polarforschung, 1981. - Vols. 51 (1): 21-37.

Shotaro Uto Takenobu Toyota, Haruhito Shimoda, Kazutaka Tateyama, Kunio Shirasawa Ship-borne electromagnetic induction sounding of sea-ice thickness in the southern Sea of Okhotsk [Conference] // Annals of Glaciology 44. - Dunedin : National Maritime Research Institute, 2006. - pp. 253-260.

SMHI [Online] // Swedish Meteorological and Hydrological Institute (SMHI). - April 23, 2014. - November 11, 2014. - http://www.smhi.se/en/theme/sea-ice-1.11198.

Tina Tin Martin O. Jeffries Morphology of deformed first-year sea ice features in the Southern Ocean [Conference] // Cold Regions Science and Technology 36. - Fairbanks : Geophysical Institute, University of Alaska, 2003. - pp. 141-163.

Toyota Takenobu, Haas Christian and Tamura Takeshi Size distribution and shape properties of relatively small sea-ice floes in the Antarctic marginal ice zone in late winter [Journal]. - [s.l.] : Deep-Sea Research II, 2011. - Vol. 58.

University of Bremen SSMIS Sea Ice Maps of Antarctica [Online]. - February 18, 2015. - http://www.iup.uni-bremen.de:8084/ssmis/#Antarctic.

Usher Mike [Online] // Antarctica Travel Picture Gallery. - 2005. - 10 14, 2014. - http://www.coolantarctica.com/gallery/travel/antarctica0032.html.

Ville Kotovirta Risto Jalonen, Lars Axell, Kaj Riska, Robin Berglund A system for route optimization in ice-covered waters [Conference] // Cold Region Science and Technology 55. - [s.l.] : VTT Technical Research Centre of Finland, 2009. - pp. 52-62.

Worby Anthony P. [et al.] Thickness distribution of Antarctic sea ice [Journal]. - [s.l.] : Journal of Geophysical Research, 2008. - Vol. 113.

Time UTC+0 (central measurement system)							Observer	Draught [m]		snow	[cm]	brash ice	Ramming	vibration s	Ice concentration in tenths																		Ice thickness [cm] in tenths																		Floe size m (diameter) in tenths								
			start		end										open	0-	10-	20-	30-	40-	50-	60-	70-	80-	90-	sum	0-	20-	40-	60-	80-	100-	120-	140-	160-	180-	200	250	300	300+	sum	< 20	20	100	500	2000	5000+	sum	comments
year	mm	dd	hh	mm	hh	mm	initials	Fore	Aft	min	max	0-10	count	(0)-3	water	10	20	30	40	50	60	70	80	90	100		20	40	60	80	100	120	140	160	180	200	250	300				100	500	2000	5000	Level ice		
2013	12	9	11	0	11	10	KM	7.3	7.75			2		1	1								2	5	2	10			2.0	4.0	3.0	1.0								10	4	2	2	2			10	
2013	12	9	11	10	11	20	KM	7.3	7.75			3		1										1	9	10			2.0	3.0	2.0	1.0	1.0	1.0						10	3	2	3	2			10	
2013	12	9	11	20	11	30	KM	7.3	7.75			2		1										6	4	10				4.0	5.0	1.0								10	3	3	4				10	
2013	12	9	11	30	11	40	KM	7.3	7.75			2		1										3	7	10			2.0	2.0	5.0	1.0								10	3	2	1	3	1		10	
2013	12	9	11	40	11	50	KM	7.3	7.75			2		1										5	5	10			1.0	2.0	2.0	3.0		1.0		1.0				10	4	1	2	3			10	almost stopped by ice.
2013	12	9	11	50	12	0	KM	7.3	7.75			1		1										5	5	10					2.0	5.0	2.0	1.0							10	3			6	1		10	
2013	12	9	12	0	12	10	BB	7.3	7.75			1		1										5	5	10					1.4	2.4	3.5	1.8	.9						10	2	3			5		10	
2013	12	9	12	10	12	20	BB	7.3	7.75			2		1										7	3	10					.9	2.2	4.8	1.1			1.0				10	3	2	5				10	
2013	12	9	12	20	12	30	BB	7.3	7.75			2		1.5									2	6	2	10			.2	2.1	3.0	3.0	1.4	.3						10	2	5		3			10	
2013	12	9	12	30	12	40	BB	7.3	7.75			1		1									4	1	5	10					1.4	1.9	1.4	3.0	2.3						10	1	3	2	4			10	
2013	12	9	12	40	12	50	BB	7.3	7.75			3		1.5										3	7	10					.0	.5	2.1	2.6	2.5	2.1	.2				10		1	2	7			10	
2013	12	9	12	50	13	0	BB	7.3	7.75			4		1										8	2	10		.8	1.3	.7	1.6	2.2	2.8	.6							10	3	5	2				10	
2014	1	23	21	0	21	10	KS	6.76	7.13	10	30	3		1.5										2	8	10				1.0	3.0	4.0	2.0							10	3	3	4				10	
2014	1	23	21	10	21	20	KS	6.76	7.13	15	40	6		2										2	8	10					1.0	4.0	2.0	3.0							10	3	6	1				10	
2014	1	23	21	20	21	30	KS	6.76	7.13	10	30	4		1										1	9	10		2.0	4.0	3.0	1.0									10	2	5	3				10	
2014	1	23	21	30	21	40	KS	6.76	7.13	5	30	2		1										2	8	10				3.0	2.0	3.0	2.0							10	4	4	2				10	
2014	1	23	21	40	21	50	KS	6.76	7.13	5	20	3		1										2	8	10				1.0	2.0	4.0	3.0							10	2	4	4				10	
2014	1	23	21	50	22	0	KS	6.76	7.13	5	20	3		1										3	7	10					2.0	5.0	3.0								10	2	3	5				10	
2014	1	23	22	0	22	10	KS	6.76	7.13	10	30	4		1										4	6	10		1.0	2.0	3.0	4.0									10	3	5	2				10	
2014	1	23	22	10	22	20	KS	6.76	7.13		20	4		1										3	7	10		2.0	3.0	3.0	2.0									10	4	4	2				10	
2014	1	23	22	20	22	30	KS	6.76	7.13		20	3		1							3			2	5	10				2.0	3.0	5.0								10	2	5	3				10	
2014	1	23	22	30	22	40	KS	6.76	7.13	5	30	3		1								4			6	10		1.0	3.0	4.0	2.0									10	3	5	2				10	
2014	1	23	22	40	22	50	KS	6.76	7.13	5	20	3		1								3		2	5	10			5.0	4.0	1.0									10	6	4					10	
2014	1	23	22	50	23	0	KS	6.76	7.13	5	20	3		1							5	3	2			10		2.0	5.0	3.0											10	3	5	2				10	
2014	1	24	2	0	2	10	PK	6.76	7.13		60	7		1									4	6		10					1.5	2.6	2.0	1.6	1.2		1.0				10	4	4	2				10	
2014	1	24	2	10	2	20	PK	6.76	7.13		50	5		0.5									3	7		10			.1	1.4	2.1	2.6	1.4	1.4	1.2						10	2	6	2				10	
2014	1	24	2	20	2	30	PK	6.76	7.13		30	3		0.5								2		4	4	10		.7	1.4	2.0	1.6	1.4	1.4	.9	.6					10		5	5				10	
2014	1	24	2	30	2	40	PK	6.76	7.13		50	3		1									10			10		.7	1.4	1.4	1.7	2.0	1.4	.9	.6					10	2	4	4				10	
2014	1	24	2	40	2	50	PK	6.76	7.13		30	2		1								2		4	4	10		.7	1.4	1.4	2.1	2.6	1.4	.5						10	4	4	2				10	
2014	1	24	2	50	3	0	PK	6.76	7.13		30	1		1									10			10		.7	1.4	1.4	1.4	1.4	1.4	1.4	1.2					10	2	4	4				10	
2014	1	24	4	0	4	10	PK	6.76	7.13		40	0		1										2	4	4	10					.8	1.6	4.1	2.4	1.2						10	2	4	4				10	
2014	1	24	4	10	4	20	PK	6.76	7.13		30	0		1										5	5	10					.8	1.6	4.1	2.4	1.2						10	5	5					10	:19 almost stopped in a old ridges field, height 1.0 m
2014	1	24	4	20	4	30	PK	6.76	7.13		40	0		0.5										4	4	2	10					.8	1.5	2.7	2.7	2.4						10	4	4	2				10	
2014	1	24	4	30	4	40	PK	6.76	7.13		40	0		0.5										5	2	3	10			.1	1.4	1.7	2.0	1.4	1.4	1.3	.7	.2				10			4	6			10	
2014	1	24	4	40	4	50	PK	6.76	7.13		40	0		1.5										6	4	10					.8	1.5	2.7	1.9	1.3	.7	1.2				10		4	6				10	:49 almost stopped in old ridge field, height 1.0
2014	1	24	4	50	5	0	PK	6.76	7.13		30	0		1.5										5	5	10					.8	1.4	2.0	1.6	1.4	1.4	1.5				10		4	6				10	
2014	1	27	4	0	4	10	PK	6.76	7.13		20	8		1											10	10					1.5	2.7	2.7	1.9	1.2						10	5	5					10	
2014	1	27	4	10	4	20	PK	6.76	7.13		30	9		0.5										8	2	10					.0	.2	2.7	2.7	2.4		2.0				10	2	8					10	:18 good hit
2014	1	27	4	20	4	30	PK	6.76	7.13		30	9		1										6	4	10					.0	.2	2.7	2.7	2.5	1.4	.5				10	4	6					10	
2014	1	27	4	30	4	40	PK	6.76	7.13		30	9												4	6	10					.0	.2	2.7	2.7	2.5	1.4	.5				10	4	6					10	slowly
2014	1	27	4	40	4	50	PK	6.76	7.13		30	10		0.5											10	10					1.5	2.7	2.7	1.9	1.2						10	5	5					10	
2014	1	27	4	50	5	0	PK	6.76	7.13		40	7												5	5	10			.1	1.4	1.4	1.5	2.7	1.9	1.2						10	6	4					10	
2014	1	31	21	0	21	10	KS	7.12	7.08		40	4		1									2	5	3	10			4.0				4.0	2.0							10	4	6					10	
2014	1	31	21	10	21	20	KS	7.12	7.08		30	4		1									1	6	3	10			3.0				5.0	2.0							10	5	5					10	
2014	1	31	21	20	21	30	KS	7.12	7.08		30	3		1						3			1	4	2	10			4.0	3.0			3.0								10	6	4					10	
2014	1	31	21	30	21	40	KS	7.12	7.08		20	2		1					3	4				3		10			5.0	2.0			3.0								10	5	5					10	
2014	1	31	21	40	21	50	KS	7.12	7.08		60	3		1						5		3	2			10			5.0	1.0			4.0								10	4	6					10	
2014	1	31	21	50	22	0	KS	7.12	7.08		40	3		1					2	5	3					10			4.0	3.0					3.0						10	5	5					10	
2014	2	1	4	0	4	10	PK	7.12	7.08		30	1		1								4	6			10			.1	1.4	1.4	1.4	1.4	1.4	1.4	.3				10	5	5					10	
2014	2	1	4	10	4	20	PK	7.12	7.08		30	0		1										10		10			.1	1.4	2.2	2.5	1.4	1.4	1.0						10	1	9					10	
2014	2	1	4	20	4	30	PK	7.12	7.08		30	0		2										10		10			.1	1.4	2.2	2.5	1.4	.9	.7	.7	.1				10	1	9					10	
2014	2	1	4	30	4	40	PK	7.12	7.08		20	0		1									4	6		10			.2	2.7	2.7	2.4	.7	.7	.5						10	4	6					10	
2014	2	1	4	40	4	50	PK	7.12	7.08		20	0		2									6	4		10			.1	1.4	2.2	2.5	1.4	.9	.7	.7	.1				10	2	8					10	
2014	2	1	4	50	5	0	PK	7.12	7.08		30	0		1.5									5	5		10			.1	1.4	1.4	1.4	1.4	1.4	1.4	.3				10	2	8					10	
2014	2	1	8	0	8	10	BB	7.12	7.08	0	30	2	0	1										10		10			.7	1.6	3.4	2.1	1.3	.7	.2						10	10						10	
2014	2	1	8	10	8	20	BB	7.12	7.08	0	30	0	0	1										10		10			.4	.9	3.4	3.0	2.3								10	9	1					10	
2014	2	1	8	20	8	30	BB	7.12	7.08	0	20	0	0	1										10		10			.7	1.4	2.1	2.9	2.8								10	10						10	
2014	2	1	8	30	8	40	BB	7.12	7.08	0	20	0	0	1										10		10			.7	1.4	2.1	2.1	1.9	1.4	.4						10	10						10	
2014	2	1	8	40	8	50	BB	7.12	7.08	0	20	0	0	1										10		10			.7	1.6	3.4	2.6	1.7								10	10						10	
2014	2	1	8	50	9	0	BB	7.12	7.08	0	20	0	0	1										10		10			1.1	2.1	2.7	1.9	1.3	.7	.2						10	10						10	

Appendix 2

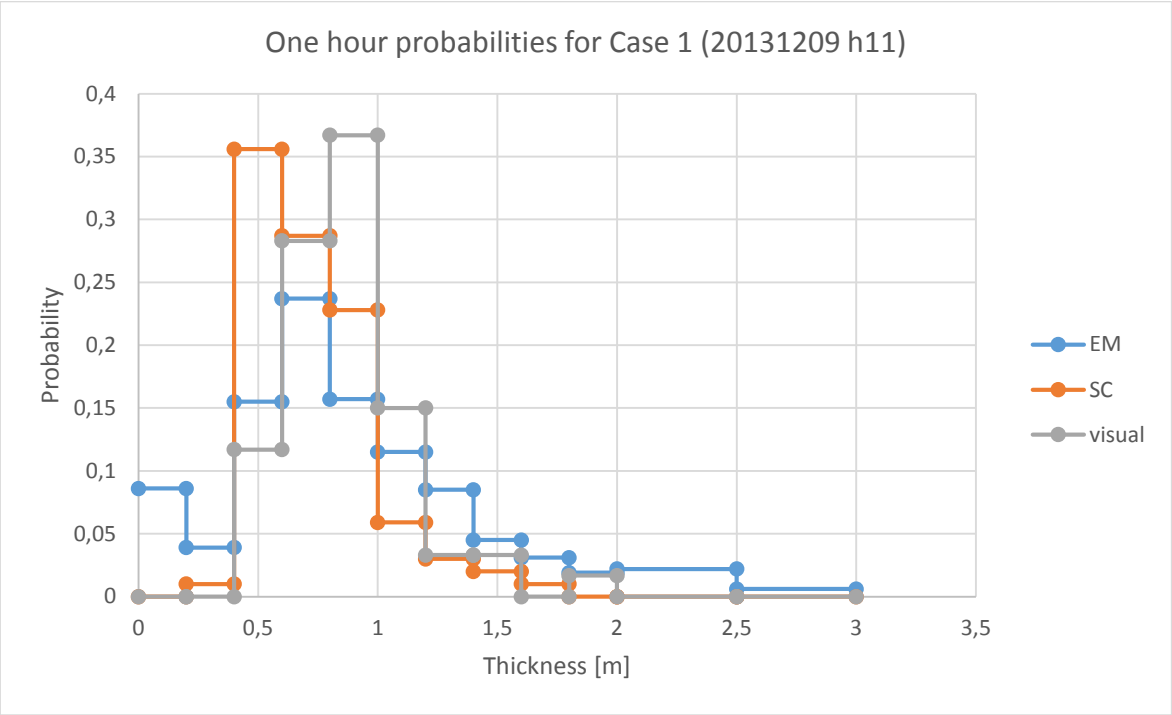
One hour probabilities for Case 1 (20131209 h11)
Probability
0,4
0,35
0,3
0,25
0,2
0,15
0,1
0,05
0
0
0,5
1
1,5
2
2,5
3
3,5
Thickness [m]
EM
SC
visual

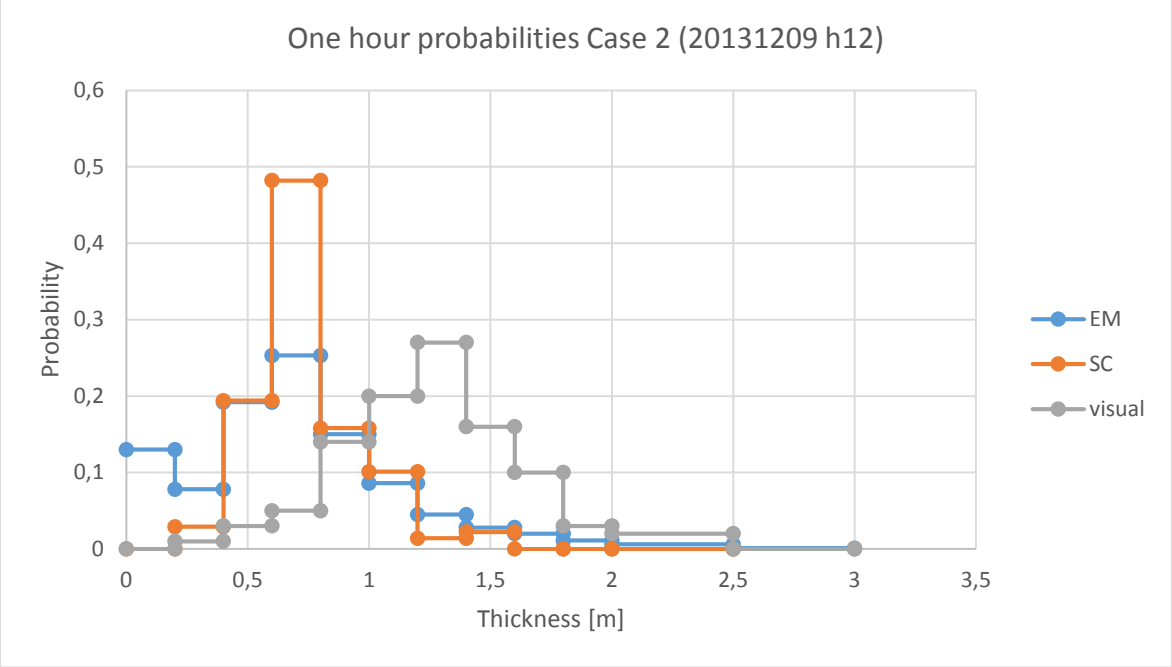
One hour probabilities Case 2 (20131209 h12)
Probability
0,6
0,5
0,4
0,3
0,2
0,1
0
0
0,5
1
1,5
2
2,5
3
3,5
Thickness [m]
EM
SC
visual

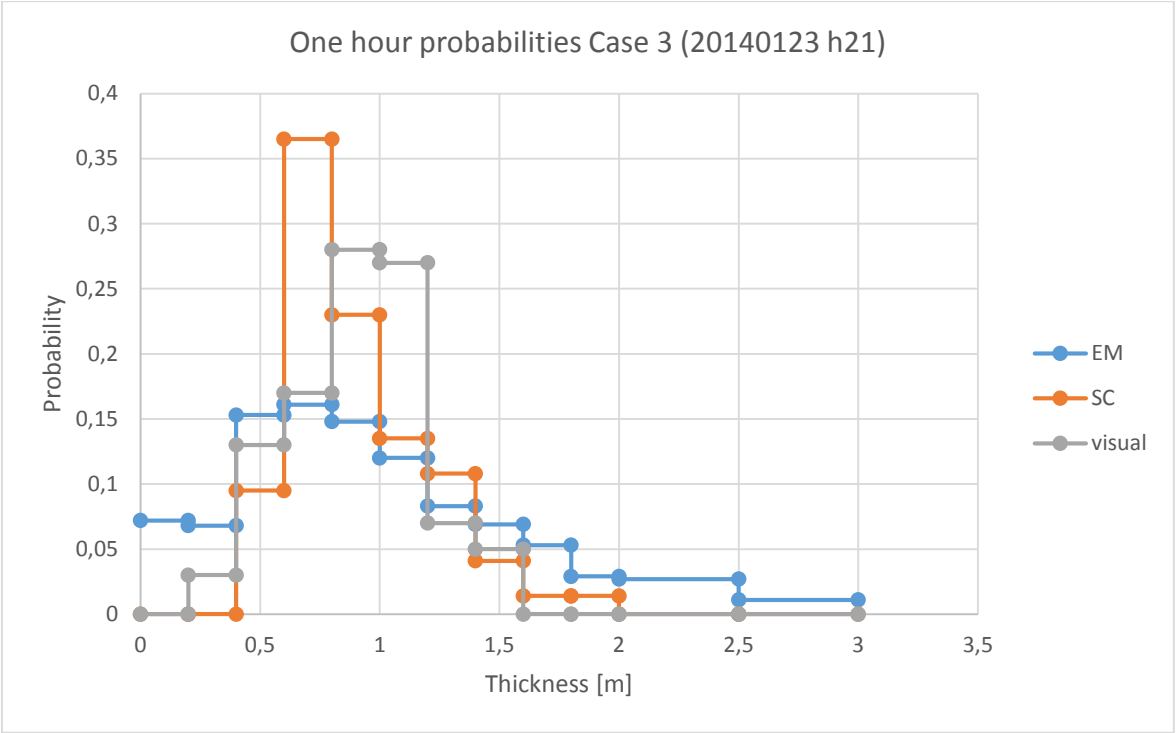
One hour probabilities Case 3 (20140123 h21)
Probability
0,4
0,35
0,3
0,25
0,2
0,15
0,1
0,05
0
0
0,5
1
1,5
2
2,5
3
3,5
Thickness [m]
EM
SC
visual

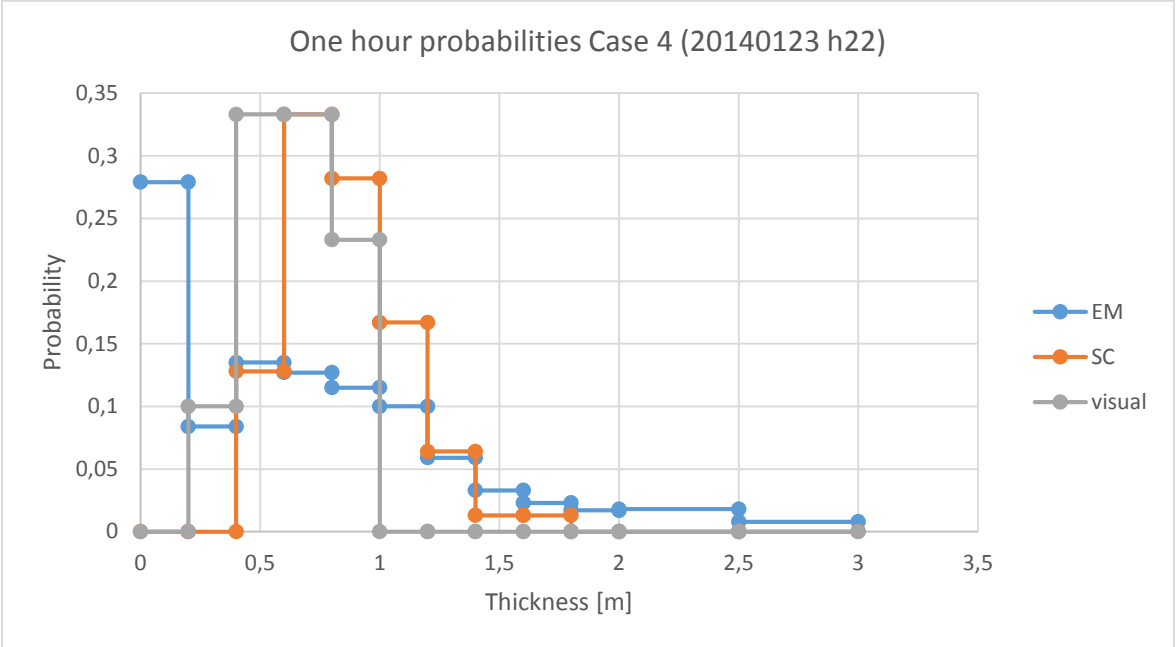
One hour probabilities Case 4 (20140123 h22)
Probability
0,35
0,3
0,25
0,2
0,15
0,1
0,05
0
0
0,5
1
1,5
2
2,5
3
3,5
Thickness [m]
EM
SC
visual

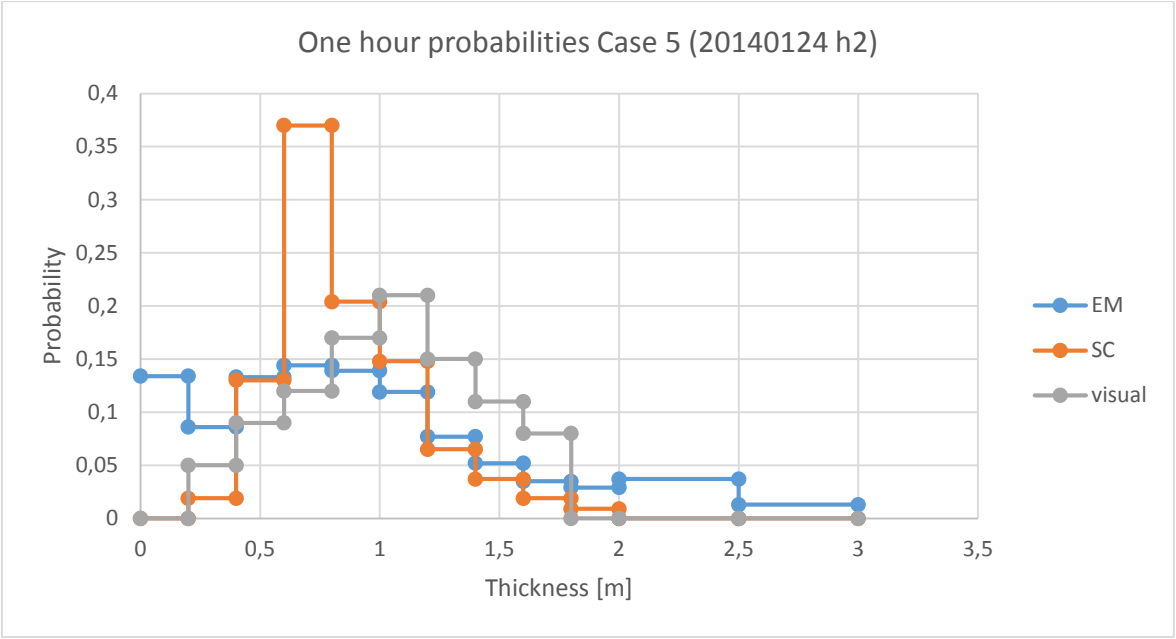
One hour probabilities Case 5 (20140124 h2)
Probability
0,4
0,35
0,3
0,25
0,2
0,15
0,1
0,05
0
0
0,5
1
1,5
2
2,5
3
3,5
Thickness [m]
EM
SC
visual

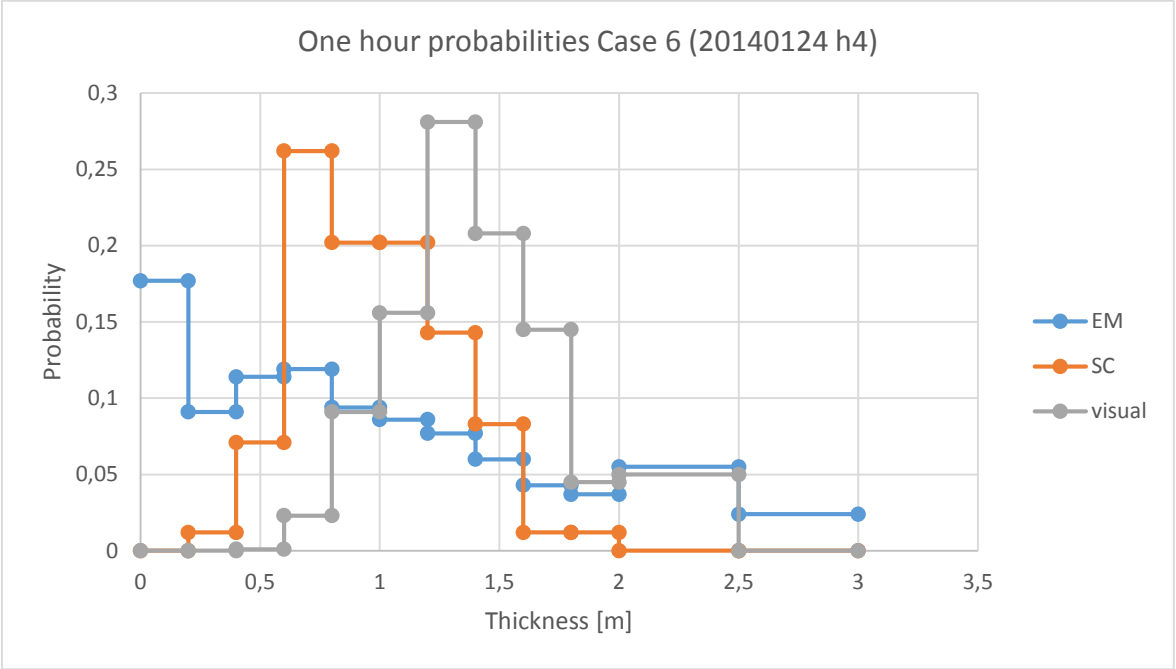
One hour probabilities Case 6 (20140124 h4)
Probability
0,3
0,25
0,2
0,15
0,1
0,05
0
0
0,5
1
1,5
2
2,5
3
3,5
Thickness [m]
EM
SC
visual

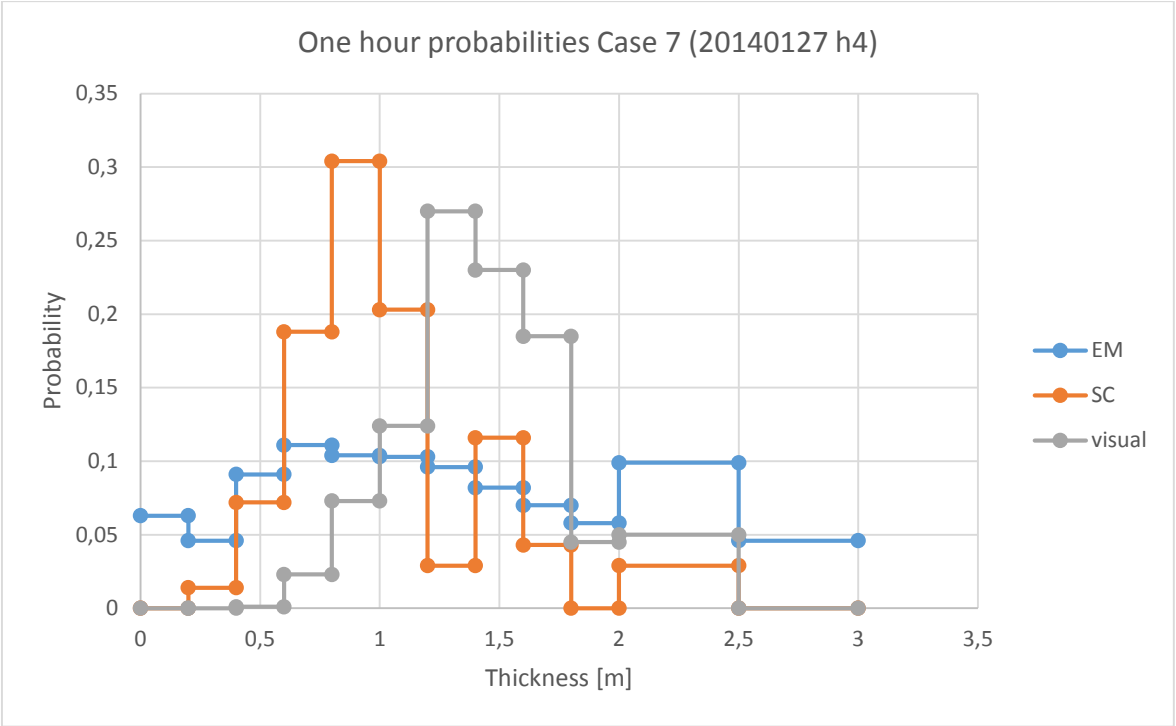
One hour probabilities Case 7 (20140127 h4)
Probability
0,35
0,3
0,25
0,2
0,15
0,1
0,05
0
0
0,5
1
1,5
2
2,5
3
3,5
Thickness [m]
EM
SC
visual

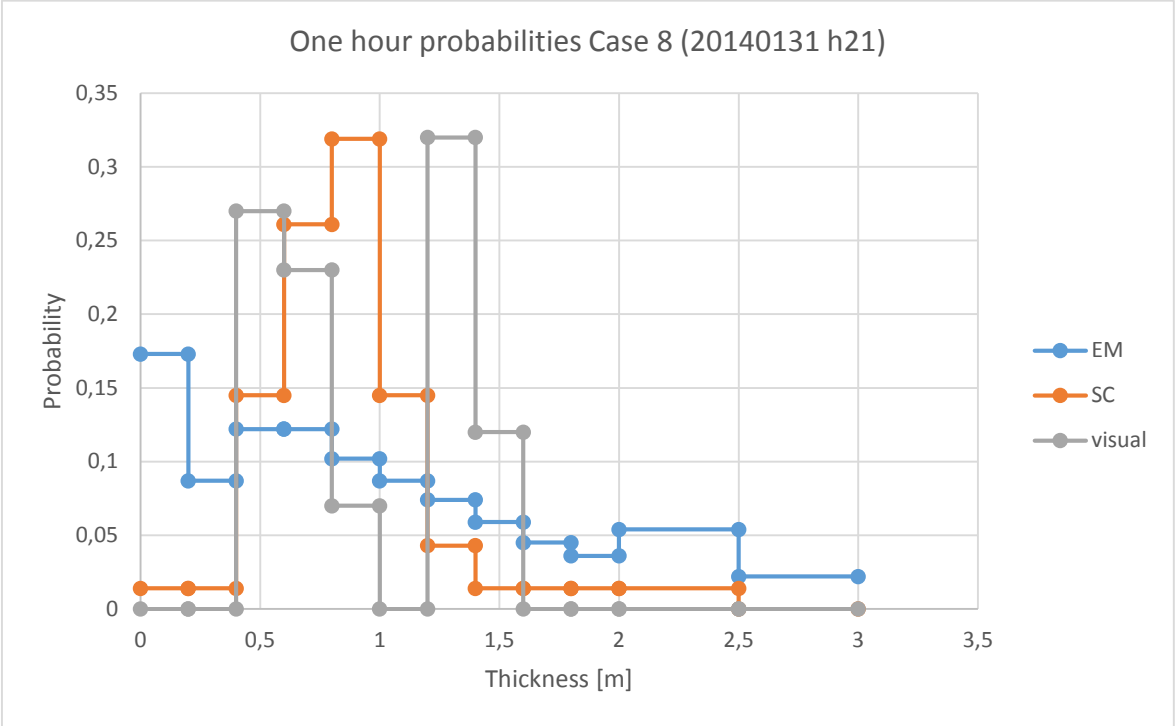
One hour probabilities Case 8 (20140131 h21)
Probability
0,35
0,3
0,25
0,2
0,15
0,1
0,05
0
0
0,5
1
1,5
2
2,5
3
3,5
Thickness [m]
EM
SC
visual

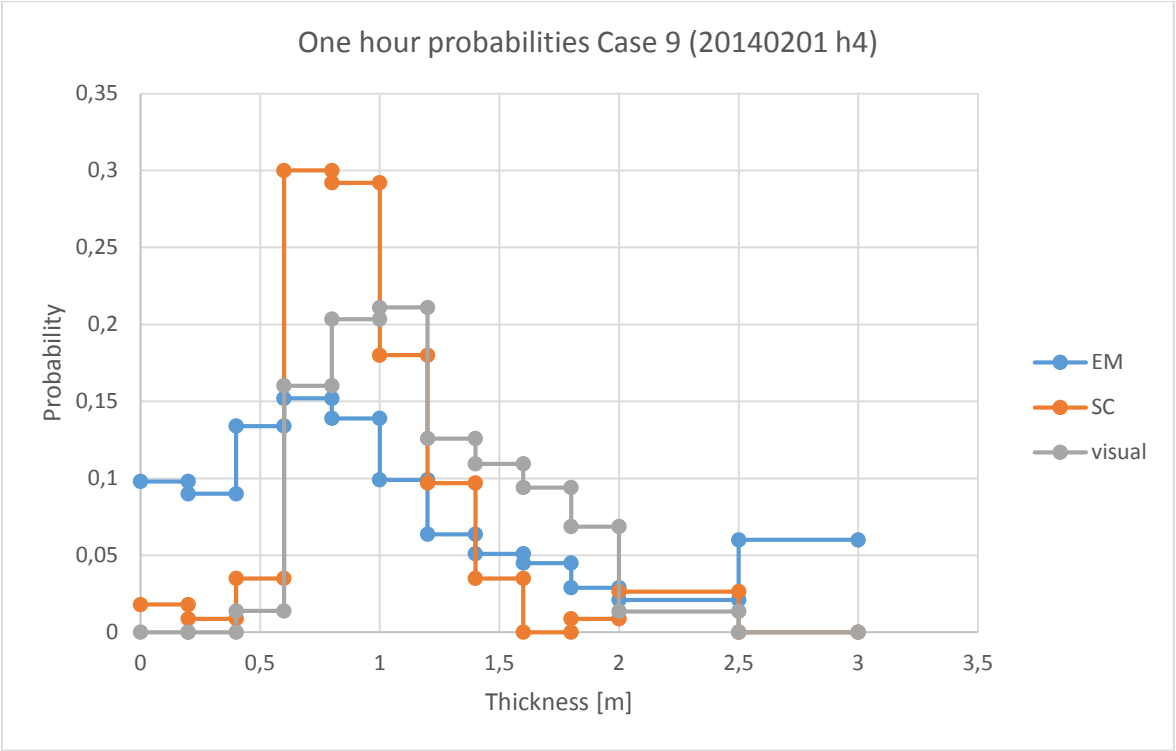
One hour probabilities Case 9 (20140201 h4)
Probability
0,35
0,3
0,25
0,2
0,15
0,1
0,05
0
0
0,5
1
1,5
2
2,5
3
3,5
Thickness [m]
EM
SC
visual

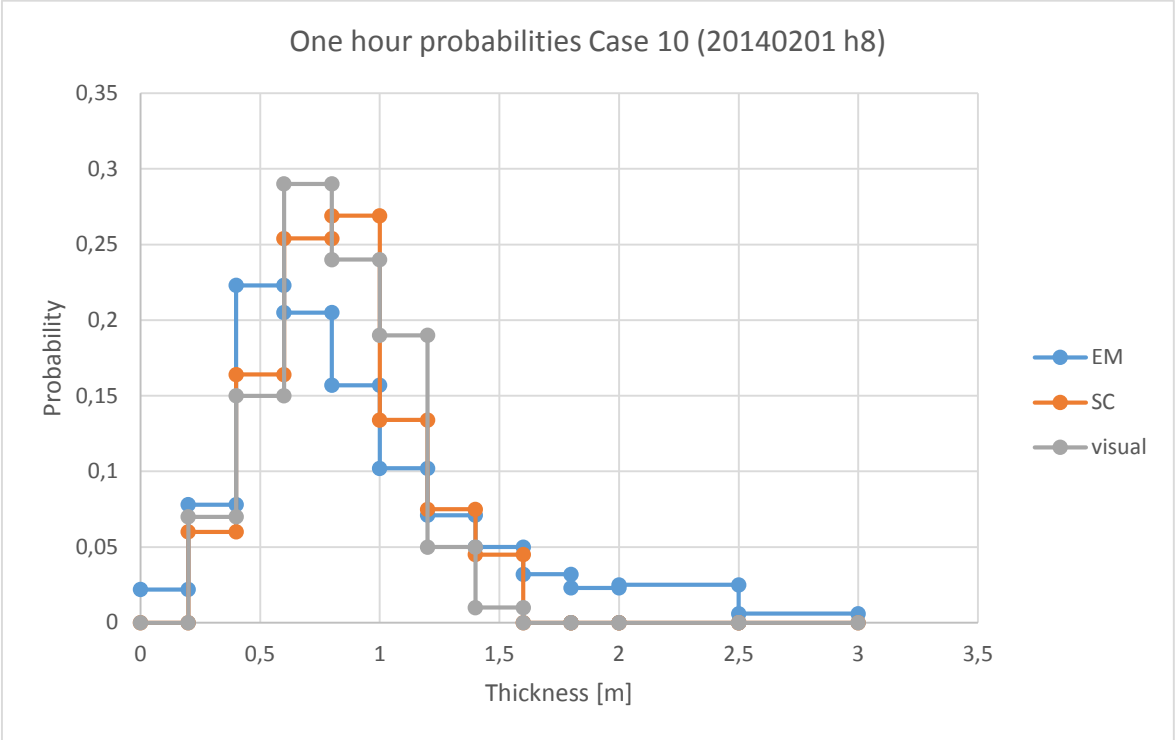
One hour probabilities Case 10 (20140201 h8)
Probability
0,35
0,3
0,25
0,2
0,15
0,1
0,05
0
0
0,5
1
1,5
2
2,5
3
3,5
Thickness [m]
EM
SC
visual

Appendix 3

Thrust and speed ratio charts for one hour and short period data.

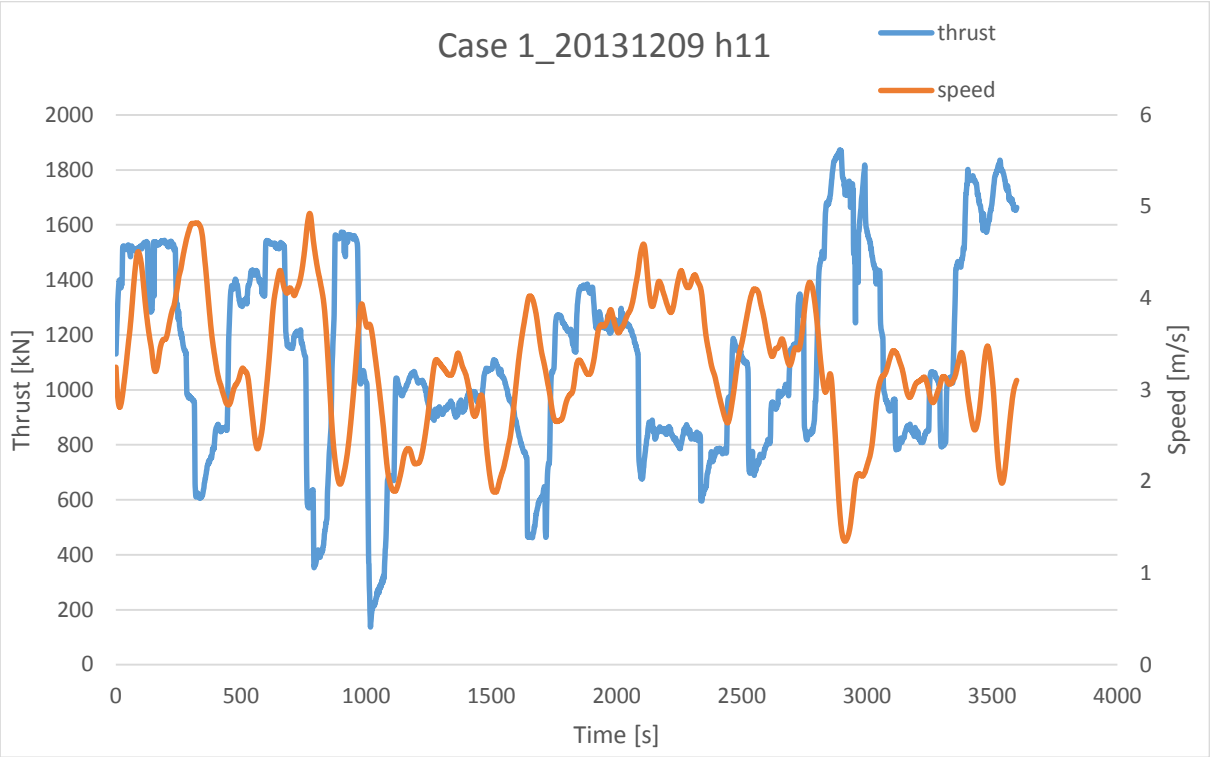

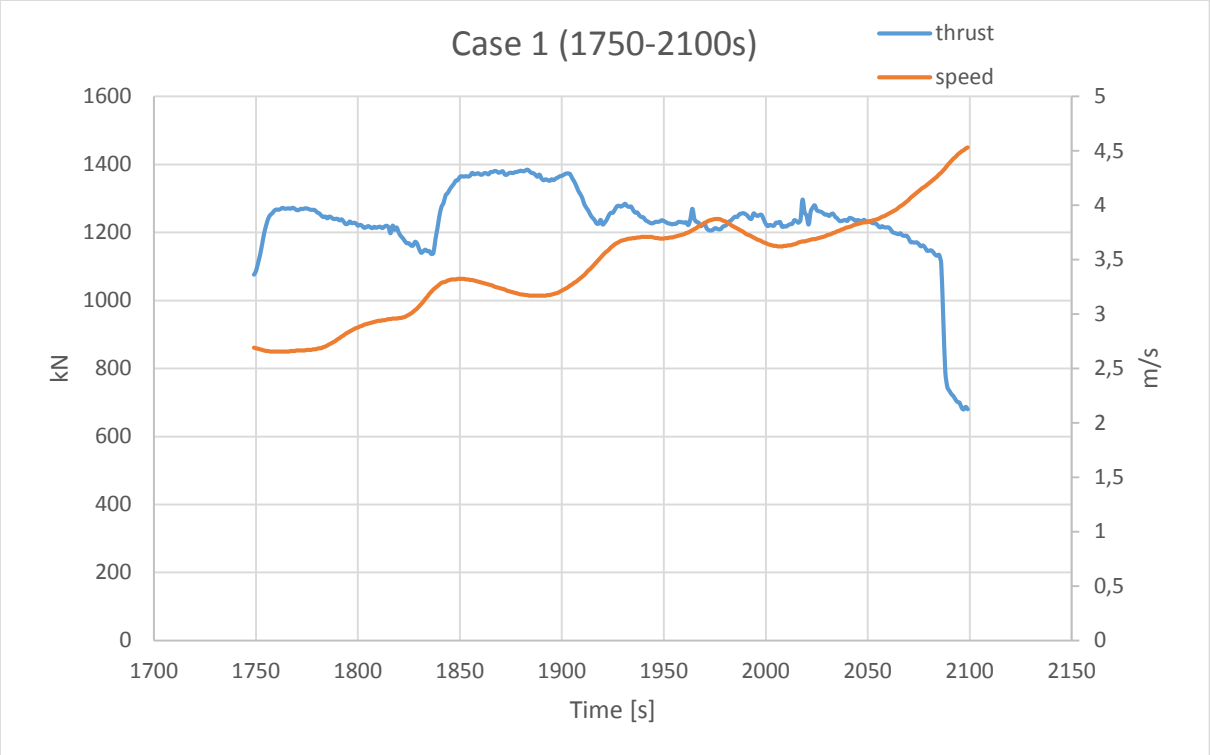

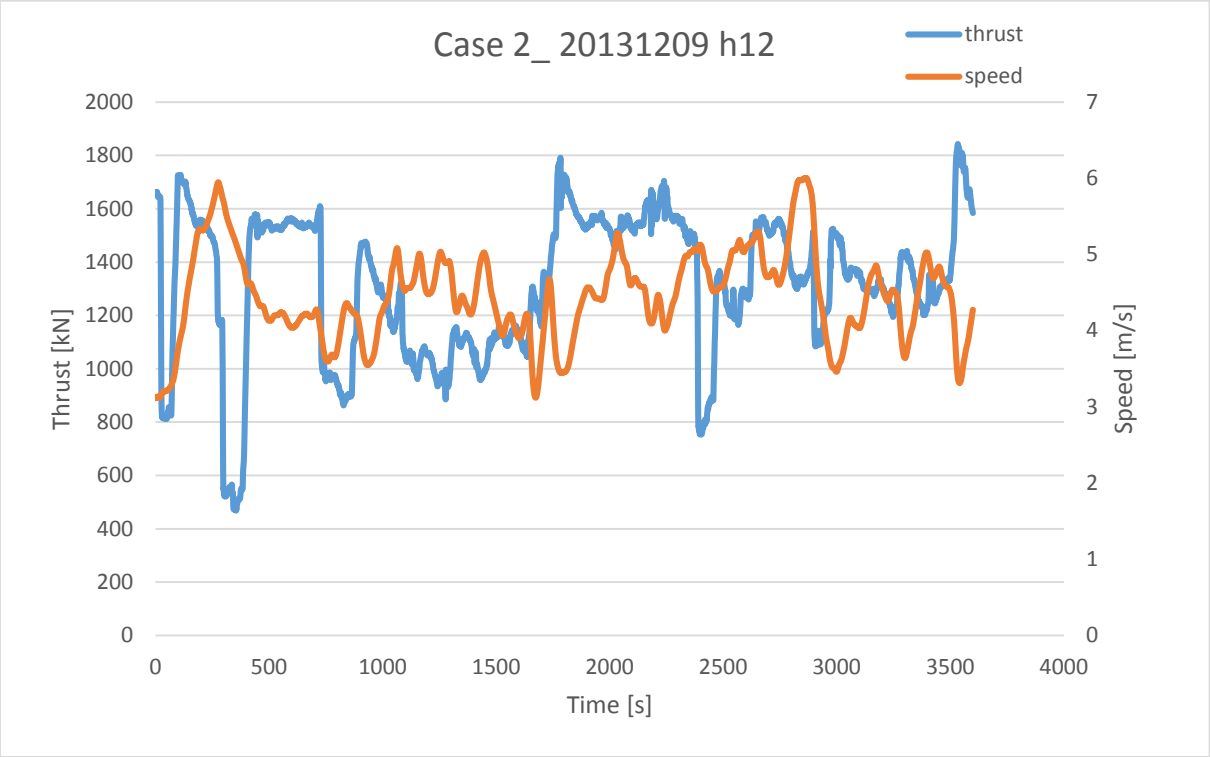
Case 2_ 20131209 h12
thrust
speed
Thrust [kN]
Speed [m/s]
Time [s]
2000
1800
1600
1400
1200
1000
800
600
400
200
0
7
6
5
4
3
2
1
0
0
500
1000
1500
2000
2500
3000
3500
4000

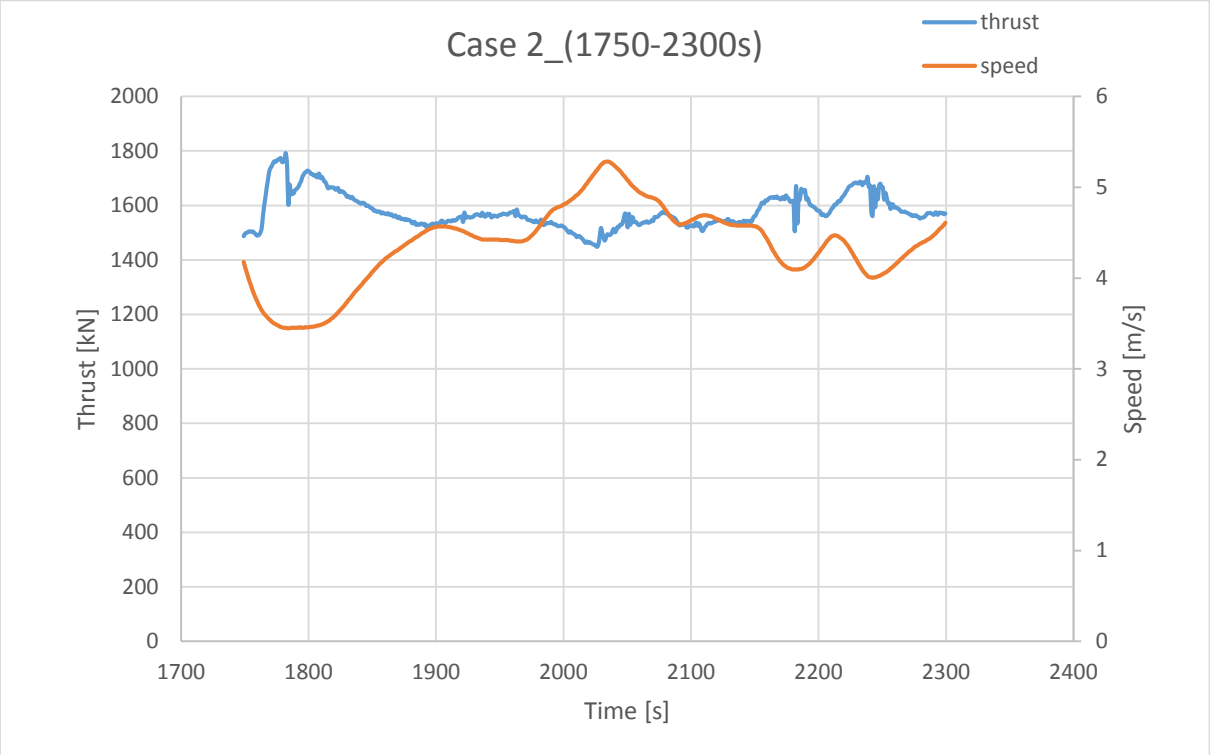
Case 2_(1750-2300s)
thrust
speed
Thrust [kN]
Speed [m/s]
Time [s]
2000
1800
1600
1400
1200
1000
800
600
400
200
0
6
5
4
3
2
1
0
1700
1800
1900
2000
2100
2200
2300
2400

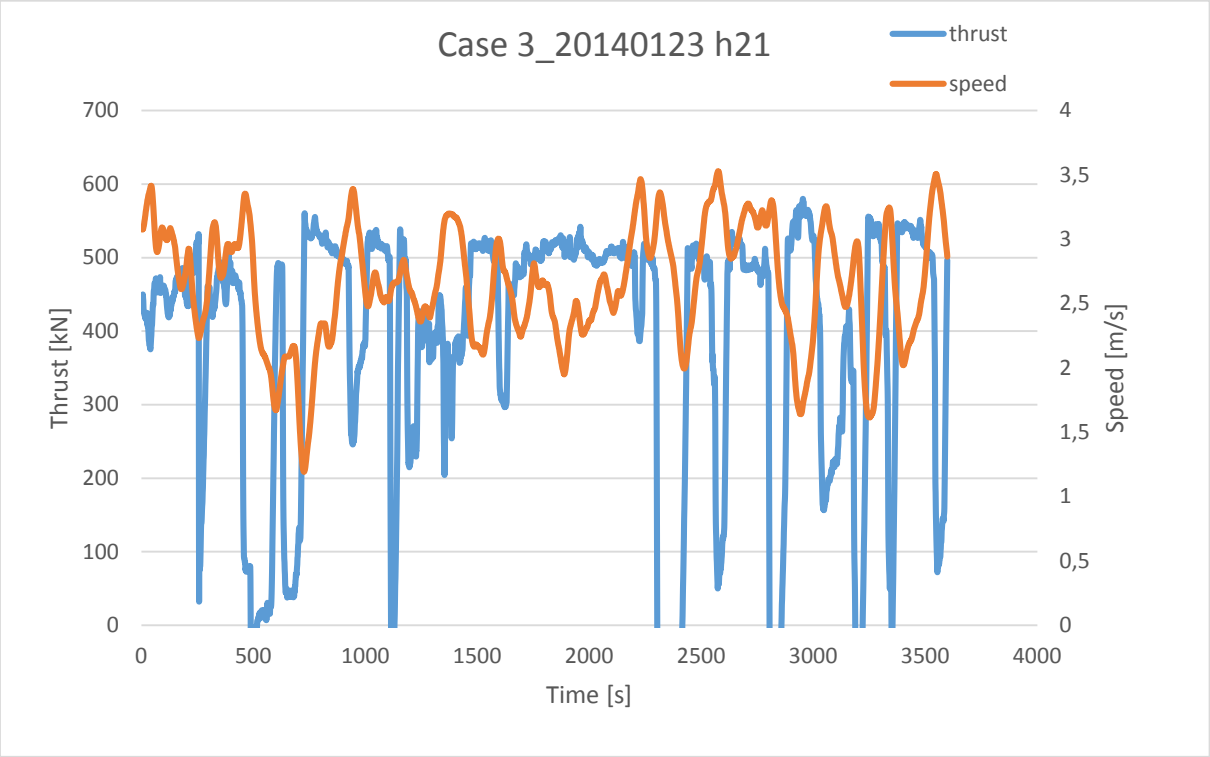
Case 3_20140123 h21
thrust
speed
700
600
500
400
300
200
100
0
Thrust [kN]
4
3,5
3
2,5
2
1,5
1
0,5
0
Speed [m/s]
0
500
1000
1500
2000
2500
3000
3500
4000
Time [s]

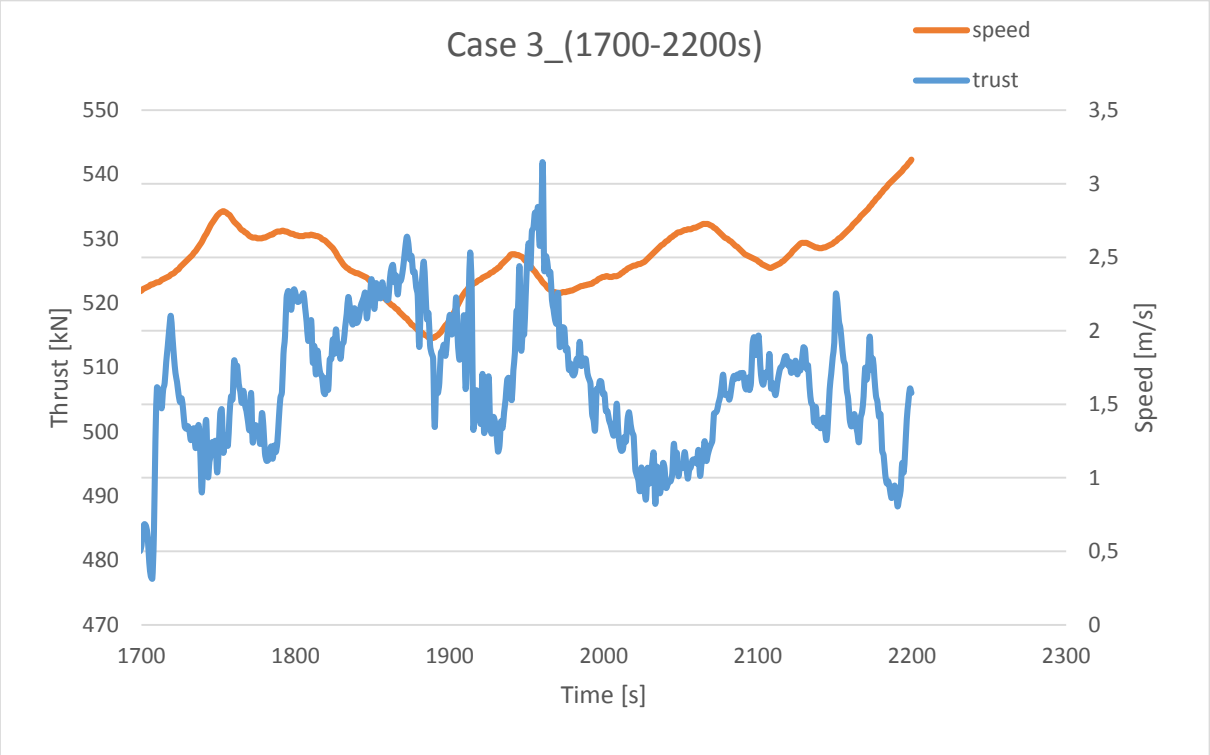
Case 3_(1700-2200s)
speed
trust
550
540
530
520
510
500
490
480
470
Thrust [kN]
3,5
3
2,5
2
1,5
1
0,5
0
Speed [m/s]
1700
1800
1900
2000
2100
2200
2300
Time [s]

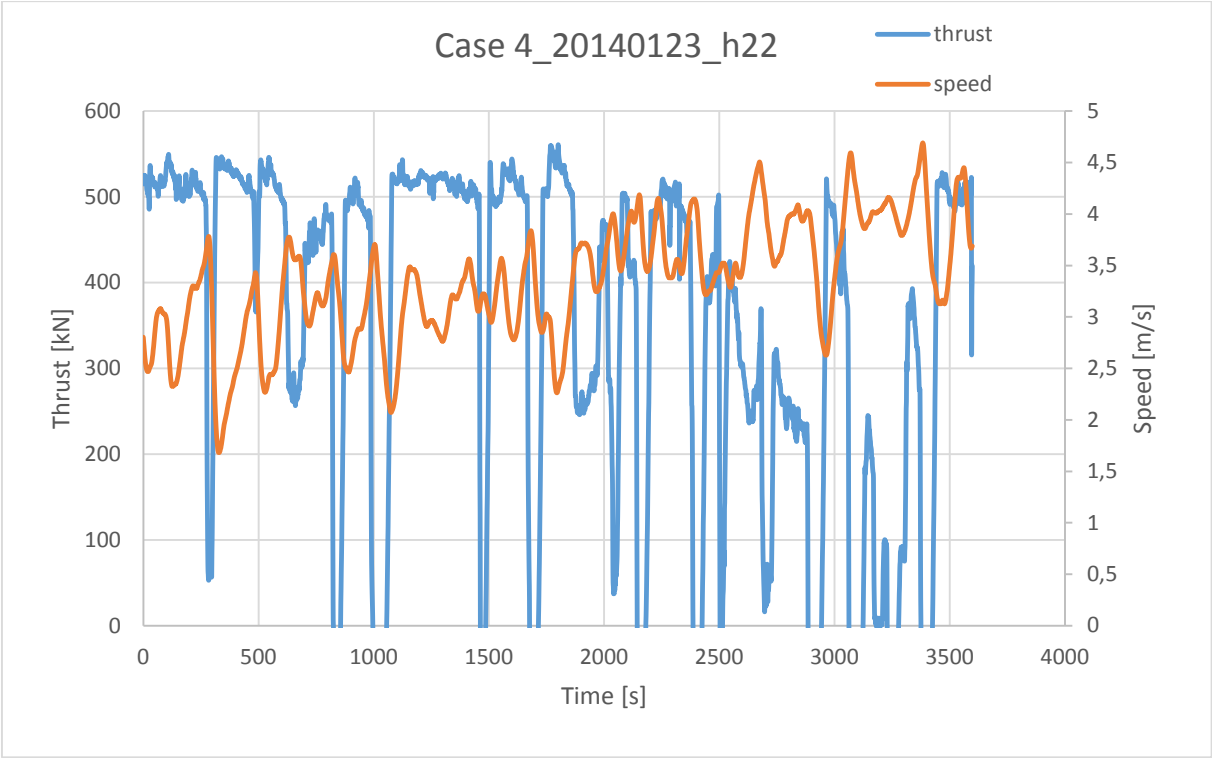
Case 4_20140123_h22
thrust
speed
Thrust [kN]
Speed [m/s]
Time [s]
0
100
200
300
400
500
600
0
0,5
1
1,5
2
2,5
3
3,5
4
4,5
5
0
500
1000
1500
2000
2500
3000
3500
4000

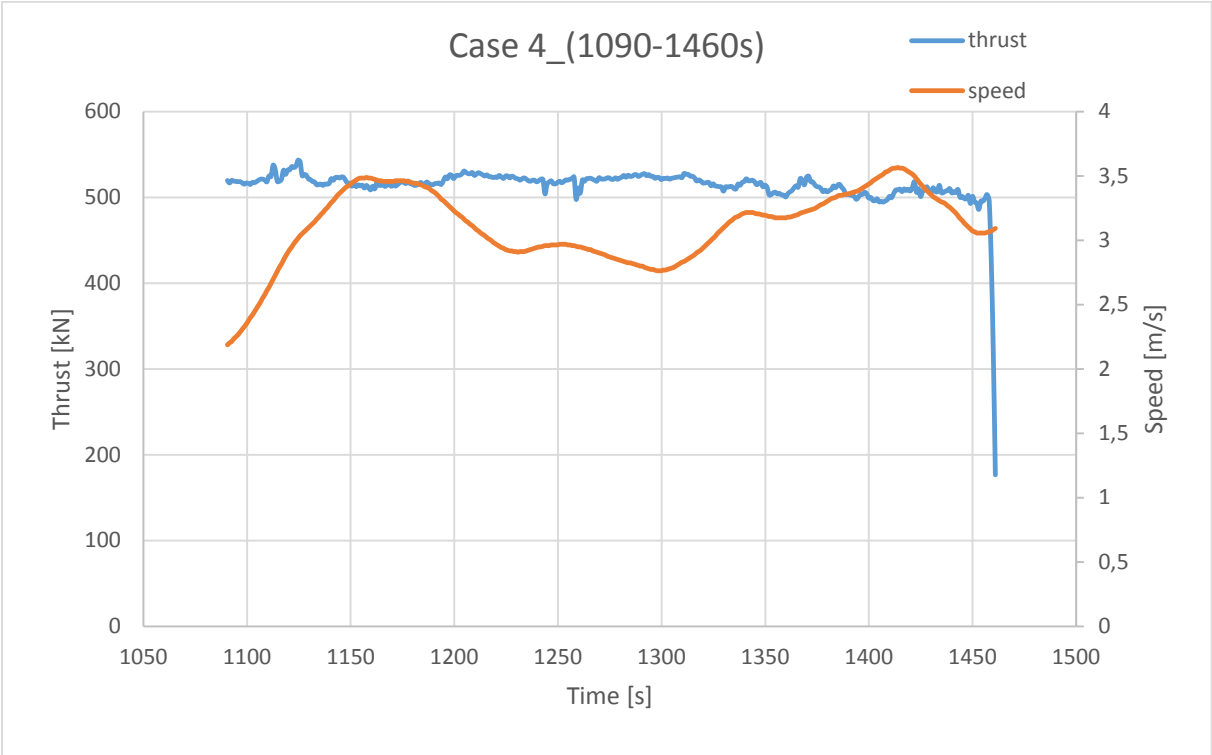
Case 4_(1090-1460s)
thrust
speed
Thrust [kN]
Speed [m/s]
Time [s]
0
100
200
300
400
500
600
0
0,5
1
1,5
2
2,5
3
3,5
4
1050
1100
1150
1200
1250
1300
1350
1400
1450
1500

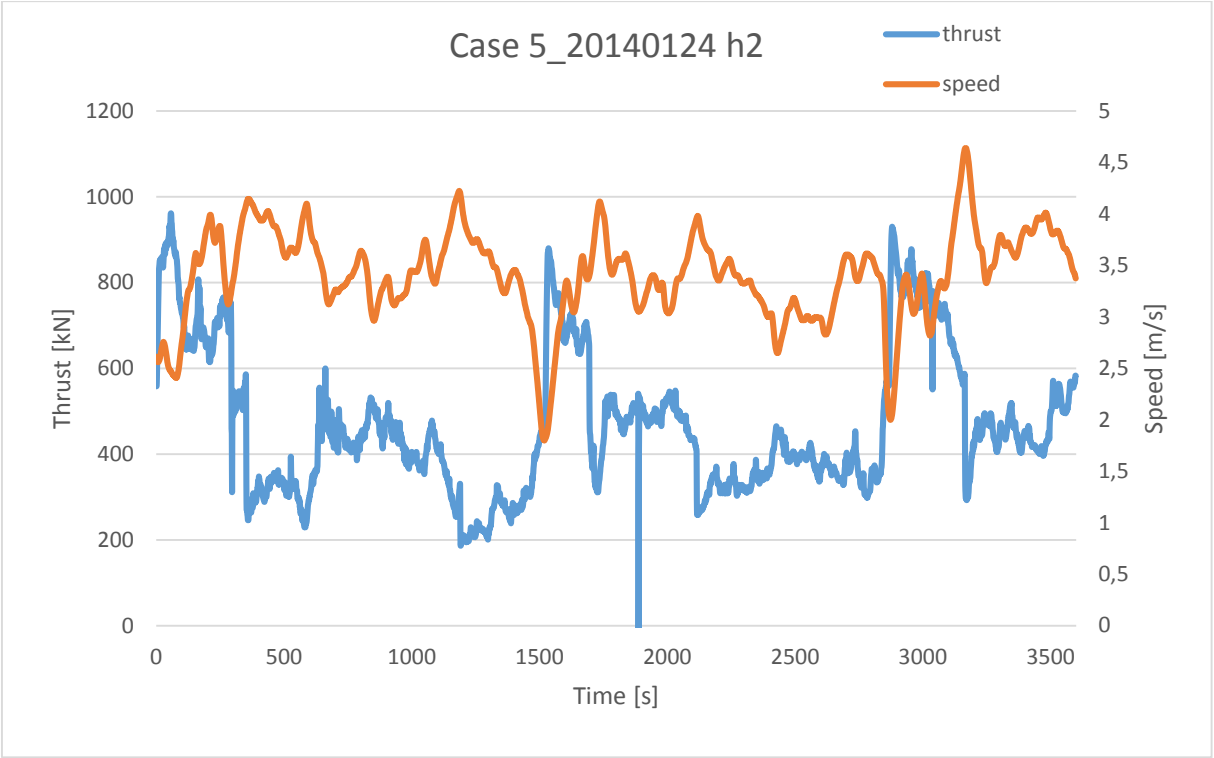
Case 5_20140124 h2
thrust
speed
Thrust [kN]
Speed [m/s]
Time [s]
0
200
400
600
800
1000
1200
0
0,5
1
1,5
2
2,5
3
3,5
4
4,5
5
0
500
1000
1500
2000
2500
3000
3500

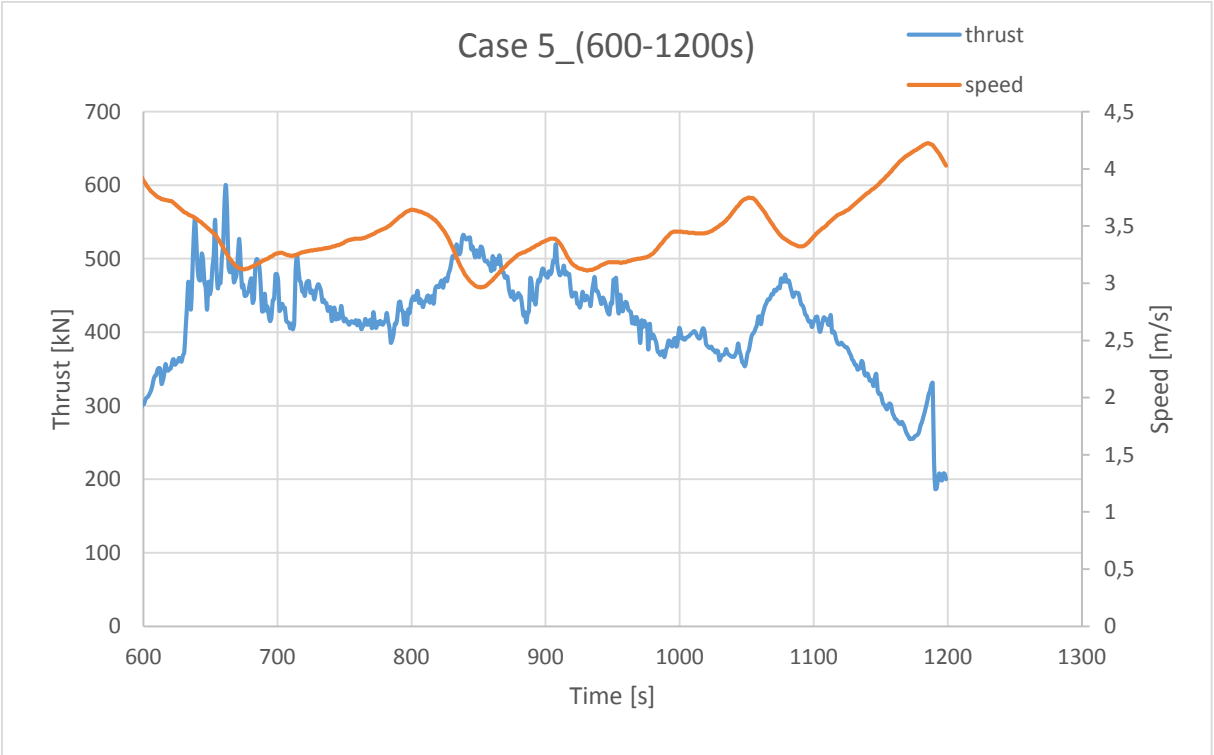
Case 5_(600-1200s)
thrust
speed
Thrust [kN]
Speed [m/s]
Time [s]
0
100
200
300
400
500
600
700
0
0,5
1
1,5
2
2,5
3
3,5
4
4,5
600
700
800
900
1000
1100
1200
1300

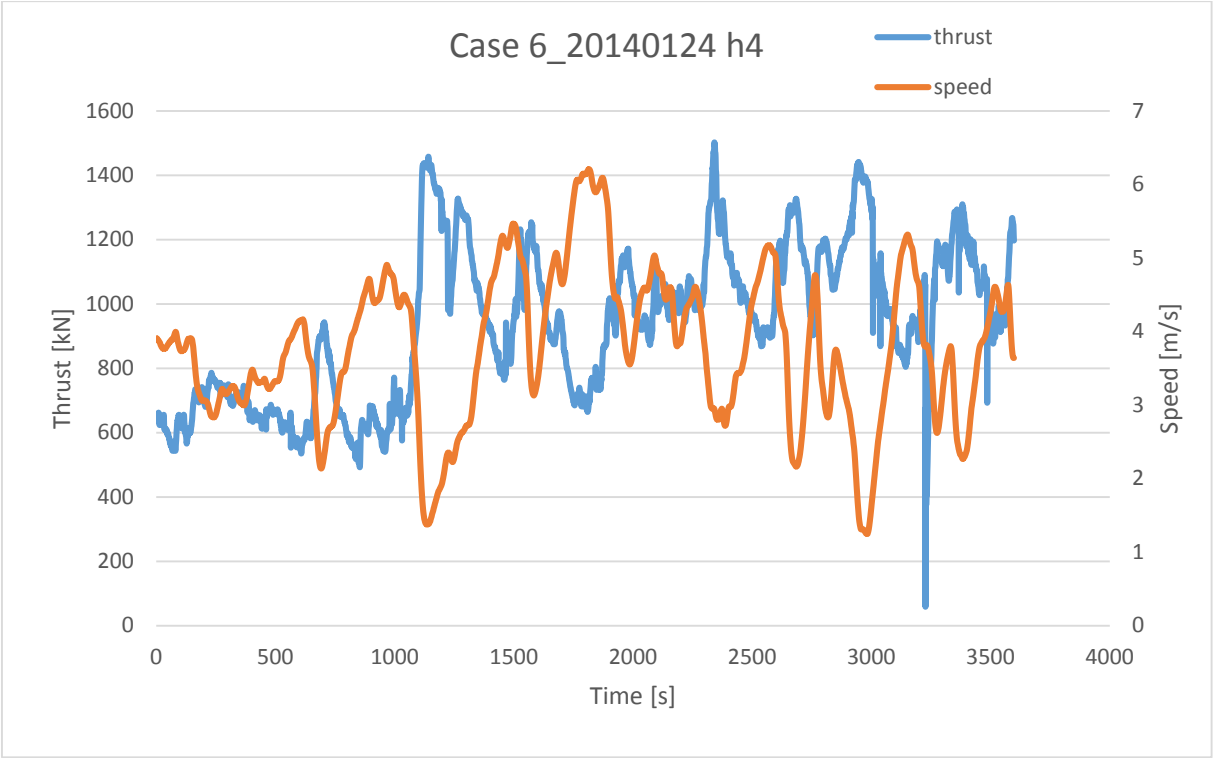
Case 6_20140124 h4
thrust
speed
Thrust [kN]
Speed [m/s]
Time [s]
0
200
400
600
800
1000
1200
1400
1600
0
1
2
3
4
5
6
7
0
500
1000
1500
2000
2500
3000
3500
4000

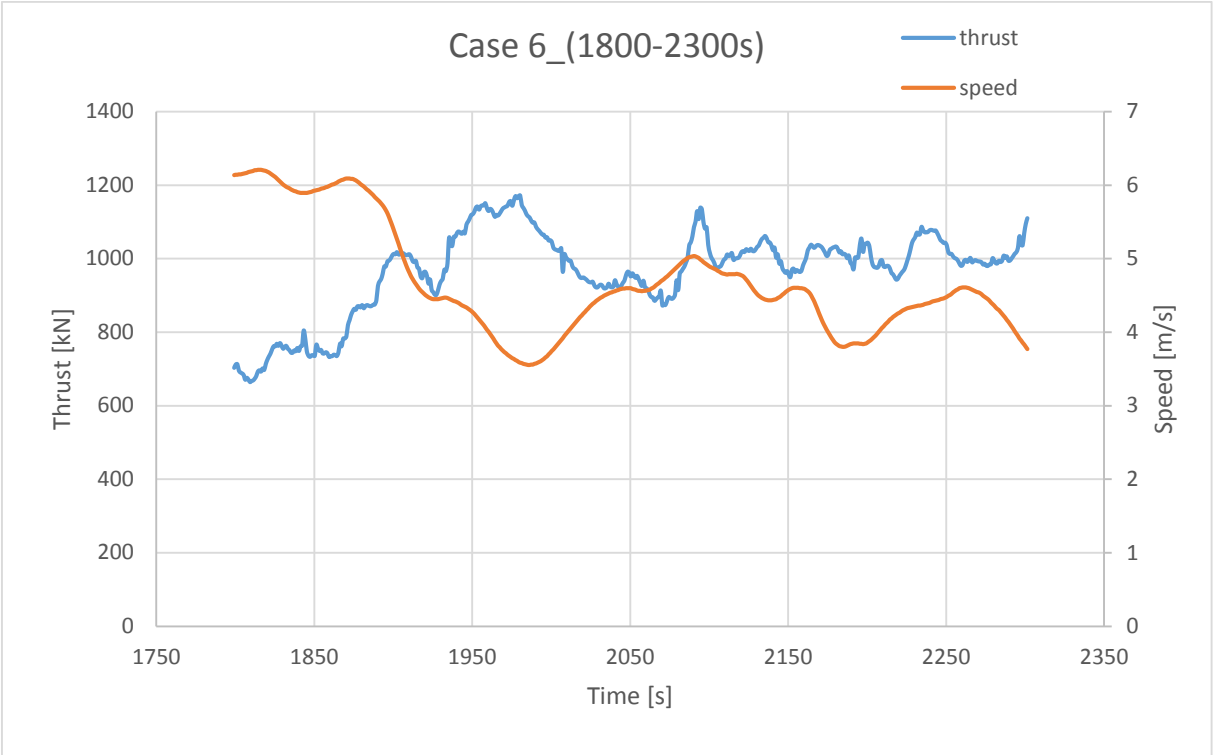
Case 6_(1800-2300s)
thrust
speed
Thrust [kN]
Speed [m/s]
Time [s]
0
200
400
600
800
1000
1200
1400
0
1
2
3
4
5
6
7
1750
1850
1950
2050
2150
2250
2350

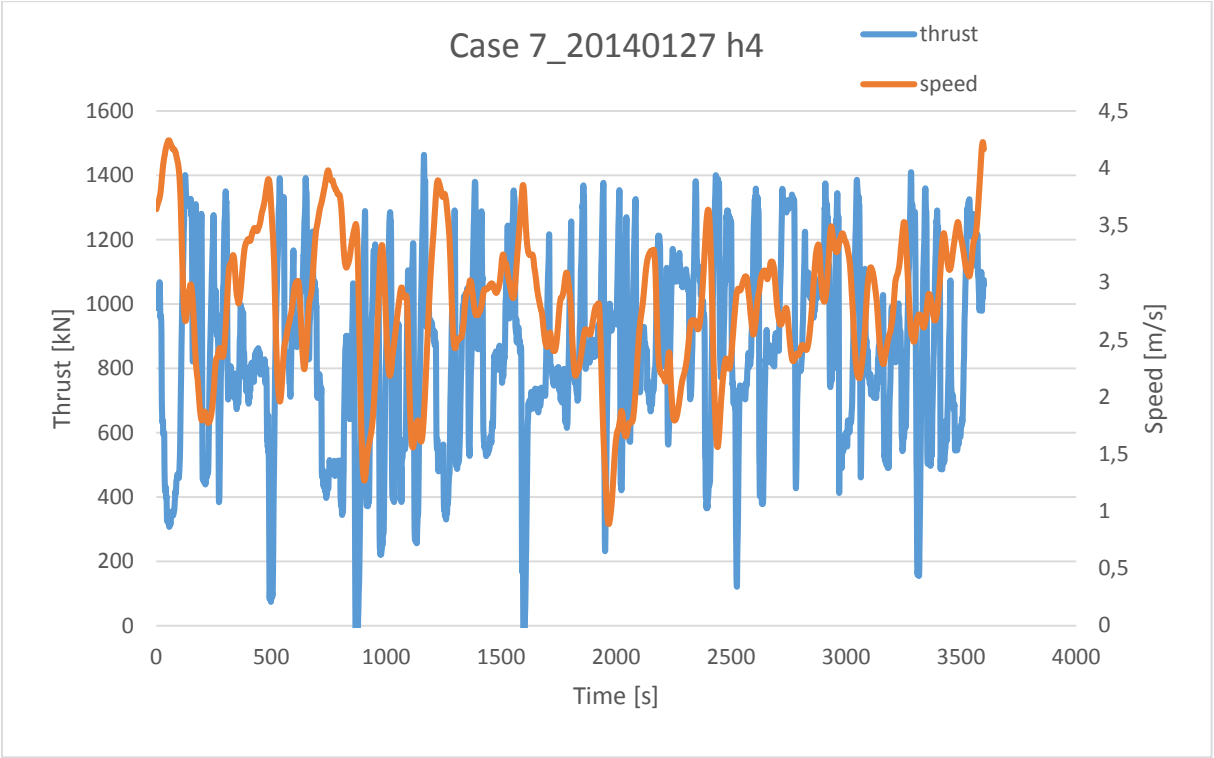
Case 7_20140127 h4
thrust
speed
Thrust [kN]
Speed [m/s]
Time [s]
0
200
400
600
800
1000
1200
1400
1600
0
0,5
1
1,5
2
2,5
3
3,5
4
4,5
0
500
1000
1500
2000
2500
3000
3500
4000

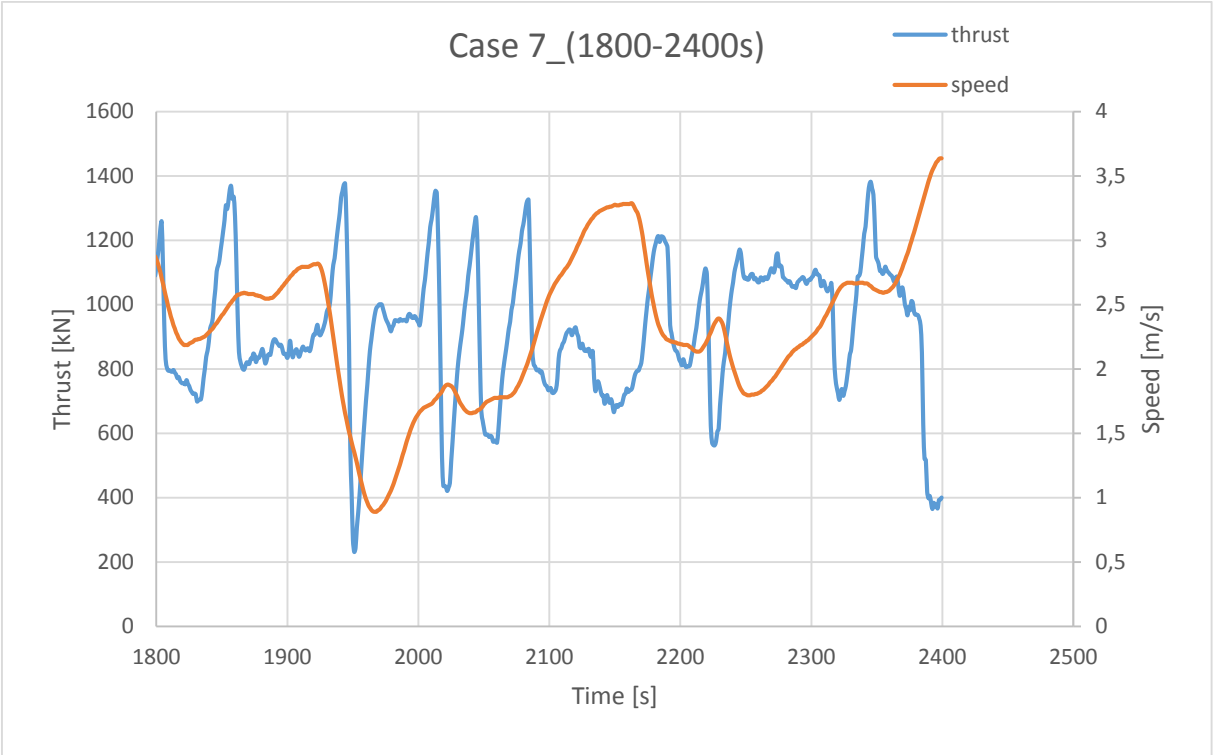
Case 7_(1800-2400s)
thrust
speed
Thrust [kN]
Speed [m/s]
Time [s]
0
200
400
600
800
1000
1200
1400
1600
0
0,5
1
1,5
2
2,5
3
3,5
4
1800
1900
2000
2100
2200
2300
2400
2500

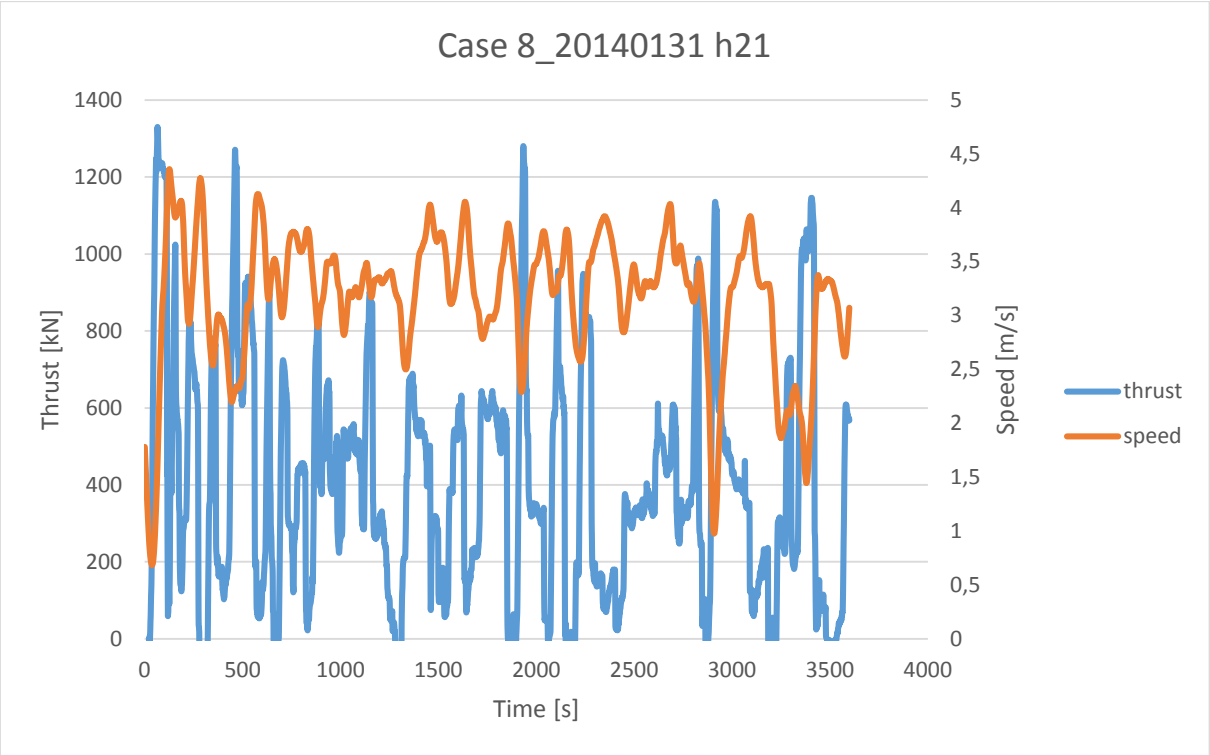
Case 8_20140131 h21
Thrust [kN]
Speed [m/s]
Time [s]
thrust
speed
0
200
400
600
800
1000
1200
1400
0
0,5
1
1,5
2
2,5
3
3,5
4
4,5
5
0
500
1000
1500
2000
2500
3000
3500
4000

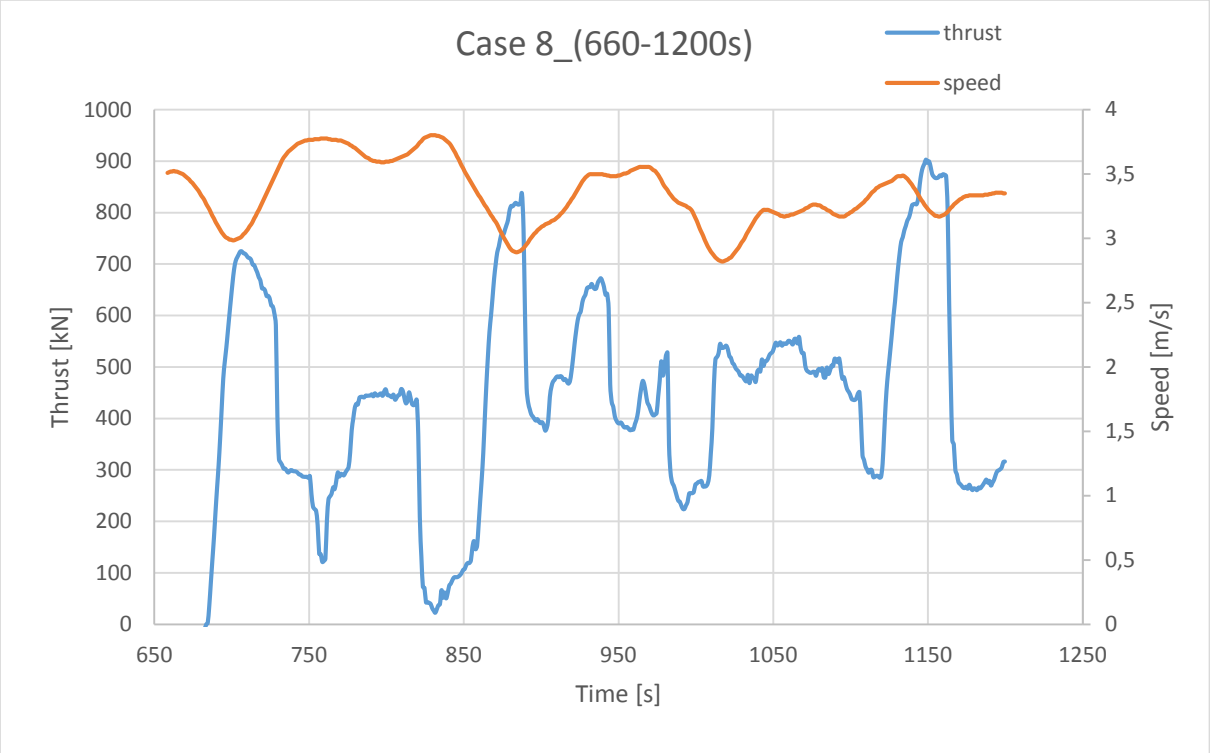
Case 8_(660-1200s)
thrust
speed
Thrust [kN]
Speed [m/s]
Time [s]
0
100
200
300
400
500
600
700
800
900
1000
0
0,5
1
1,5
2
2,5
3
3,5
4
650
750
850
950
1050
1150
1250

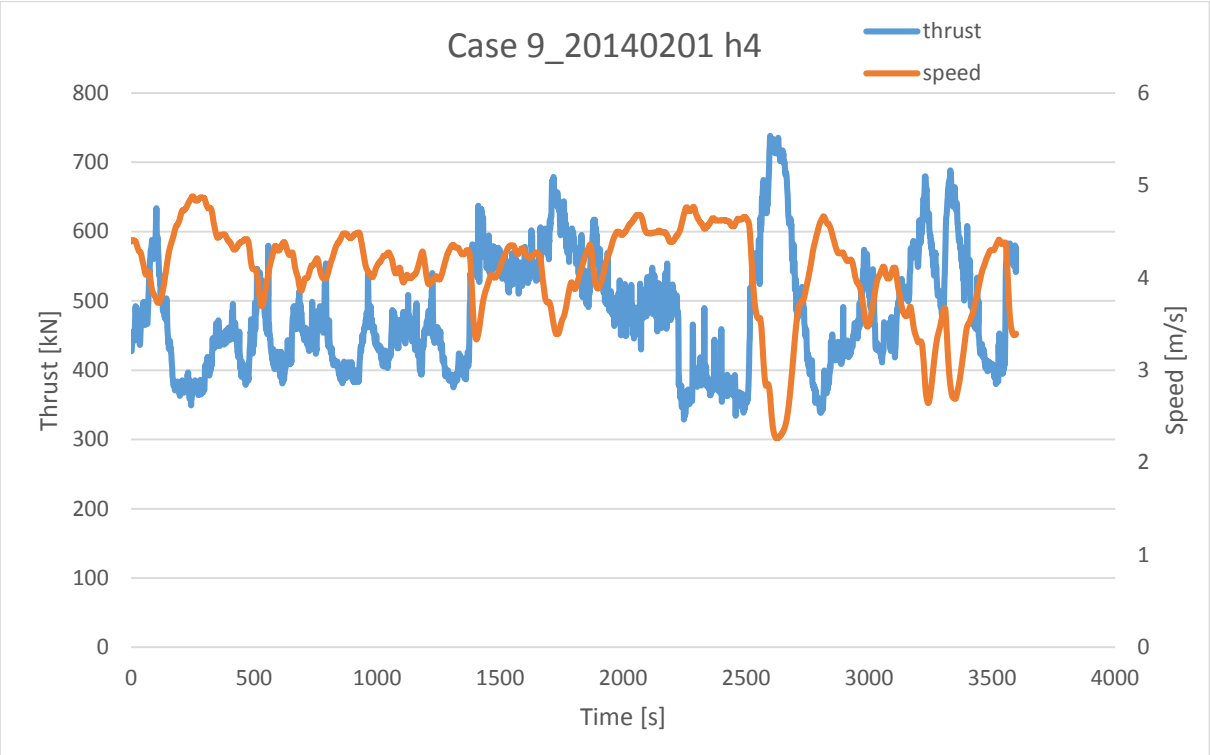
Case 9_20140201 h4
thrust
speed
Thrust [kN]
Speed [m/s]
Time [s]
0
100
200
300
400
500
600
700
800
0
1
2
3
4
5
6
0
500
1000
1500
2000
2500
3000
3500
4000

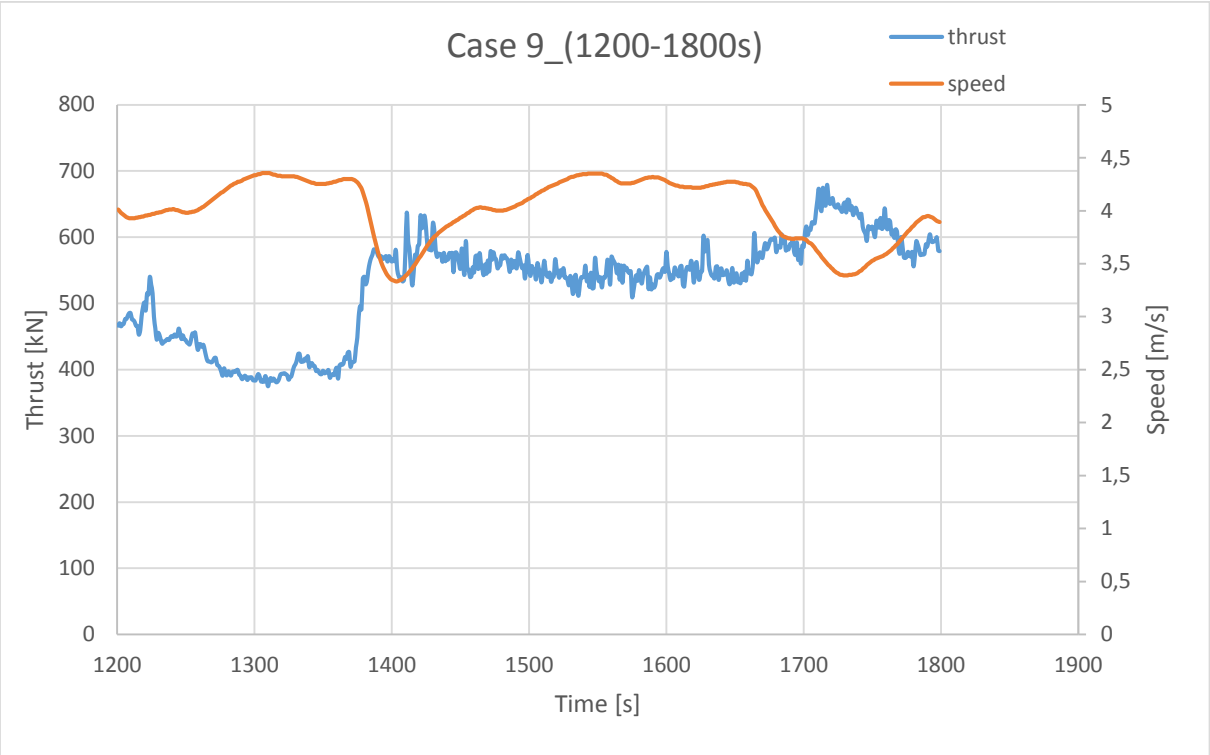
Case 9_(1200-1800s)
thrust
speed
Thrust [kN]
Speed [m/s]
Time [s]
0
100
200
300
400
500
600
700
800
0
0,5
1
1,5
2
2,5
3
3,5
4
4,5
5
1200
1300
1400
1500
1600
1700
1800
1900

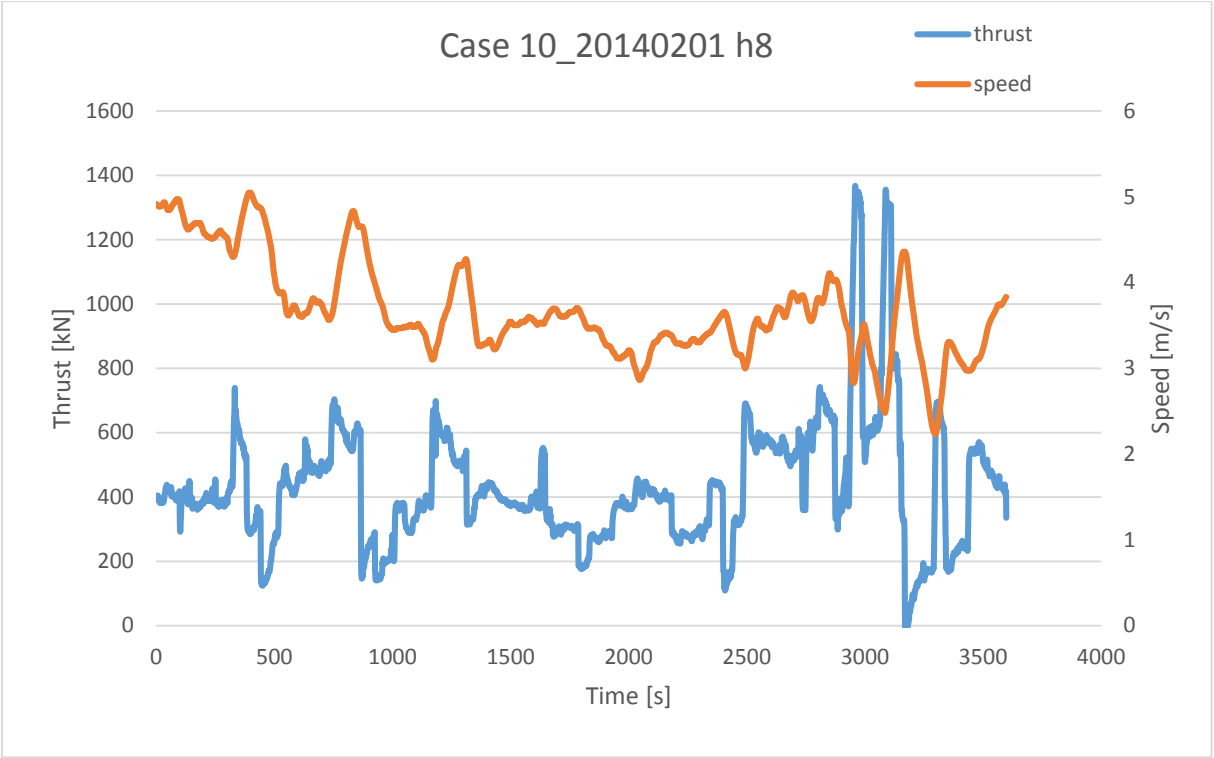
Case 10_20140201 h8
thrust
speed
Thrust [kN]
Speed [m/s]
Time [s]
0
200
400
600
800
1000
1200
1400
1600
0
1
2
3
4
5
6
0
500
1000
1500
2000
2500
3000
3500
4000

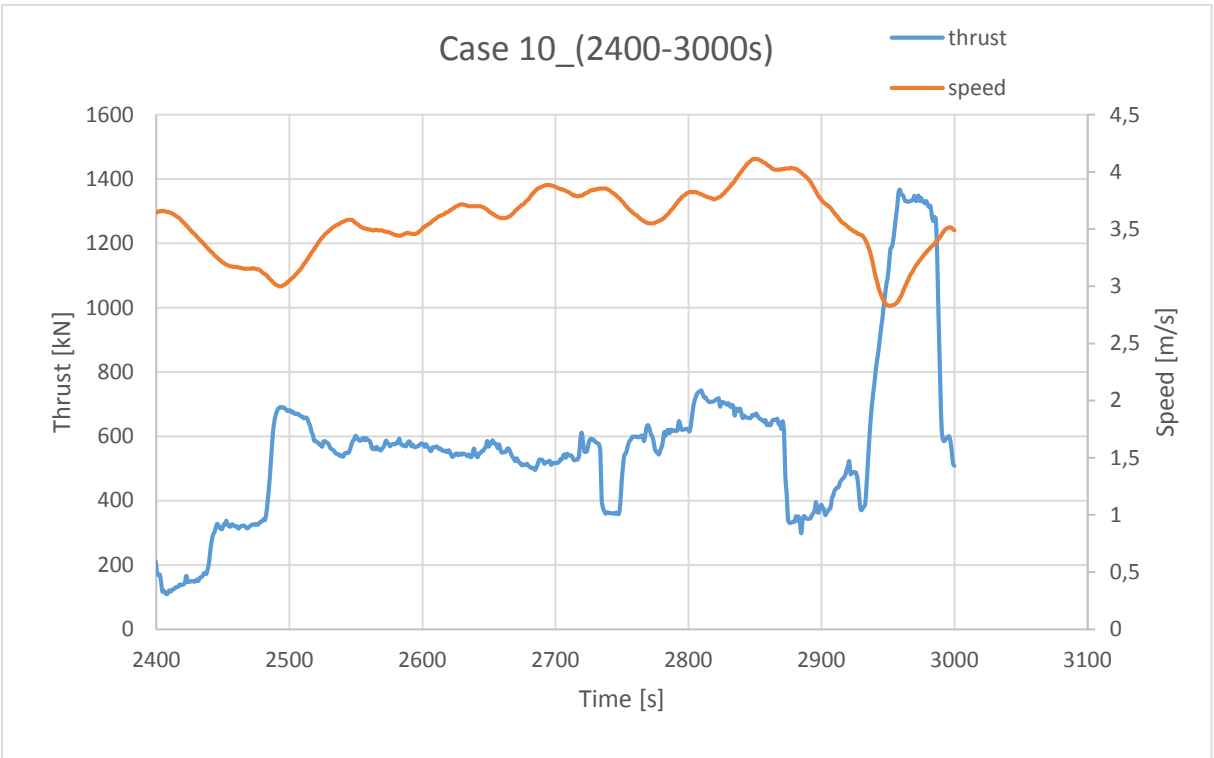
Case 10_(2400-3000s)
thrust
speed
Thrust [kN]
Speed [m/s]
Time [s]
0
200
400
600
800
1000
1200
1400
1600
0
0,5
1
1,5
2
2,5
3
3,5
4
4,5
2400
2500
2600
2700
2800
2900
3000
3100

Appendix 4 Bending strength

Salinity of the sea water 3,35 % , salinity of the measured specimen 0,24 %

Date	Test nro	Layer			Bending Direction		Height	Width	Support span	Density	Ice temperature	Bending Strength	Comments
		Bottom	Middle	Surface	Down	Side	[m]	[m]	[m]	[kg/m3]	[C^0]	[kPa]	
26.12.2013 These measurements were done when was waiting fuel, ice thickness 1.5 m, snow 0.5 m, ice had a lot of porosity	Bending 1			*	*		0,1503	0,1105	1,11	824,8	-1,2	171,7	
	Bending2			*	*		0,1455	0,11375	1,11	824,8	-1,4	128,1	

Salinity of the sea water 3,39 % , salinity of the measured specimen 0,06 %

The ice salinity was measured in-situ being from the top layer 0,74 % (T -1.1 C^o)

Date	Test nro	Layer			Bending Direction		Height	Width	Support span	Density	Ice temperature	Bending Strength	Comments
		Bottom	Middle	Surface	Down	Side	[m]	[m]	[m]	[kg/m3]	[C^0]	[kPa]	
25.01.2014 These measurements were done on flat ice cover close to Pinguin Bukta, ice thickness 1.75 m, snow 0.2 m	Bending 1			*	*		0,199	0,170	1,11	929,4	-0,7	116,3	Broken in 3 pieces, toplayer separated, height 38-45 mm
	Bending2			*	*		0,168	0,136	1,11	757,8	-0,6	150,0	
	Bending 3			*	*		0,156	0,13	1,11	708,6	-0,6	84,4	Broken in two places
	Bending 4			*	*		0,128	0,164	1,11	705,8	-0,5	336,6	Broken in two places .
	Bending 5			*	*		0,144	0,155	1,11	781,9	-0,2	220,7	

Appendix 5

Total ice thickness profiles

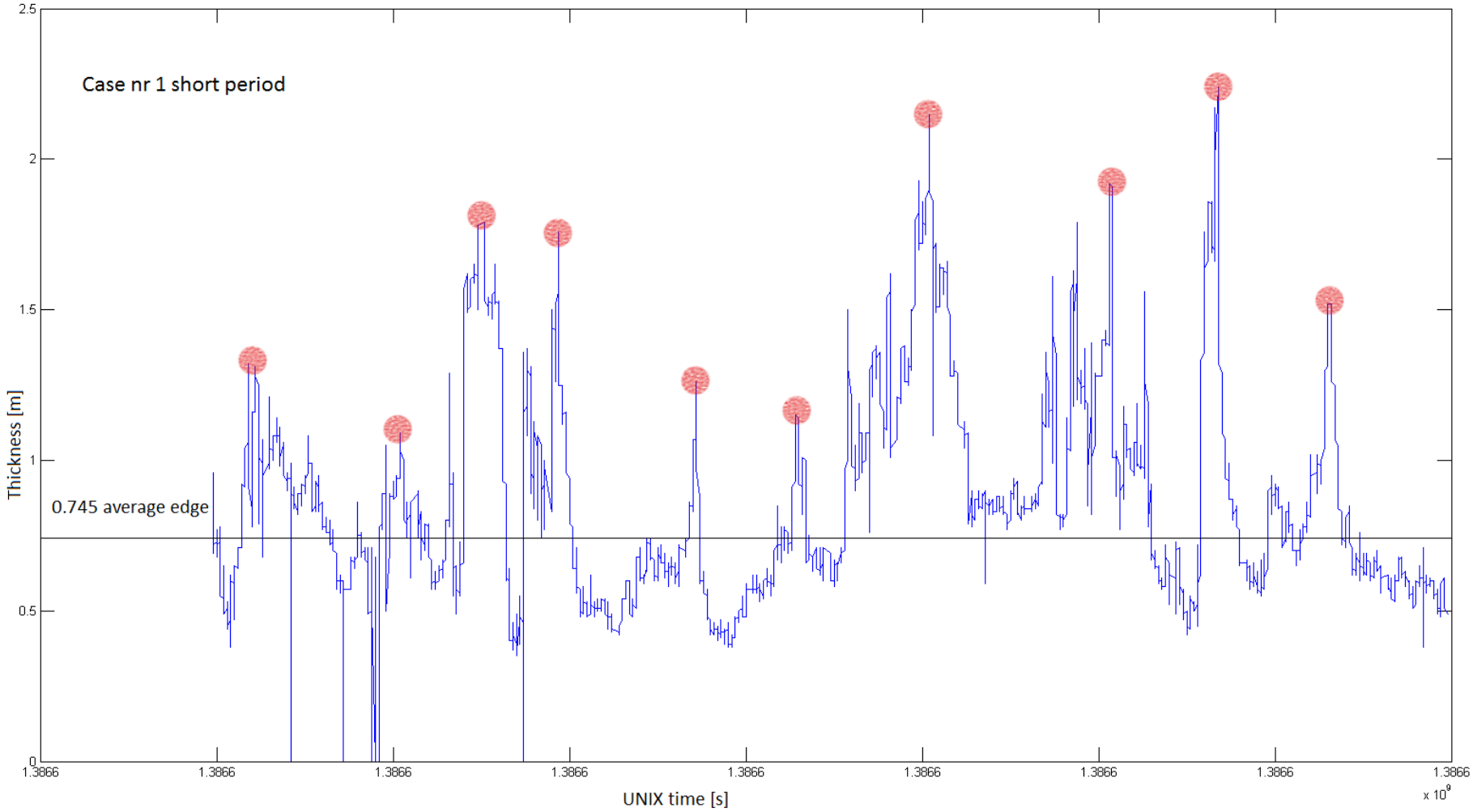

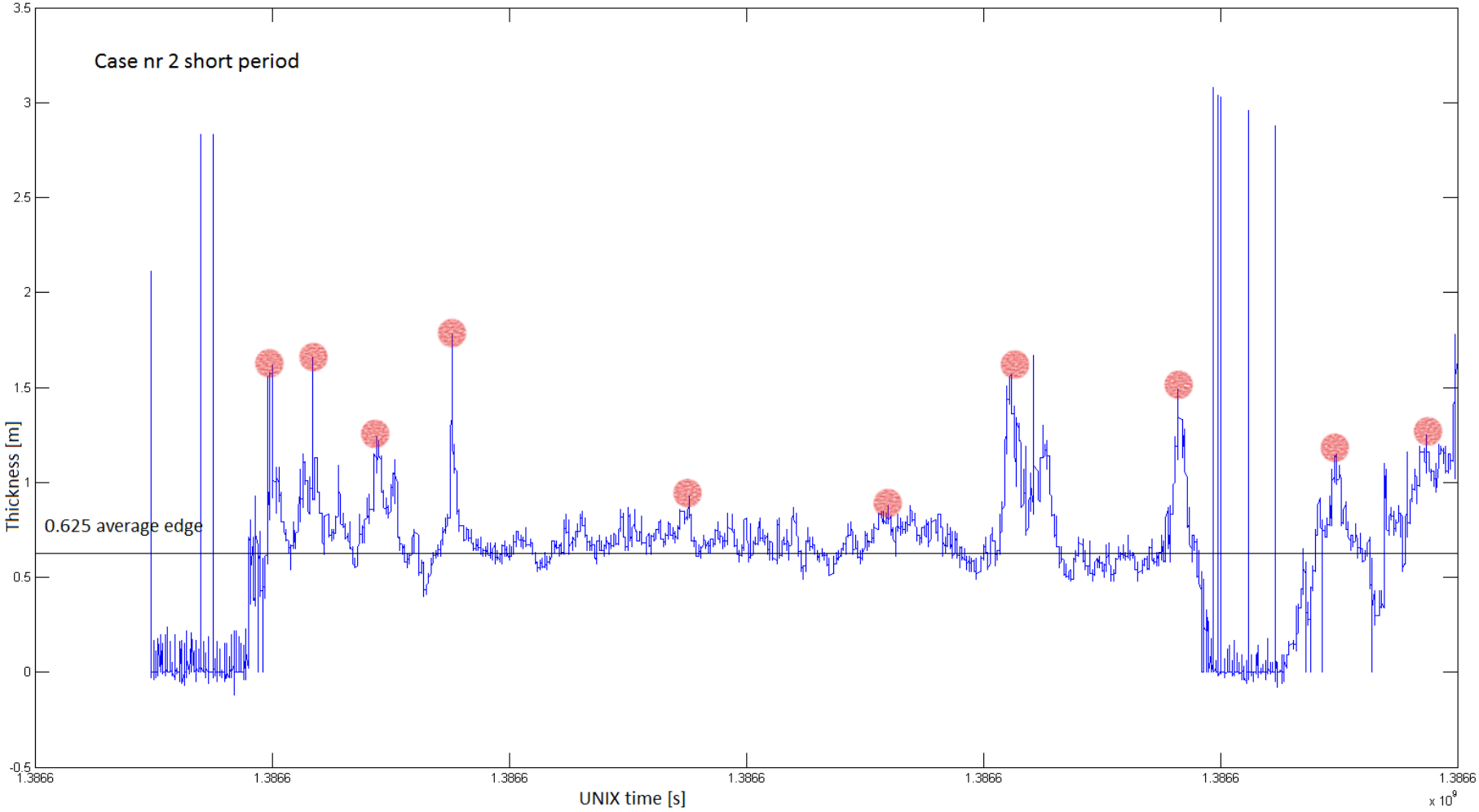
Case nr 2 short period
0.625 average edge
Thickness [m]
UNIX time [s]
x 10^9
3.5
3
2.5
2
1.5
1
0.5
0
-0.5
1.3866

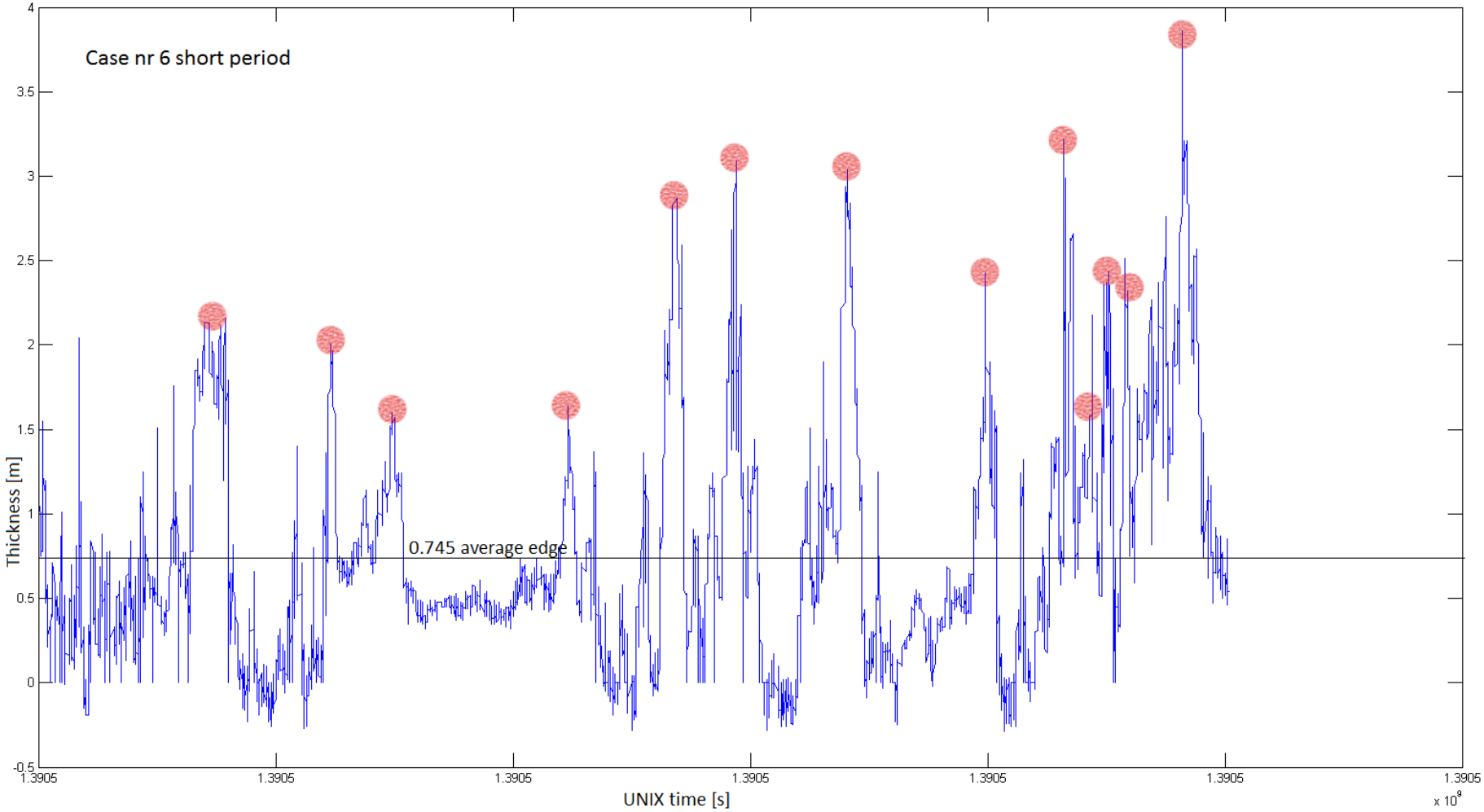
Case nr 6 short period
0.745 average edge
Thickness [m]
UNIX time [s]
x 10^9
4
3.5
3
2.5
2
1.5
1
0.5
0
-0.5
1.3905

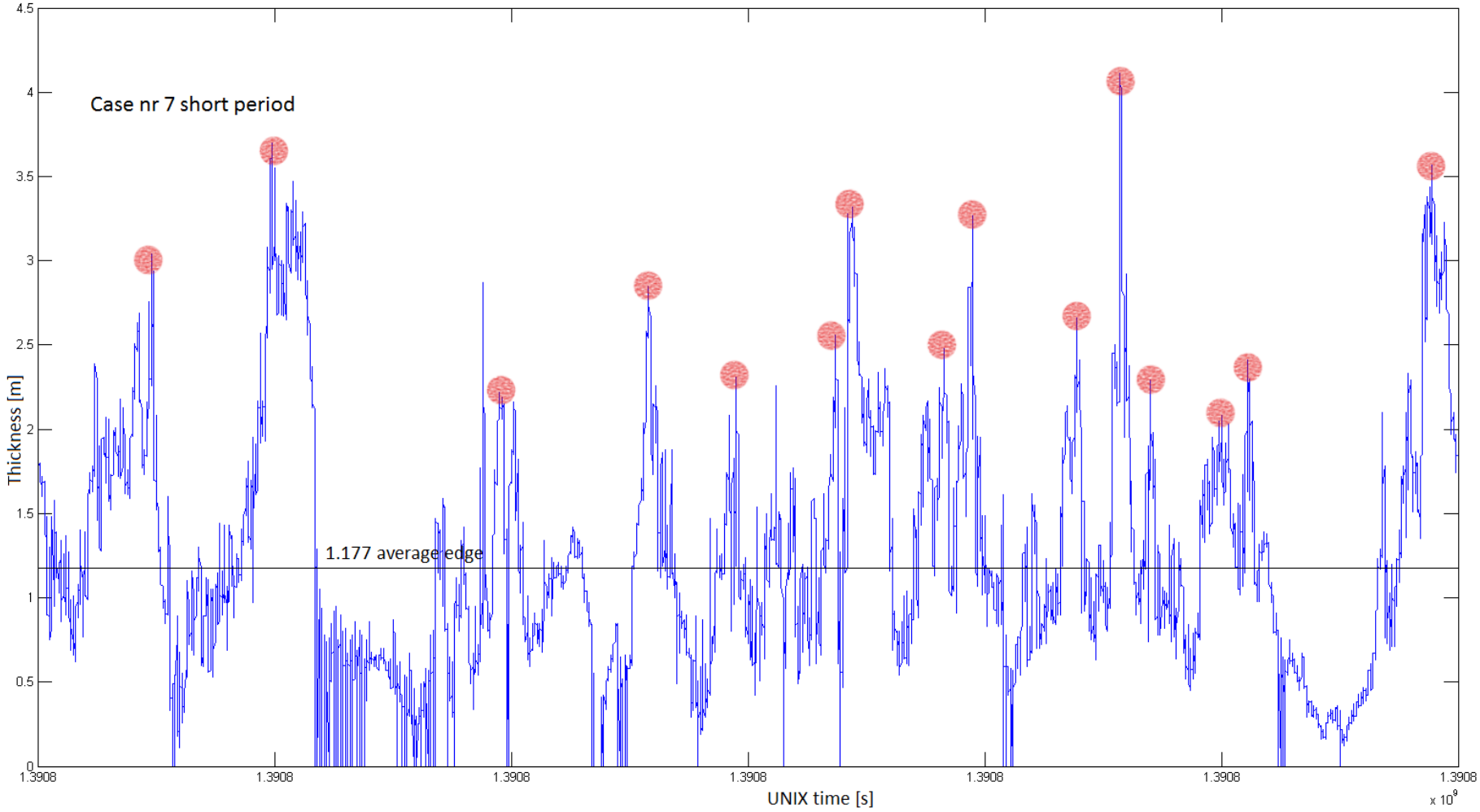
Case nr 7 short period
1.177 average edge
Thickness [m]
UNIX time [s]
x 10^9
4.5
4
3.5
3
2.5
2
1.5
1
0.5
0
1.3908

Case 1	Ridge height	height	1=66	dist	**ridges per km**	
	unit	[m]	0.015152	1.177	8.496177	**~ 9**
1	38	0.575776				
2	20	0.30304				
3	70	1.06064				
4	54	0.818208				
5	22	0.333344				
6	27	0.409104				
7	76	1.151552				
8	78	1.181856				
9	97	1.469744				
10	52	0.787904				
		Average	**0.809**	**[m]**		

Case 2	Ridge height	height	1=41.5	dist	**ridges per km**	
	unit	[m]	0.024096	2.331	4.290004	**~ 4**
1	40	0.96384				
2	22	0.530112				
3	22	0.530112				
4	29	0.698784				
5	13	0.313248				
6	11	0.265056				
7	39	0.939744				
8	29	0.698784				
9	22	0.530112				
10	24	0.578304				
		Average	**0.605**	**[m]**		

Case 6	Ridge height	height	1=37	dist	**ridges per km**	
	unit	[m]	0.027027	2.247	5.785492	**~ 6**
1	51	1.378377				
2	45	1.216215				
3	30	0.81081				
4	27	0.729729				
5	78	2.108106				
6	81	2.189187				
7	80	2.16216				
8	43	1.162161				
9	83	2.243241				
10	31	0.837837				
11	59	1.594593				
12	58	1.567566				
13	90	2.43243				
		Average	**1.572**	**[m]**		

Case 7	Ridge height	height	1=37	dist	**ridges per km**	
	unit	[m]	0.027027	1.419	9.161381	**~ 9**
1	58	1.567566				
2	79	2.135133				
3	36	0.972972				
4	56	1.513512				
5	32	0.864864				
6	41	1.108107				
7	76	2.054052				
8	38	1.027026				
9	61	1.648647				
10	42	1.135134				
11	48	1.297296				
12	32	0.864864				
13	81	2.189187				
		Average	**1.414**	**[m]**		

Appendix 6

Equivalent ice thickness calculations
Case 1

Ice concentration $C := 0.87$

Ridge density $\mu := \frac{10}{1177}$ per km

Ridge sail angle $\kappa := (15 \cdot \text{deg})$

Ridge porosity $p := 0.35$

$C_p := 1 - p$

Ridge height $H_R := 0.809$ m

Level ice thickness $h_i := 0.745$ m

Ridged ice equivalent $h_{eq} := \frac{1}{\tan(\kappa)} \cdot \mu \cdot H_R^{\,2} \cdot C_p$

Snow thickness as level ice $h_s := \frac{1}{3} 0.186$

Equivalent ice thickness $H_{eq} := (h_i + h_s + h_{eq}) \cdot C$

$H_{eq} = 0.714$ m

Case 1 resistance calculations with Lindqvist

Input parameters for the ice resistance

Ice bending strength $\sigma_b := 173000$ Pa

Friction coefficient $f := 0.1$

Ice density $\rho_{ice} := 790$ kg/m^3

Water density $\rho_w := 1025$ kg/m^3

Length of the ship $L := 121.52$m

Draft $T := 7.65$ m

Breadth $B := 22$ m

Waterline angel $\alpha := 28 \cdot \frac{\pi}{180}$ deg

Stem angle $\phi := 21 \cdot \frac{\pi}{180}$ deg

Gravitational const. $g := 9.81$ m/s^2

Ice thickness $h_{ice} := 0.714$ m

Speed $v := 3.40$ m/s

$$\Delta\rho := \rho_w - \rho_{ice} = 235 \qquad \psi := \operatorname{atan}\left(\frac{\tan(\phi)}{\sin(\alpha)}\right)$$

Crushing component:

$$R_c(h_{ice}) := 0.5 \cdot \sigma_b \cdot h_{ice}^2 \cdot \frac{\tan(\phi) + f \cdot \frac{\cos(\phi)}{\cos(\psi)}}{1 - f \cdot \frac{\sin(\phi)}{\cos(\psi)}}$$

Bending component:

$$R_b(h_{ice}) := 0.003 \cdot \sigma_b \cdot B \cdot h_{ice}^{1.5} \cdot \left(\tan(\psi) + f \cdot \frac{\cos(\phi)}{\sin(\alpha)\cdot\cos(\psi)}\right) \cdot \left(1 + \frac{1}{\cos(\psi)}\right)$$

Submersion component:

$$R_s(h_{ice}) := \Delta\rho \cdot g \cdot h_{ice} \cdot B \cdot \left[T \cdot \frac{B + T}{B + 2T} + f \cdot \left[0.7L - \frac{T}{\tan(\phi)} - \frac{B}{4\tan(\alpha)} + T \cdot \cos(\phi) \cdot \cos(\psi) \cdot \sqrt{\frac{1}{(\sin(\phi))^2} + \frac{1}{(\tan(\alpha))^2}}\right]\right]$$

Total resistance:

$$R_{ice} := \left(R_c(h_{ice}) + R_b(h_{ice})\right) \cdot \left(1 + 1.4 \cdot \frac{v}{\sqrt{g \cdot h_{ice}}}\right) + R_s(h_{ice}) \cdot \left(1 + 9.4 \cdot \frac{v}{\sqrt{g \cdot L}}\right)$$

$$R_{ice} = 1.049 \times 10^6 \quad \text{N}$$